Nantes | Hamburg | Helsinki

Deliverable due date: M36 – November 2019

D2.10 DISTRICT HEATING MONITORING AND OPTIMIZATION

WP2, Task 2.5 (Subtask 2.5.3)

Transition of EU cities towards a new concept of Smart Life and Economy

This project has received funding from the European Union's Horizon 2020 research and innovation programme under grant agreement No 731297.

Project Acronym	mySMARTLife
Project Title	**Transition of EU cities towards a new concept of Smart Life and Economy**
Project Duration	1st December 2016 – 30th November 2021 (60 Months)
Deliverable	D2.10 District heating monitoring and optimization
Diss. Level	PU
Status	☐ Working ☐ Verified by other WPs ■ Final version
Due date	30/11/2019
Work Package	WP2
Lead beneficiary	ARMINES [ARM]
Contributing beneficiary(ies)	[ARM] via its Linked Third Party IMT Atlantique
Task description	The urban platform and the decision aiding action with the necessary information for decision making related to the District Heating will be the basis to optimise the operation of the District Heating and to offer a mean to assess the impacts of actions (cost, energy, CO_2). Data will be collected from the monitoring of a selection of district heating substations (on the Ile de Nantes). Definition of load profiles at the substations to input in the modelling tool. In this subtask led by ARM, tests of different scenarios of actions will be done in order to deploy an optimisation strategy of the DH. Extension, sub-net connexion, assessment of energy efficiency actions on connected buildings, assessment of new energy carriers for DH energy supply and new energy systems, awareness of end users will be part of this subtask.

Date	Version	Author	Comment
15/10/2019	0.1	[ARM] M. T. Mabrouk[1], P. Haurant[1], B. Lacarrière[1]	
09/11/2019	0.2	[ARM] M. T. Mabrouk[1], P. Haurant[1], B. Lacarrière[1]	
12/11/2019	0.2	[NAN] G. Chanson	Contribution monitoring section
18/11/2019	1	[ARM] M. T. Mabrouk[1], P. Haurant[1], B. Lacarrière[1]	

[1] IMT Atlantique (ARMINES' Linked Third Party)

This project has received funding from the European Union's Horizon 2020 research and innovation programme under grant agreement No 731297.

This project has received funding from the European Union's Horizon 2020 research and innovation programme under grant agreement No 731297.

Table of Content

This project has received funding from the European Union's Horizon 2020 research and innovation programme under grant agreement No 731297.

This project has received funding from the European Union's Horizon 2020 research and innovation programme under grant agreement No 731297.

This project has received funding from the European Union's Horizon 2020 research and innovation programme under grant agreement No 731297.

Table of Figures

This project has received funding from the European Union's Horizon 2020 research and innovation programme under grant agreement No 731297.

This project has received funding from the European Union's Horizon 2020 research and innovation programme under grant agreement No 731297.

This project has received funding from the European Union's Horizon 2020 research and innovation programme under grant agreement No 731297.

This project has received funding from the European Union's Horizon 2020 research and innovation programme under grant agreement No 731297.

Table of Tables

This project has received funding from the European Union's Horizon 2020 research and innovation programme under grant agreement No 731297.

Abbreviations and Acronyms

Acronym	Description
mySMARTLife	Transition of EU cities towards a new concept of Smart Life and Economy
DH	District Heating
CHP	Combined Heat and Power
HP	Heat Pump
HEx	Heat Exchanger
SH	Space Heating
DHW	Domestic Hot Water
P	Power (W)
E	Energy (Wh)
UIOM	Waste incineration plant
RES&R	Renewable and recovery heat
T	Temperature (°C)
m	Mass flow rate (Kg/s)
N	Number
subs	Sub-station
PID	Proportional Integral Derivative (relates to the valves control)
TD	Typical Days
MCDA	Multi Criteria Decision Aiding
DM	Decision Maker

This project has received funding from the European Union's Horizon 2020 research and innovation programme under grant agreement No 731297.

1. Executive Summary

This document presents the work achieved on the Nantes District Heating monitoring and optimization. The purpose of this action is to provide stakeholders (District Heating operator, local authorities, clients, third parties…) with a methodology able to assess any scenarios of District Heating improvement. These scenarios can relate on management actions, infrastructure modification (energy systems, extension, retrofitting…) as well as any actions on the buildings connected (improvement of the envelop, of the systems…).

The action has been developed with the will to be flexible enough for being used by different parties. It is illustrated with a set of actions at different scales of the District Heating. The methodology is implemented thanks to modelling and optimization tools from ARMINES, without making it dependent on them. Thus alternative solutions are presented in the document to allow other tools to be used in the application of this methodology.

One of the key aspect of the methodology is to fit to the reality of the monitoring with its variable quality of information regarding the physical variables needed for evaluating the performance indicators. Solutions are given in this work to supplement these lack of data which is common in a supervision.

The proposed solution makes possible the analyse of the District Heating at different geographical scales and time spans. It can be applied to a fraction of the network or to the whole District Heating depending of the operational objectives. It can handle optimization of the District Heating in complement of the usual energy systems management tools used by the operators.

This action has been done with the objective of being strongly connected with other actions in the network. The main connection is with the action 2.5.3 which proposes a Decision Aiding tool. This link between these actions is documented in the deliverable D2.8. In addition, the present action has been thought with the idea to be connected to the urban platform. Thus, the data from the District Heating operator supervision are uploaded in the urban platform for making the assessment solution available for various stakeholders. Last, thanks to its connection to the urban platform, input data and complementary information can come from other actions which focus on urban systems which can affect the District Heating (e.g. Modelling solution of the building stock, proposed in the action 1.4.1 can be used as input for assessing impacts of building renovation actions on the District Heating performances).

All these characteristics of this action and the flexibility they offer make the solution scalable and replicable for other District Heating Networks in the future, in Nantes or elsewhere.

This project has received funding from the European Union's Horizon 2020 research and innovation programme under grant agreement No 731297.

2. Introduction

2.1 Purpose and target group

District Heating improvement is of interest for multiple parties. The district Heating operator first, for which assessing innovative scenarios is essential for anticipating the transformation of its system (new connections, development of low temperature district heating networks, energy harvesting from renewable sources or surplus, definition of its objectives …).

The local authorities are also concerned as they are in charge of energy planning on the territory. The methodology offers them mean to assess the impacts of urban energy actions on the District Heating systems. It is also an efficient tool for improving the discussion with the District Heating operator.

In an idea of open data, the proposed methodology coupled with the information and data collected by the urban platform offers a potential of innovation too, in particular innovation of services associated to the District Heating and its systems. This services can be directly studied by the operator or the local authority as well as potential third parties (existing or to be created).

2.2 Contributions of partners

Table 1 depicts the main contributions from participant partners in the development of this deliverable.

Table 1: Contribution of partners

Participant short name	Contributions
ERENA (District Heating Operator; ARM subcontractor)	Provide the raw material (data from their supervision tool). Deep and continuous discussion with expert engineers to assess at each step the relevance of the choices in the development of the action
NAN	Continuous discussion with different departments to include the different parties consideration in the development of the action
NAN	Link with the Urban Platform and the relevant MySMARTLife actions to be connected with the present action
ARM (LTP IMT Atlantique)	Development of the present action
ARM (LTP IMT Atlantique)	Link with the action on Decision Aiding

2.3 Relation to other activities in the project

Table 2 depicts the main relationship of this deliverable to other activities (or deliverables) developed within the mySMARTLife project and that should be considered along with this document for further understanding of its contents.

This project has received funding from the European Union's Horizon 2020 research and innovation programme under grant agreement No 731297.

Table 2: Relation to other activities in the project

Deliverable Number	Contributions
D1.12	Description of 3D model for each pilot
D2.8	Decision aiding tool
D2.7	Development of improved services in Nantes Urban Platform

This project has received funding from the European Union's Horizon 2020 research and innovation programme under grant agreement No 731297.

3. District heating description

3.1 District heating fundamentals

3.1.1 Concept and role of district heating

District heating (DH) is an old concept based on moving heat from available heat sources to be consumed immediately by end users located in other locations. DH appeared in the late 19th century to allow a centralized generation in a location generally far away from the end users. Nowadays, the concept has evolved and DH offer the ability to use local heat sources which otherwise would be wasted or renewable sources. In this configuration, energy sources are smaller and more distributed. Five types of heat sources are currently considered as strategic local heat sources in DH (Frederiksen and Werner, 2013):

- **Combined Heat and Power (CHP)** which consists in harvesting heat excess from thermal power plants.
- **Waste-to-Energy** which consists in using heat from waste incineration.
- Using **excess heat from industrial processes.**
- Using **renewable Combustible** that are usually difficult to handle in small boilers such as wood waste, straw or olive residues...
- **Geothermal heat sources.**

Other renewable energy sources could be considered in DH such as renewable electricity generated by large solar fields or wind farms coupled to large heat pumps (HP) to convert electricity to heat. The penetration rate of these technologies is still very low for different raisons including cost, the intermittency of the sources and the lack of effective storage solutions.

From a practical point of view, a DH is constituted of three subsystems (Figure 1):

- **Production:** heat production plants use available sources to increase the temperature of a heat transfer fluid. In all recent networks liquid water is used.
- **Distribution:** the fluid is pumped in a distribution network constituted of a double piping system (supply and return).
- **Utilization:** The heat is transferred to the heating network of the consumer building (secondary network). The heat transfer occurs in the heat exchanger (HEx) of the substation usually located in the building.

DH is used mainly to meet heat demand for space heating (SH) and domestic hot water (DHW). It can also be used for industrial processes which increases the complexity of the system as industrial heat demand covers a wide range of temperature levels. In 2007, about 30 % of heat supplied by DH in the Europe where used for industrial purposes which is not negligible.

This project has received funding from the European Union's Horizon 2020 research and innovation programme under grant agreement No 731297.

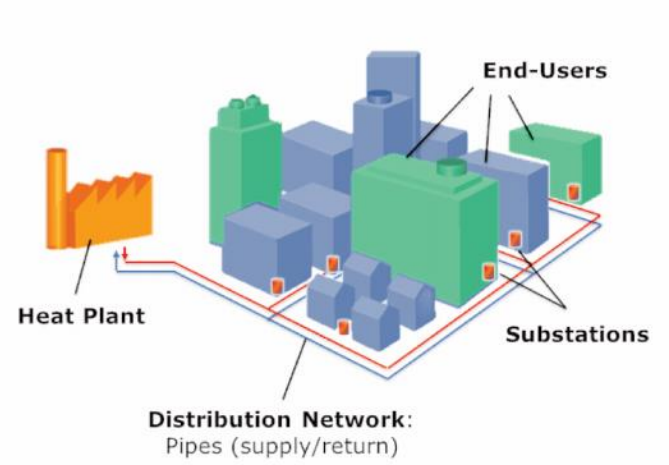

Figure 1: Concept of a DH (Castro Flores, 2018)

DH systems are usually classified into different generations going from the first to the 4th generation depending essentially on level of the supply temperature (Lund et al., 2014). Indeed, the first generation of the DH used steam as heat carrier with supply temperatures higher than 100°C. Steam was distributed through concrete ducts. This generation was deployed before the nineteen thirties. The second generation used pressurized water instead of steam with supply temperature also higher than 100°C and had been deployed until the nineteen eighties. Supply temperature dropped under 100°C since the third generation. Pre-insulated pipes and the possibility to use low grade heat coming from industry surpluses or CHP power plants participated to the development of third generation of DH. In fact, most of the current DH belong to this generation. Fourth generation DH are likely to be developed in the future and offer lower supply temperature levels ranging between 50°C and 60°C and the possibility to connect more energy sources such as geothermal, solar farms, data centers. This generation offers also the possibility to connect electrical power sources coupled to HP.

3.1.2 District heating substations

The heat transfer at the substation is illustrated in Figure 2 which shows the hot fluid taken from the supply piping system passes through the HEx and is rejected to the return pipe. This side of the HEx is called “primary side”. In the HEx, heat is transferred by indirect contact to the fluid coming from the internal heating distribution network of the building. The heated fluid circulates through the SH system of the building (radiators, floor heating or air conditioning systems). This side of the HEx is called “secondary side”.

Figure 2 shows the simplest design of a substation. Depending on the usage of heat in the substation, this could be more complex. In the case of SH and DHW production for instance, one, two or three HEx could be used in different configurations (parallel, series, 2-stages, 3-stages etc…). Storage for DHW can also be installed in the substation.

HEx used in district heating substations are almost exclusively plate HEx. This type of HEx is cheap and compact. Besides, it is easy to adapt the size of the HEx to the building’s requirements by selecting the appropriate number of

This project has received funding from the European Union's Horizon 2020 research and innovation programme under grant agreement No 731297.

plates. These HEx replaced “shell and tube” technologies which were widely used in the past but less compact and more subject to leaking and corrosion.

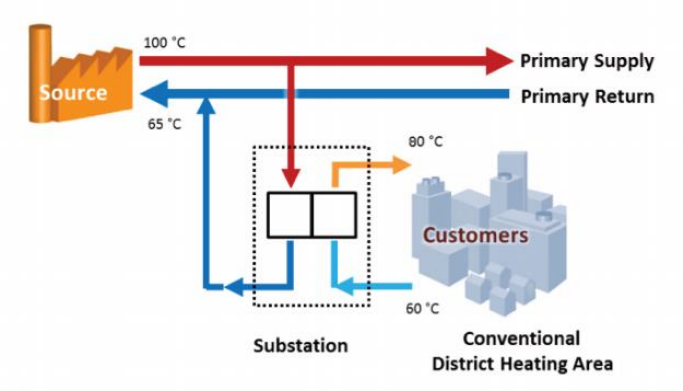

Figure 2: District heating substation (Castro Flores, 2018)

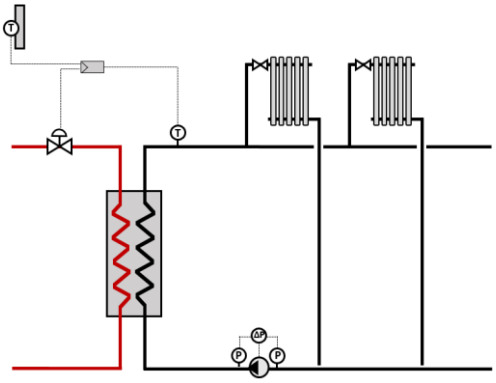

Figure 3: Simplified layout of substation with variable mass flow rate and temperature control (only SH is showed)

From the control point of view, motorized valves are often used in substations to control the temperature. For SH, the primary side’s valve is controlled to keep the supply temperature at the secondary side close to the set point (Figure 3). A PID-type control system is used most of the time. In an “ambient temperature compensation strategy”, the temperature set point varies with respect to the outside air temperature following a control curve. For hot water preparation, tap supply temperature set point is usually fixed to a constant temperature between 55°C and 65°C. It is important for the water to be heated enough to avoid legionella growth but not too much to avoid skin burns from hot water.

3.1.3 Heat distribution systems

In a DH, heat is distributed in pipes thermally isolated to prevent excessive heat losses during the transport. These pipes are in most cases underground. Over the years, many designs have been developed with more or less success. The goals of these developments were to reduce investment and operation costs, space footprint and installation times and to increase the reliability of the system by reducing the number of premature fails.

Over the generations, different designs were used. The Figure 4 illustrates the evolution of the technology caused by the changes in the temperature levels and the technical requirements. The main changes between the first and third generations are the use of pre-insulated pipes delivered by trucks in standard lengths. These pipes are bonded together and directly buried what reduces the costs. The insulation also changed from generation to generation and the most used insulating material is Polyurethane foam because of its good thermal properties. A jacket made of high density Polyurethane is also used to protect the insulating material.

The choice of pipes’ diameters is a critical decision during the design phase. If the diameter is too large, the velocity of the heat transfer fluid will be small and its residency time in the pipes will increase which causes high heat losses and a slow dynamic behaviour of the network. In the contrary, if the diameter of the pipe is too small, the velocity of the fluid will be too high resulting in too high pressure drops in the system and high pumping costs. Planning plays an

This project has received funding from the European Union's Horizon 2020 research and innovation programme under grant agreement No 731297.

important role too in this choice because choosing small diameters reduces the possibility to extend the network by connecting new buildings in the future. Therefore, in some cases, designers might choose oversized diameters with more heat losses in order to allow network extension in the future.

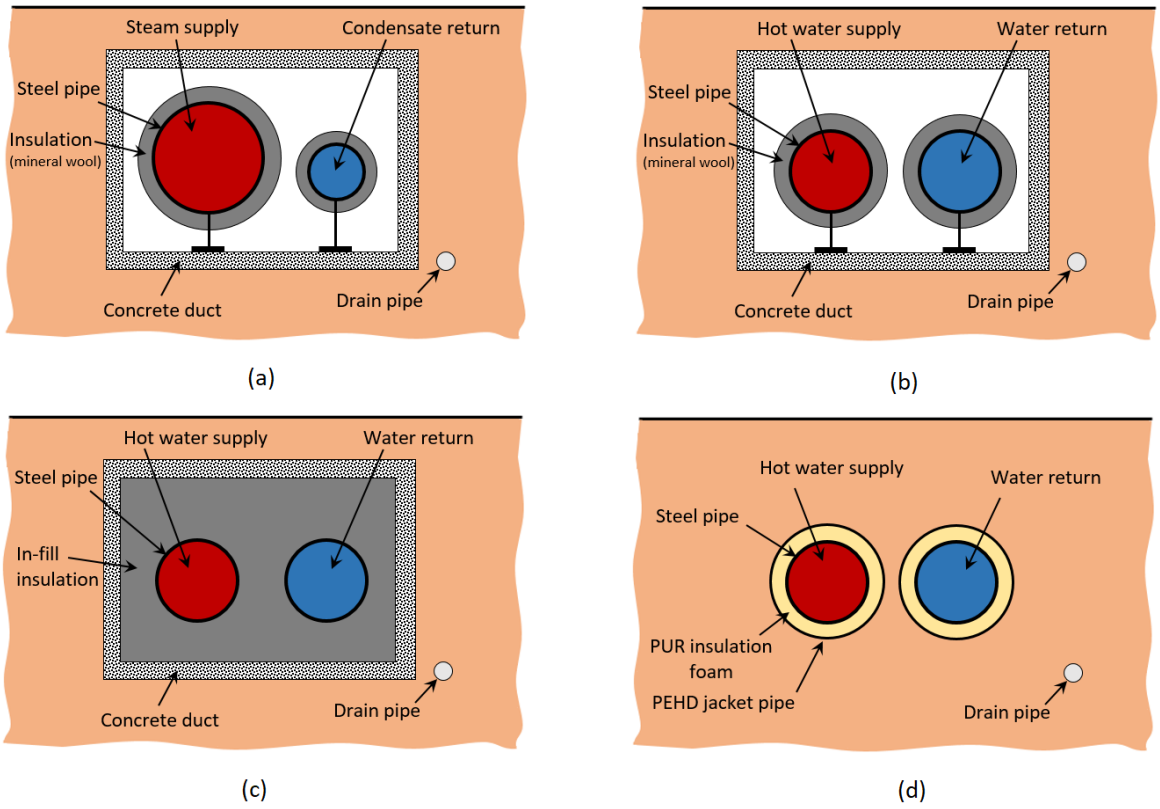

Figure 4: Different designs of heating distributions technologies : (a) Steam pipes in concrete ducts for 1st generation DH ; (b) Hot water pipes in ducts for 2nd generation DH ; (c) pipes with in-fill insulation (transitional technology towards 3rd generation DH ; (d) Pre-insulated directly buried pipes for 3rd generation DH.

This project has received funding from the European Union's Horizon 2020 research and innovation programme under grant agreement No 731297.

4. District heating “Centre Loire”

4.1 DH Overview

Nantes’ agglomeration area includes three DH, among which "Nantes Centre Loire" DH, the biggest one with a fast development dynamic since 2012, the beginning of the public service delegation contract between Nantes Métropole and ERENA, the DH operator in charge of its management and development.

In 2017, it connected more than 380 substations with about 85 km of pipes versus only 22 km in 2012. It supplies heat to more than 16 000 dwellings and many public facilities (swimming pools, hospital, schools, museums…). *Nantes Centre Loire* DH is composed of 3 subnets (or main branches): the *Beaulieu* branch which provides heat to Nantes Island substations, the *Centre ville* for the substations in the city centre, and the *Nord* branch supplies heat to the northern part of the city (Figure 5). The total capacity of heat production units hits 202 MW with an energy mix composed of 84 % of the heat coming from renewable sources or waste heat recovery, fulfilling the commitments of renewable rate in the contractual agreement between the DH operator ERENA and Nantes Métropole (Table 3).

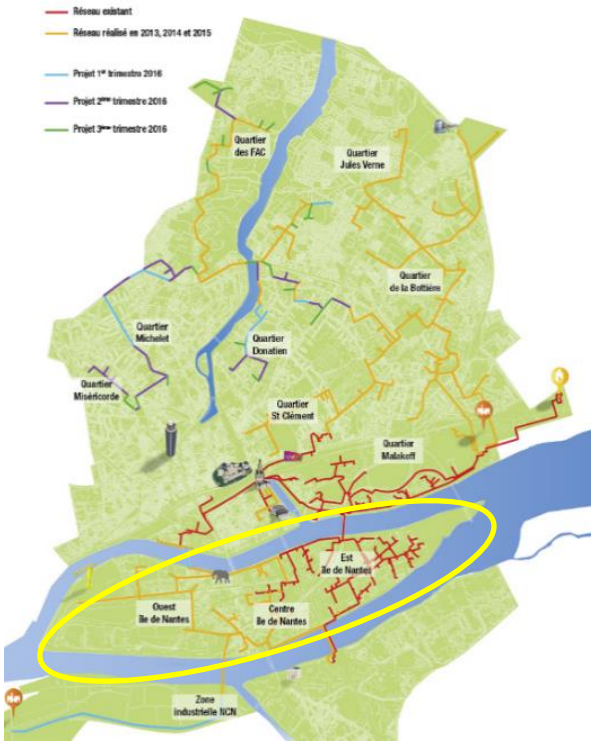

Figure 5: *Nantes Centre Loire* DH (source : ERENA website[2]). In yellow, the *Beaulieu* branch: the DH zone considered in this study

[2] http://erena-nantes.reseau-chaleur.com/votre-reseau-de-chaleur/plan-du-reseau/

This project has received funding from the European Union's Horizon 2020 research and innovation programme under grant agreement No 731297.

In the present study, the mySMARTLife H2020 area project focuses on the Beaulieu – île de Nantes branch of the network. The branch is a good sample of a city sized district heat, as it fuels 170 substations of various uses: public facilities, social or private dwellings, offices or sports equipment. However, it must be noticed that this area does not include production plants. The action of the mySMARTLife project does not include scenarios on energy systems modification and/or implementation.

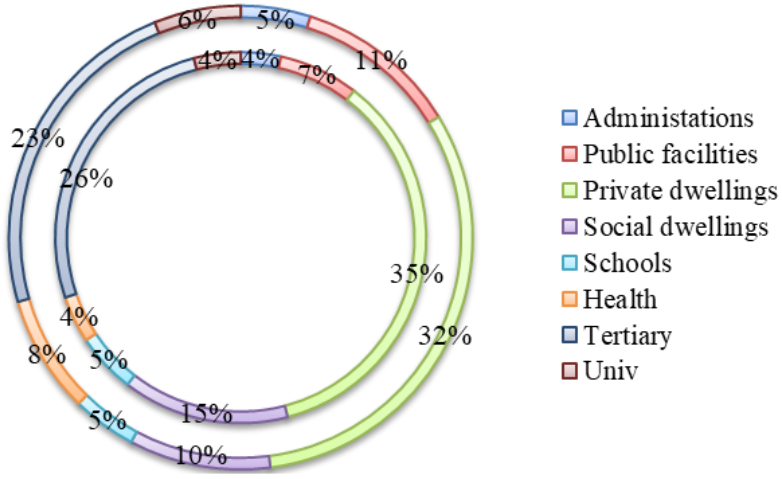

Figure 6: Substations by uses in *Nantes Centre Loire* DH (Outer ring : ratio in terms of cumulative subscribed power, inner ring : ratio in terms of amount of substations belonging to each category)

Figure 6 show the uses distribution in terms of subscribed powers and types of final use of the substations connected. We can observe that private dwellings and tertiary sector represent the biggest shares with 35 % and 26 % of the substations respectively, representing 32 % and 23 % of the subscribed powers. The other uses represent less than 10 %. We can note that contrary to dwellings and tertiary sector, public facilities, university and health facilities represent bigger shares in terms of subscribed powers than in terms of number. These last facilities need more heat since they represent bigger area to be heated.

Most of the substations of the *Beaulieu* branch belong to the historical part of the DH. They constituted the base of its development, when the public service delegation contract was signed in 2012. Many other substations were connected over the last years with the cumulative subscribed power $P_{sbc,t}$ of the branch increasing from 58 MW in 2012 to 78 MW in 2017. It will achieve 85 MW in 2019 (Figure 7).

This project has received funding from the European Union's Horizon 2020 research and innovation programme under grant agreement No 731297.

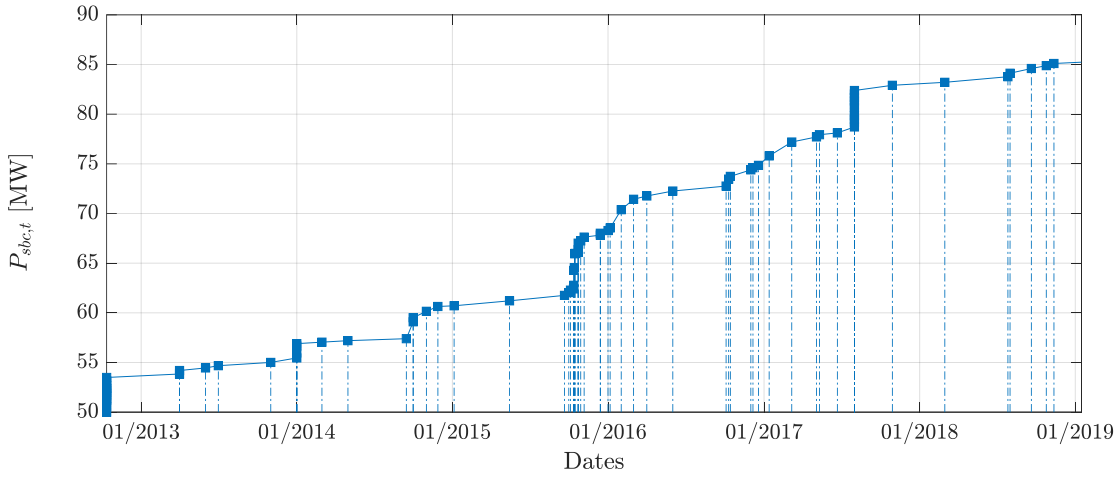

Figure 7: Cumulative subscribe power $P_{sbc,t}$ evolution

Figure 8 shows the energy heat consumptions of *Beaulieu* branch substations for the year 2015, 2016 and 2017 (sorted from the most energy intensive to the less one). We can observe that the most energy intensive substations consumed between 10 and 16 GWh during the three years. The others substations are far less energy intensive, since they consumed less than 2.5 GWh, and most of them consumed less than 0.5 GWh.

On another hand, the consumed energy for a given substation can vary from 50 % from a year to another. These variations are mostly linked to evolution of the meteorological conditions, but they can be due to refurbishment actions at substations level. In that case, the yearly energy evolution could be a parameter for evaluating this kind of actions.

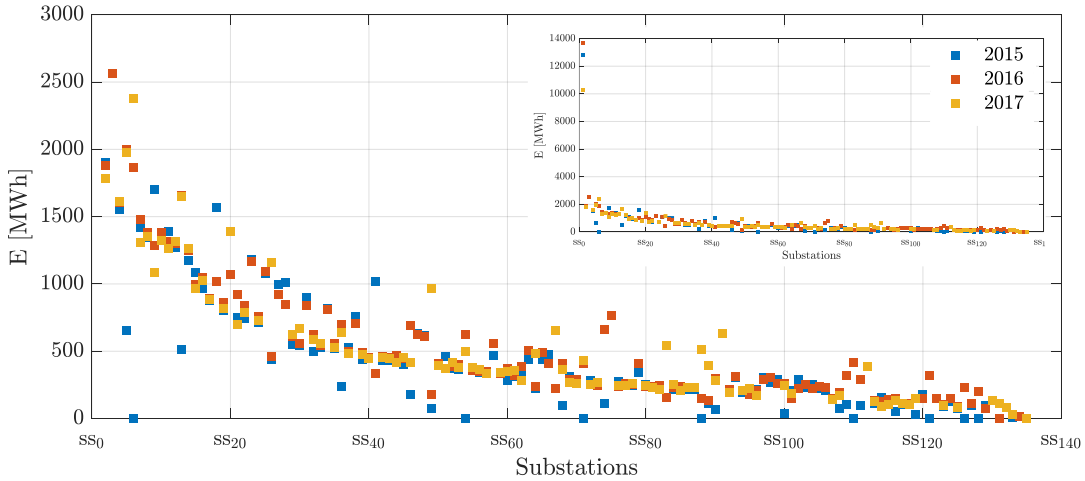

Figure 8: Substations' heat consumptions

From production side, the total capacity of heat production units for the overall DH hits 202 MW, with 68 MW of renewable and recovery heat capacity, representing 32 % of the total installed capacity (Table 3).

This project has received funding from the European Union's Horizon 2020 research and innovation programme under grant agreement No 731297.

Site	Number of units	Energy source	Installed capacity (MWth per unit)
Malakoff	2	Waste incineration	15
	2	Biomass (Wood)	15
	3	Gas	29
	3	Gas	13
La Californie	2	CHP	8
	1	Biomass (Wood)	8 (May 2019)

Table 3: Nantes Centre Loire DH production units

The time series of year 2018's *Malakoff* and *Californie* production, as well as the derived load duration curves are presented in Figure 9, Figure 10, Figure 11 and Figure 12.

For Malakoff site, we can observe the base contribution of the waste incinerator (P_{UIOM} in the Figure 9 and Figure 10). It can also be seen the incinerator only runs in summer except for few days in August due to the yearly maintenance. During this period, the gas boilers are solicited. Most of the time, the biomass boilers are used to complement the waste incinerator when needed, followed by the gas boilers. However, the gas boilers are used in priority during some specific periods (e.g. in summer and November), while the biomass are turned off. During these short periods of use, the biomass boilers are not solicited because of the constraints link to their start time and their out-of-design low efficiency.

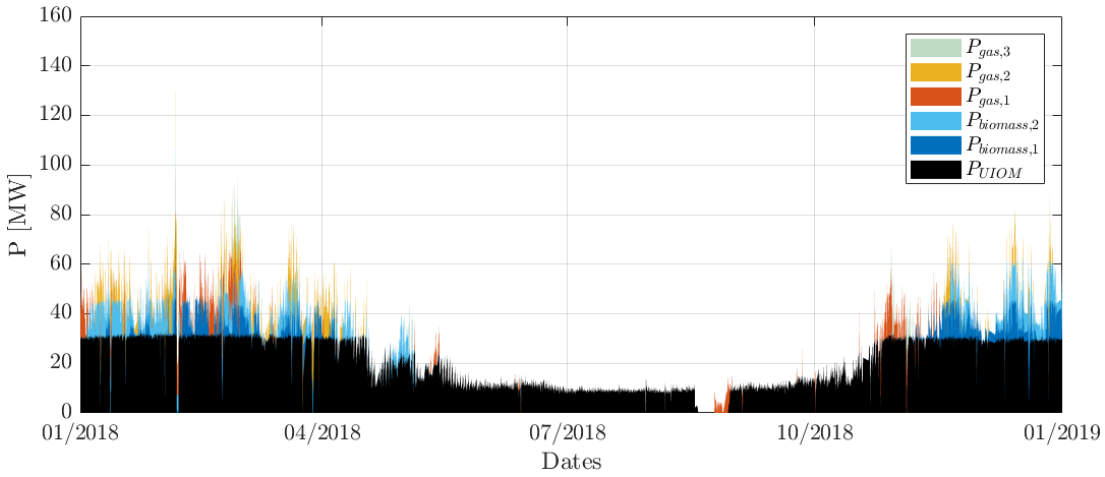

Figure 9: Heat productions times series in *Malakoff*

This project has received funding from the European Union's Horizon 2020 research and innovation programme under grant agreement No 731297.

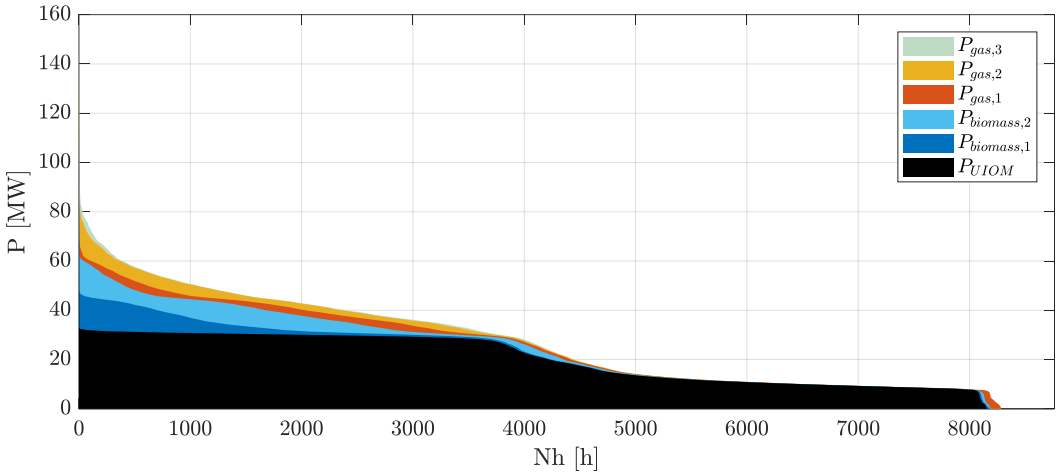

Figure 10: Load duration curve of heat productions in *Malakoff* plant (2018)

For *Californie* plant, the CHP ensures the base production during the heating period, whereas it does not run in summer (Figure 11 and Figure 12). On another hand, the gas boilers run as complementary systems, and one of them provides heat in summer, when the waste incinerator is undergoing maintenance.

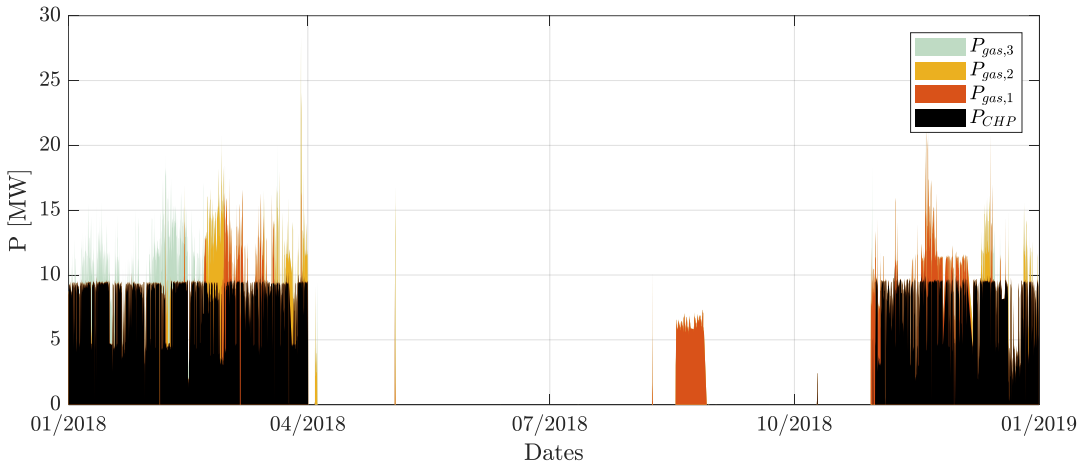

Figure 11: Heat productions times series in *Californie* plant (2018)

This project has received funding from the European Union's Horizon 2020 research and innovation programme under grant agreement No 731297.

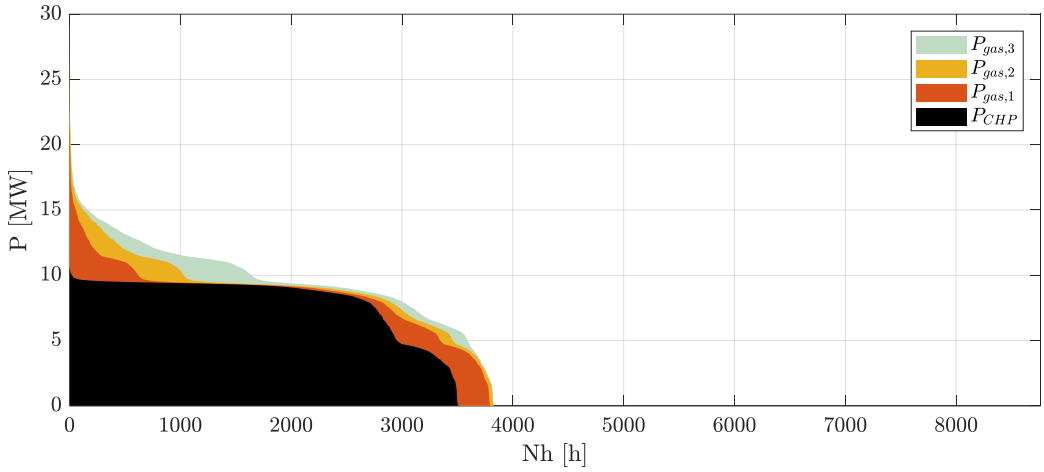

Figure 12: Load duration curve of heat productions in *Californie* plant (2018)

The two production sites being interconnected thanks to the DH it makes sense to consider the global functioning of the productions units (Figure 13 and Figure 14). We can verify the incinerator remains the base production of the whole DH, the CHP and the biomass boilers are used only during the heating season as first stage of complementary production and the gas boilers are used as second stage of complementary production for short duration (especially in summer).

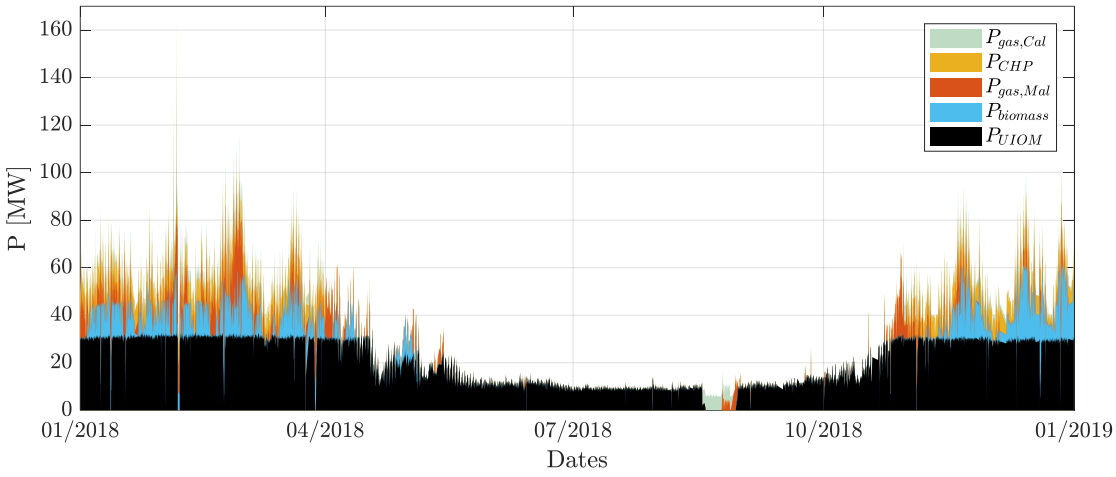

Figure 13: Heat productions times series in both production sites DH (2018)

This project has received funding from the European Union's Horizon 2020 research and innovation programme under grant agreement No 731297.

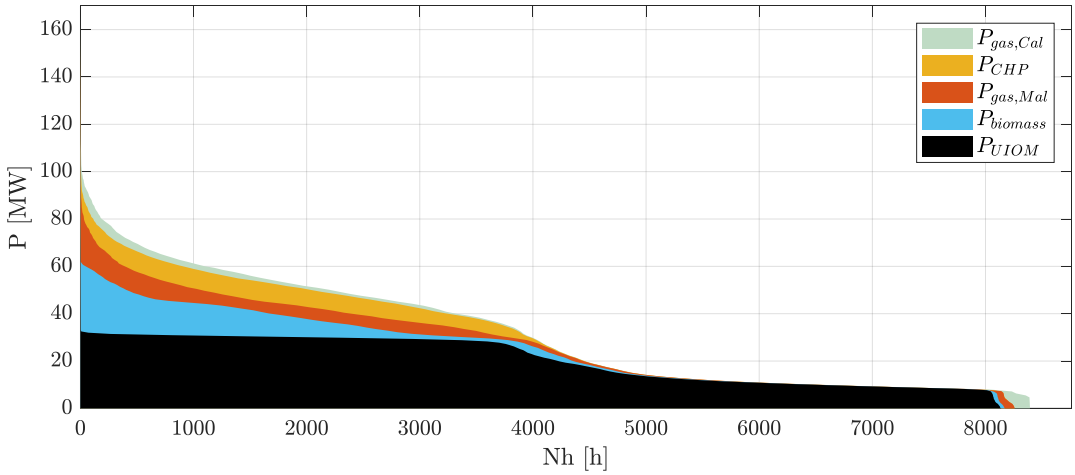

Figure 14: Load duration for in both production site for all the DH (2018)

The Renewable and recovery heat (RES&R) is provided by the incinerator and the biomass boilers. Then, we can deduce the RES&R production rate of the DH from this merit order shown in the time series and the monthly distribution in the Figure 15 and Figure 16 respectively. In particular, it can be seen RES&R cover between 60 % to 80 % of the production during the whole heating season and can reach 100 % in summer (except during the waste incinerator maintenance phases).

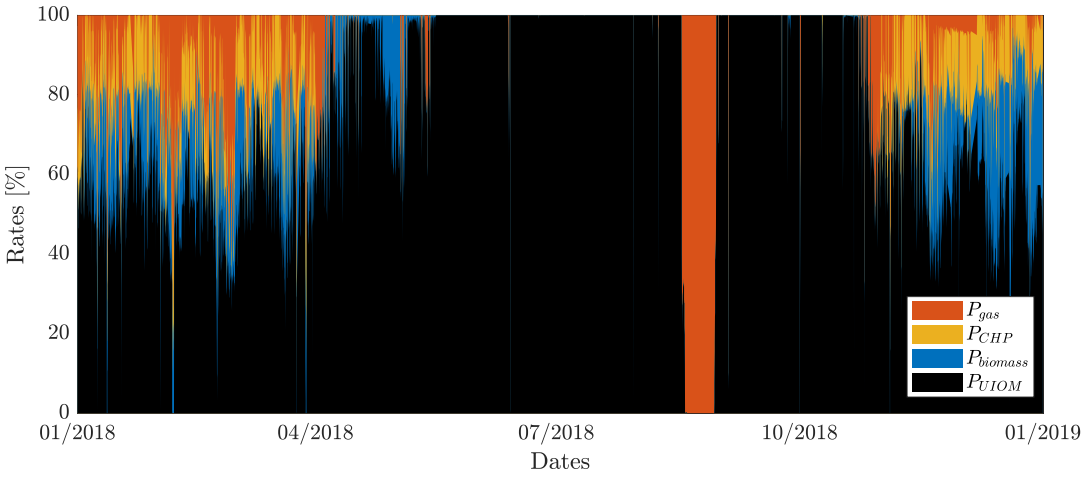

Figure 15: Contribution of each energy system in the production (year 2018)

This project has received funding from the European Union's Horizon 2020 research and innovation programme under grant agreement No 731297.

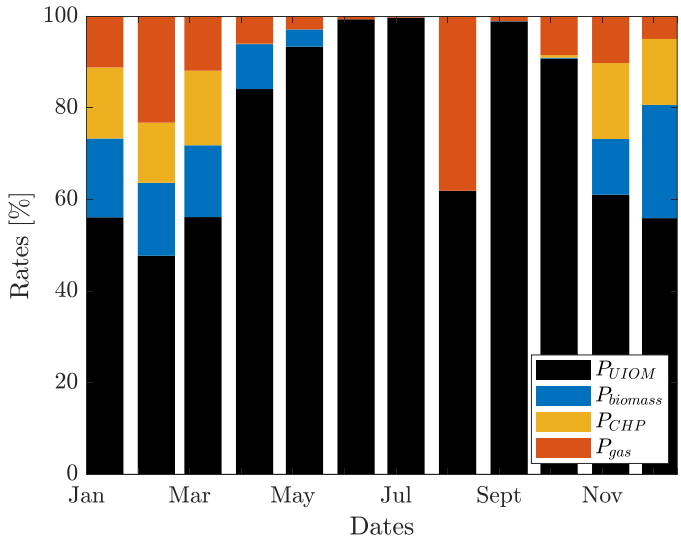

Figure 16: Monthly contribution of each energy system in the production (year 2018)

Finally, the yearly heat production as well as RES&R rates from Malakoff and Californie plants, for the year 2017 & 2018 are given in Table 4. These figures were obtained by summing over the year the hourly heat powers calculated from measured data. The used datasets are uncompleted, whatever the production plants and the considered year. In addition, the periods with no data are not the same from a plant to another, so data processing must be implemented. In our case, a filter excludes the dates when a lack of data is detected for at least one power plant, justifying the samples sizes below the 365 days of a full year. The energy produced was firstly calculated from an incomplete dataset (in brackets in the table) and extrapolated to a full year. We can see the production increased noticeably from 2017 to 2018 due to new clients connected on the DH. However, despite this evolution, the contractual objective of 84 % of the production coming from RES&R is achieved for both years. More than 75 % is provided by the waste incinerator. Due to its constant capacity and the global increase of the production, this ratio naturally decreases in 2018. The rate of RES&R is reached thanks to the biomass boiler contribution.

Table 4: Produced energy and renewable part

Year	Sample [days]	Energy produced [GWh]	Heat rate from RES&R [%]	Heat rate from the waste incinerator [%]	CO_2 emission [10^3 tons]
2017	298	226.6 (185)	83.9	77.4	8.79 (7.18)
2018	350	283.7 (272)	84.0	75.8	10.93 (10.49)

Besides, we can notice the RES&R rate of 2017 is not equal to the 71.2 % mentioned on Nantes Métropole in the activity report on the DH[3]. The difference here can be explained by the data processing. Indeed, we have calculated a

[3] https://www.nantesmetropole.fr

This project has received funding from the European Union's Horizon 2020 research and innovation programme under grant agreement No 731297.

RES&R rate of 69.4 %, closer to Nantes Métropole figure, considering all the data, without our filter. This calculation method is biased since it considers a power plant with no data does not produce and allocates then the value "0 W" of production, what impacts the average. Besides, the difference can be explained by the fact that few small capacity gas boilers are spread on the network and are not taken into account in our estimations. These distributed units can affect the RES&R rate.

Finally, the CO_2 emissions are calculated considering the equation:

$$Q_{CO_2} = E_y(1 - R_{RES\&R}).R_{CO_2} \quad (1)$$

With E_y the annual heat production, $R_{RES\&R}$ the RES&R rate and R_{CO_2} the CO_2 emissions rate[4].

4.2 Position of the action

In accordance with the Figure 1, the improvement of DH performance can relate to three categories of actions linked to the three main components of the DH: Production plants, Distribution and Substations. As it will be detailed later in the document, the actions at the substation can reflect various technical solutions on the HEx, on the energy systems inside the buildings, on their control strategies. Similarly, solutions for the distribution can reflect actions on the temperatures management, pumping effort, high return temperature valorisation… The effect of any of these scenarios could be detected in the indicators presented so far (peak consumptions, merit order, installed capacities, RES&R rate, intensity of consumption per substation, energy losses…). However, depending on the part of the system an action focuses on, the assessment of the proposed action necessitates (needs?) to consider corresponding technical variables before quantifying such macro indicators.

As mentioned previously, the studied area in mySMARTLife project focuses on Ile de Nantes where there are not production plants. In consequence, considering this as an opportunity more than a constraint, in the next sections, the scenarios used to illustrate the proposed methodology belong to actions which impact the distribution part and the substations level. It demonstrates the relevance and the power of a methodology able to analyse any part of the DH system, scalable at the whole network and replicable to other networks, with a good complementarity with usual tools for energy systems management. The different modules/steps of the methodology are illustrated with the use of codes developed by ARMINES without making the whole procedure dependent on them. That is why a section is presented on the existing solutions for replacing any of these modules by existing tools (either commercial or developed by DH operator or the municipality). This reinforces the expected flexibility and the replicability of the outcomes of this action.

In addition to this, the action intends to be connected to other actions in the project, what is done by the coupling with the action 2.5.3 on decision making tool, by the direct link with Urban platform regarding the centralization of monitoring

[4] Here we consider CO_2 emissions only due to gas combustion. Biomass and waste incineration are considered neutral. The CO_2 emission rate for the gas, on the whole cycle from the extraction to the combustion, is $R_{CO_2} = 241$ gCO_2/kWh (http://www.bilans-ges.ademe.fr).

This project has received funding from the European Union's Horizon 2020 research and innovation programme under grant agreement No 731297.

data of the DH system (not done before mySMARTLife) and the potential use of centralized information from modelling actions (e.g. Building stock energy modelling of action 1.4.1).

To ensure the action to be realistic and operational it is necessary to refer to the reality of the DH systems rather than theoretical characteristics or information assumed to be available. That is the reason why the starting point of the methodology corresponds to a data analysis regarding the information embedded in the data and their quality. (availability, errors…). Based on this, solutions for completing the lacking information are proposed to ensure a good representation of the DH.

This project has received funding from the European Union's Horizon 2020 research and innovation programme under grant agreement No 731297.

5. DH monitoring - Data quality

Like presented further in the next section the aim of the action is to propose a methodology coupling data from the monitoring and DH modelling for optimization scenarios assessment. In that view, data extracted from the DH operator's supervision tool are used. Despite a huge effort for monitoring rigorously the most relevant physical value of all the substations, the data quality and availability are unequal depending on the location on the DH and on the considered time span. In addition, some important parts of the distribution systems can be not equipped with sensors despite the importance of the information such a measure could provide (e.g. Temperature and mass flow rates along the main distribution pipes, in the junctions/split of pipes). An overview of the data availability, quantity and quality of *Beaulieu* branch is presented in this section.

Figure 17 shows the data availability (in white) or not available (in black) for different variables, for each of the *Beaulieu* substations. We can observe that all the substations are monitored and supervised: supply and return temperatures ($T_{s,Pri}$ and $T_{r,Pri}$) as well as mass flows $\dot{m}$ in the primary side of the heat exchangers are almost systematically measured so that energy loads E can be calculated. On another hand, other variables such as secondary supply and return temperatures ($T_{s,Sec}$ and $T_{r,Sec}$) or open rate of valves (PID) are usually, but not always available.

The measured data are recorded at 10 or 15 minutes' time steps, so that a huge amount of data are available for manual[5] extraction in *csv* files. Figure 18 shows the number of available data per variable for each substation (coloured scale in the figure). We can see an important disparity of the quantity of available measures from a substation to another, and from a variable to another (from a few 10 to more than $3.5.10^5$ data). Note that energy consumption estimations are always fewer because there are estimated only daily whereas the poor level of availability of other variable is either link to the late date of connection of some substation's to the supervision, or data monitoring fails[6].

[5] The necessary data treatment is not possible for external parties with the DH operator supervision tools as it requires an access which is possible only in the frame and for the time of mySMARTLife project. Thus a centralization of the DH data in the Urban Platform has been initiated in the frame of this action. This will make possible future similar treatment and monitoring from the Urban Platform.

[6] A continuous discussion with DH operator experts helped to identify the explanations for lacking data and/or divergent pattern regarding their evolution in time.

This project has received funding from the European Union's Horizon 2020 research and innovation programme under grant agreement No 731297.

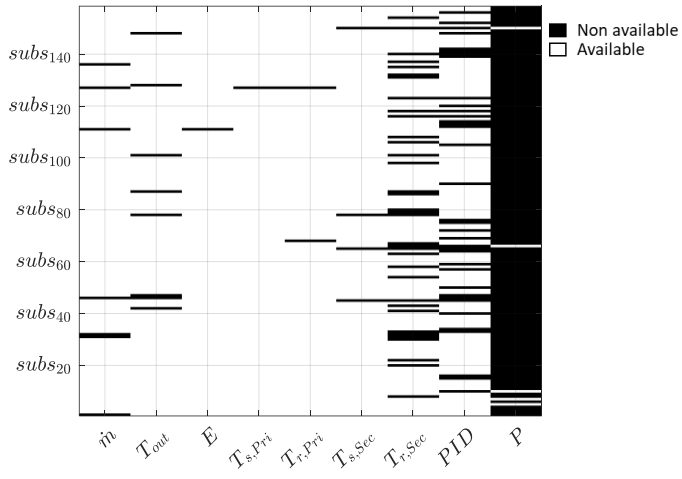

Figure 17: Availability of variables for each substations $subs_i$

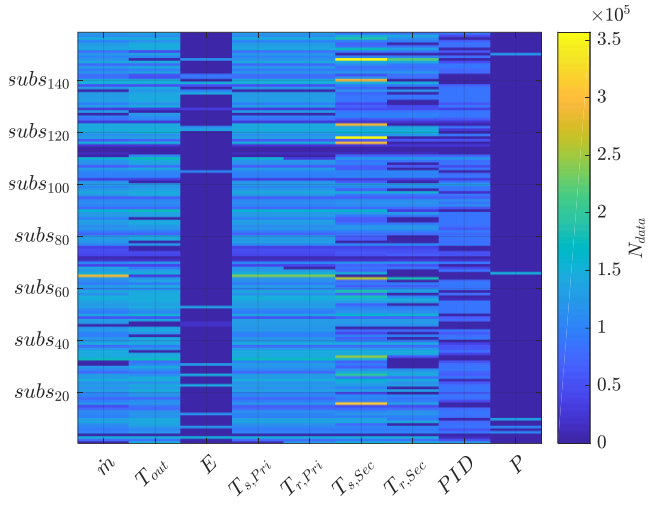

Figure 18: Number of data N_{data} available per variable for each substation $subs_i$

The lack of data for some substations and some variables as well as the disparity regarding their availability has direct effects on the capacity to characterize the DH. The main consequence is the small and sparse overlapping periods meaning when variables are altogether available. Thus, some information such as the thermal power which is calculated with the primary temperatures and the mass flow rate according to equation (2), can be determined only for a few occasional periods (see Figure 19).

$$P = \dot{m} C_p \left(T_{s,Pri} - T_{r,Pri}\right) \quad (2)$$

Figure 19 shows the amount of available data each of the three variables ($T_{s,Pri}$, $T_{r,Pri}$, $\dot{m}$), for each substations (sorted in decreasing order of amount of available data for P), and the amount of common dates where all the variables are available simultaneously (called 'Data Overlap' in the Figure 19). We can observe that for most of the substations, the amount of data for variables alone and the number of overlapping dates are similar. The three variables are, in these cases, always available at the same time so that thermal power are calculable for all the periods. However, there are some substations for which less data are available for a given variable. Then the number of overlapping dates is limited and then less powers can be calculated. Worse, some substations do not record any data for a given variable making the power impossible to be calculated.

This project has received funding from the European Union's Horizon 2020 research and innovation programme under grant agreement No 731297.

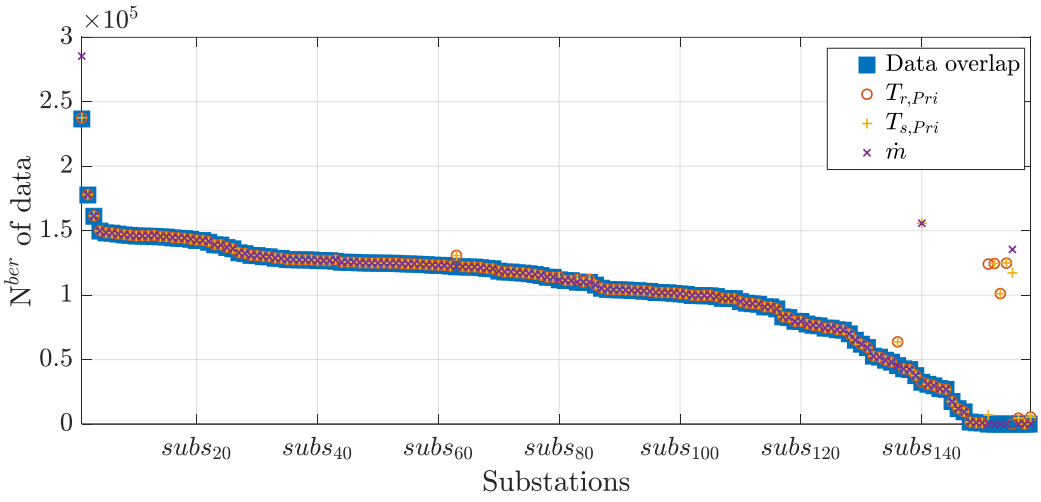

Figure 19: Availability of data for the variables $T_{s,Pri}$, $T_{r,Pri}$, and $\dot{m}$ for each sub-station

The timelines in the Figure 20 show the dates when heat load can be calculated, for each substation. The colour gradient refers to the normalized daily energy consumption that clearly identifies heating and non-heating seasons. We can observe a high disparity of heat load data availability from a substation to another. It is linked to random data losses due to transmission or monitoring issues (e.g. the substations 60 to 80 have hole in the timelines in summer 2016 due to information transmission issues) or to late connection of substations (e.g. substations 140 to 158 which were connected in the middle 2018 or after).

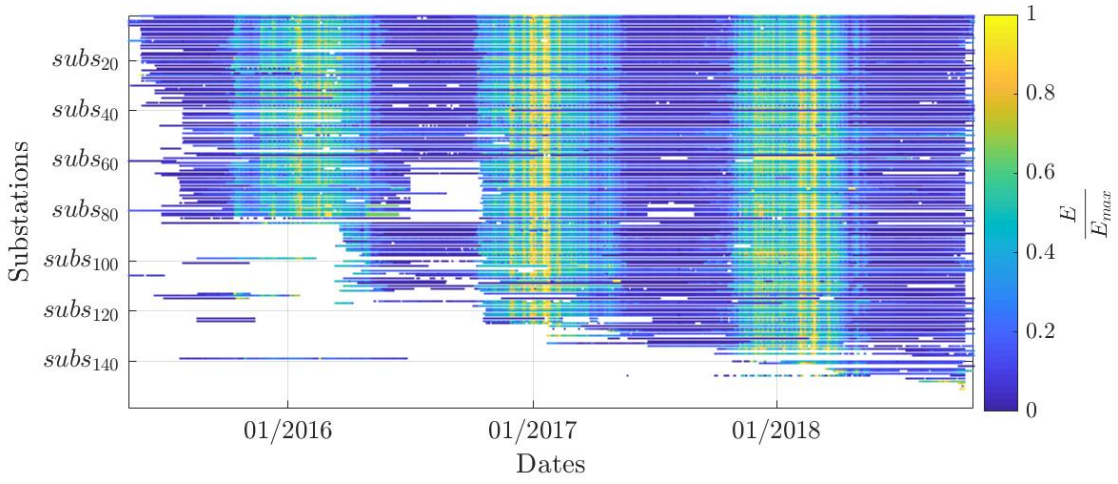

Figure 20: Timelines of heat consumption rates of available measurements

Besides, the disparity of available overlapping dates between the substations strongly limits the periods when powers can be calculated for all the substations simultaneously. Indeed, from this timeline we can deduce numbers of overlapping dates N_d as a function of the number of substation considered N_{subs} i.e the number of days when heat powers can be estimated simultaneously for a given number of substations (Figure 21). We can observe the number of overlapping dates drops when the amount of considered substations increases: from more than 800 days for when

This project has received funding from the European Union's Horizon 2020 research and innovation programme under grant agreement No 731297.

only 20 substations are considered together, to 400 days for sets of substations between 80 and 110, and 0 days when more than 135 substations are considered at the same time.

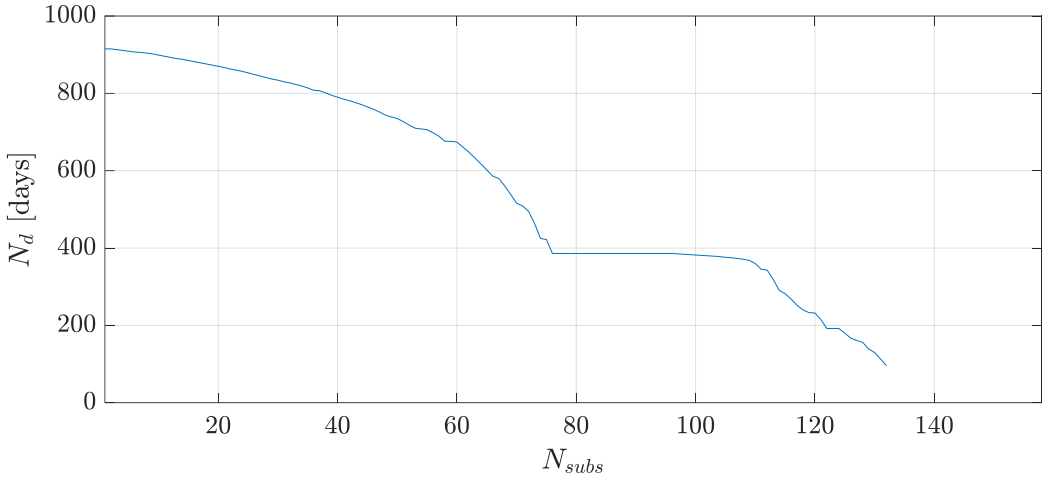

Figure 21: Numbers of overlapping dates N_d for which heat powers can be calculated, as a function of the number of substation

Similarly to the Figure 19, the Figure 22 shows the amount of available measures of $T_{s,Pri}$, $T_{r,Pri}$, $T_{s,Sec}$ and $T_{s,Sec}$. These variables are essential for characterizing the HEx of each substation (see section 6.3.2.1). In many cases at least one variable limits the number of overlapping dates as it presents less measures than the other variable. Thus, in the best cases, 1.5 10^5 data of each variable are measured simultaneously while less than 120 substations of the set have all the four variables available.

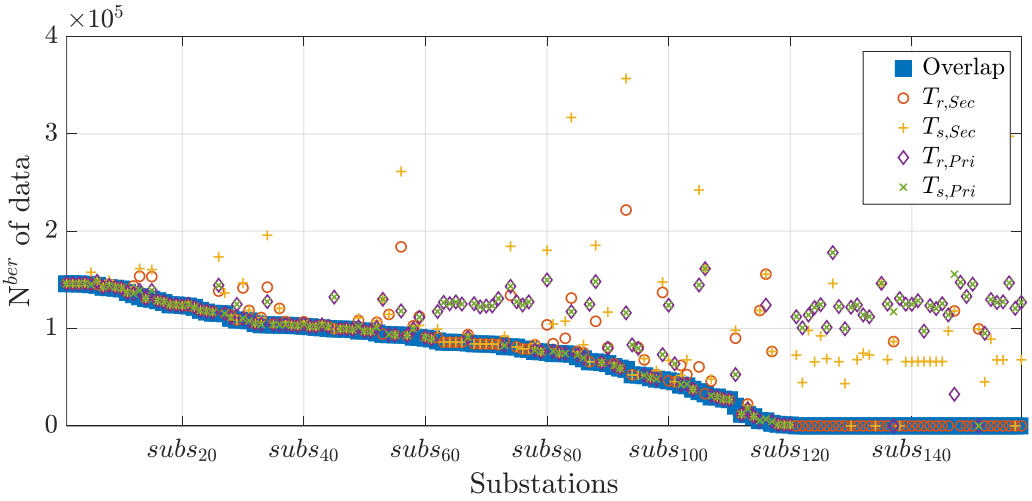

Figure 22: Simultaneous availability of $T_{s,Pri}$, $T_{r,Pri}$, $T_{s,Sec}$ and $T_{r,Sec}$ variables at both primary and secondary side of the HEx

This first data analysis underlines the difficulty to collect useful data for studying the historical behaviour of the DH despite a systematic monitoring of the substations. Some solutions must be then implemented to overcome the partial knowledge of the system (section 6.3.1).

This project has received funding from the European Union's Horizon 2020 research and innovation programme under grant agreement No 731297.

6. Methodology for district heating optimization

6.1 Current challenges

Some general remarks arise from this preliminary analysis of data which gives an idea about the baseline of the existing network. These observations concern essentially the distribution efficiency and the behaviour of the substations. In fact, some general aspects in the measurements give a first idea about the main issue to be tackled. In this section flaws and weaknesses of the actual network are illustrated and their impacts are discussed. Then, some improvements are suggested to enhance the efficiency of the network.

Energy losses in the pipes of a DH, which is of major importance as seen previously, grow linearly with the temperature difference between the ambient/ground temperature and the temperature of the water inside the pipes. For this reason, high-temperature levels in the supply and return pipes cause high energy losses and are indicators of the efficiency level of the network.

In the supply pipes, high-temperature levels are caused by high supply temperatures at the production units' level. It is unavoidable in some cases and it depends on the building's needs/performance. Indeed, buildings equipped with classical heating technologies need high supply temperatures (usually higher than 70°C) compare to buildings equipped with more modern heating technologies (floor heating, HP to raise the temperature level, etc…) for which lower temperatures are compatible with the needs (usually between 40°C and 70°C).

In the return pipes, high temperatures are most of the time caused by high return temperatures of water coming from the buildings (the more the buildings reject water to the return pipe at a high temperature, the higher the mean temperature in the return pipe). High return temperature indicates flaws either in the control of the heating system of the building or the control of the substation which delivers heat to it.

Moreover, high temperatures in return pipes lead to high return temperatures at the level of the production units and alter their efficiencies which is another drawback of high return temperatures.

6.1.1 Return temperature[7]

Low operational temperatures (supply and return) with high temperature differences are important conditions for increasing the efficiency of DH. However, a focus on return temperatures of substations revealed that they used to inject quit high temperatures in the primary return pipe. This is illustrated here with the example of a branch (Figure 24) of the DH located in the East of *Ile de Nantes* subnet (Figure 23).

[7] Results published in *Mabrouk, M.T., Haurant, P., Dessarthe, V., Meyer, P., Lacarrière, B., 2018. Combining a dynamic simulation tool and a multi-criteria decision aiding algorithm for improving existing District Heating. Energy Procedia 149, 266–275. https://doi.org/10.1016/j.egypro.2018.08.191*

This project has received funding from the European Union's Horizon 2020 research and innovation programme under grant agreement No 731297.

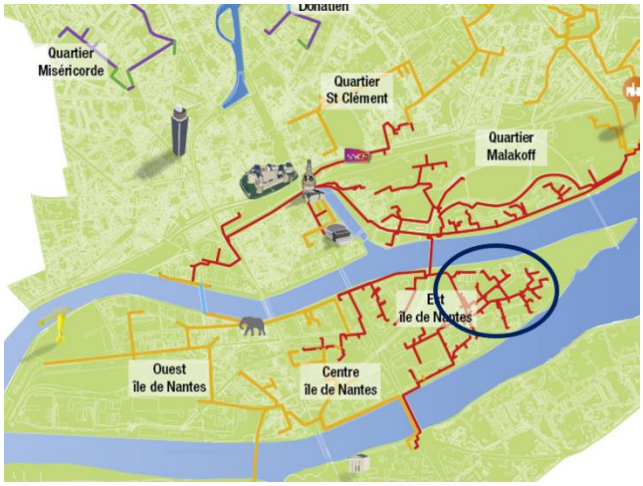

Figure 23: Situation of the studied part of the DH

Figure 24: Map of the substations in *Millerand*

The selected branch topology is presented by an oriented graph in Figure 25. In this oriented graph, the edges represent the supply and return pipes which link the substations represented by vertices.

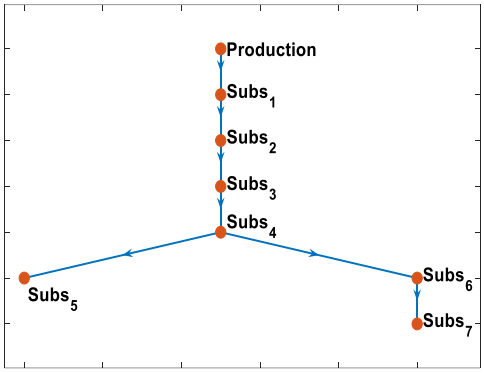

Figure 25: Branch's topology.

Figure 26 show statistics of supply and return temperatures: the squares represent the median of the sample, and the error bars link the first and last quartile of the temperature values..

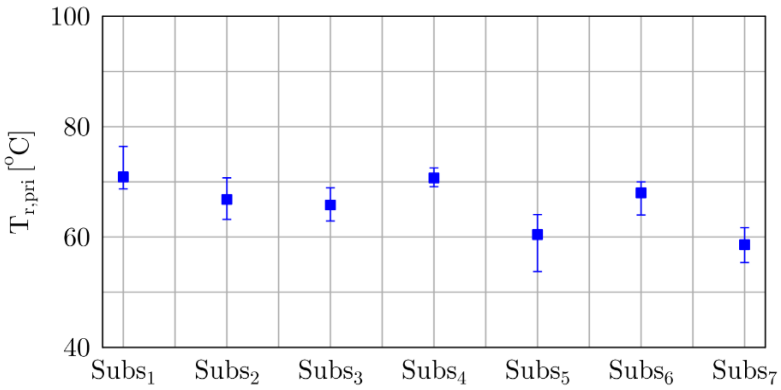

Figure 26: Median and range between first and third quartile of return temperatures $T_{r,Pri}$ in the studied branch.

This project has received funding from the European Union's Horizon 2020 research and innovation programme under grant agreement No 731297.

Here, the return temperatures of most of its seven substations are usually over 60°C: we can observe that the median, 25th and 75th centiles of return temperatures at $Subs_6$, $Subs_4$, $Subs_3$, $Subs_2$ and $Subs_1$ are between 62°C and 75°C. These substations present high potential residual heat in their return pipe to be valorised, and particularly at $Subs_6$

We define the heat recovery potential as the difference between the power in the return pipe of a given substation at its functioning temperature and the power at a temperature of 55°C. Figure 27 shows monthly heat potential statistics at $subs_6$ (in red in the top left corner subfigure) and consumption at substations $Subs_5$, $Subs_4$, $Subs_3$, $Subs_2$ and $Subs_1$ (in blue in the other subfigures). In these graphs, the lines represent median values while the darker coloured areas fill the range between 25th and 75th centiles, and the lighter coloured areas fill the range between 10th and 90th centiles. We can observe on Figure 27 that for the $Subs_6$ the recovery potential heat power varies from 80 kW in the less favourable times (10th centile) to 200 kW in the most favourable ones (90th centiles) in winter months, while the heat consumptions of $Subs_4$, $Subs_3$, $Subs_2$ and $Subs_1$ are always below 100 kW. It suggests that the high amount of heat available on the return pipe after $subs_6$ could be used by the other substations. Any solution is this way could lower the return temperature and then improve the efficiency of a network.

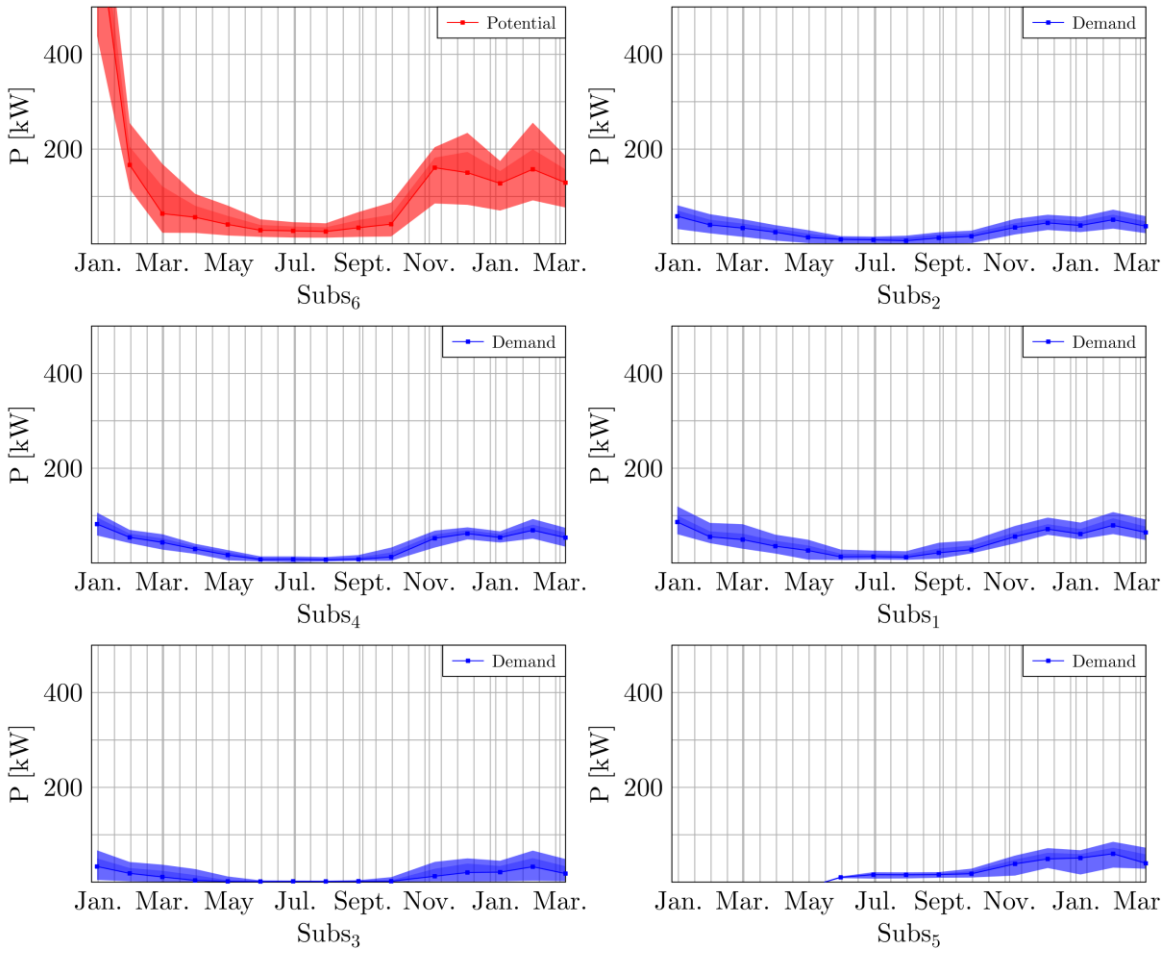

Figure 27: Monthly heat potential at $subs_6$ and heat consumptions at $Subs_5$, $Subs_4$, $Subs_3$, $Subs_2$ and $Subs_1$ (Median and range between first and third quartile)

This project has received funding from the European Union's Horizon 2020 research and innovation programme under grant agreement No 731297.

6.1.2 Supply temperature

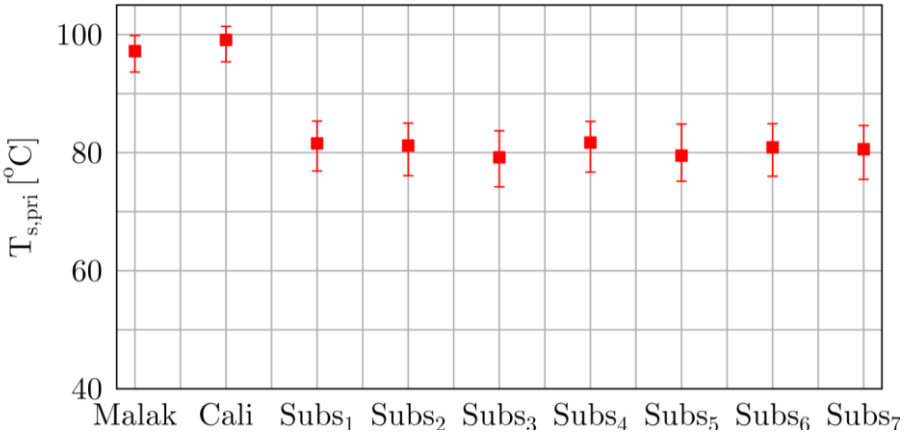

Figure 28: Median and range between first and third quartile of supply temperatures $T_{s,Pri}$ out of the productions (Malak stands for Malakoff plant and Cali for Californie plant) and in the studied branch.

Figure 28 sums up the statics of supply temperatures $T_{s,Pri}$, of the heat production units outlet and in the substations of the branch studied previously. We can observe that $T_{s,Pri}$ out of *Malakoff* and *Californie* are closed to 100°C while they are only around 80°C when the fluid arrives to the substation. These temperatures differences are usually over 20°C. They are due to heat losses during the heat transport in the supply pipes.

6.2 Potential solutions

Many actions could be taken to enhance the performance of the DH in terms of energy consumption, CO_2 emissions and renewable energy share. As seen in section 4, although the DH has an installed capacity of renewable and recovery heat energy of 68 MW (32 % of the total installed capacity), the renewable energy share in the annual energy production reaches 84 %. Added to the discussion about the importance of reducing the losses thanks to a good control of the temperatures, the proposed scenarios will focus on the enhancement of the efficiency of the distribution. In the end, this will allow a reduction of the energy production which can be converted into avoid CO_2 emissions. Based on this preliminary remarks, the energy efficient actions can be undertaken at different levels: the buildings, the distribution (pipes and substations).

6.2.1 Solutions at the building level

At the building level, many actions with different impacts could be taken. Thermal retrofitting of the envelop, for example, will have a direct impact on the heating demand by reducing it. For instance, in France, a building complying with RT2012 standard consumes five times less energy than a building complying with RT2005 standard.

Another type of action at the building's level is the retrofitting of the heating systems such as pipes, circulating pumps, thermostats, heating emitters (radiant or convection radiators, air conditioning systems, floor).

A performant heating system needs also to be efficiently controlled to have the lowest return temperature from the building at the HEx. Keeping a low return temperature is very important because when the return temperature at the

This project has received funding from the European Union's Horizon 2020 research and innovation programme under grant agreement No 731297.

secondary side of the substation is high, the return temperature at the primary side is inevitably high also. The use of variable speed pumps and suitable control of the mass flow rate in the building is primordial to achieve this goal.

Besides, replacing traditional heat emitters by more recent technologies could be considered too. Some proven technologies exist on the market such as underfloor heat emitters or low-temperature heat emitters by using heat radiation to intensify the heat exchange ambient air. These technologies are good candidates and allow to reduce temperature levels of the water flowing in the building.

6.2.2 Solutions at the network level

At the network level, different solutions could be done to enhance the efficiency of heat distribution. For instance, replacing the HEx by bigger ones could drop return temperature in the substations resulting in lower temperature levels in the return pipes. This is only true when the high return temperature is not the result of a high return temperature in the secondary side. In this case, reducing the primary side return temperature cannot be done without actions at the building side.

In France, in most of the cases, the distribution network and the secondary side network are operated by different stakeholders and the DH operator cannot directly proceed to modifications in the secondary side. In this case, as explained before, the high temperature of water flowing in the return pipe could be an interesting source of energy. Connecting some substations to the return pipe could be an interesting solution to harvest this energy (Figure 29) before using the heat from the supply pipe (what would be done as a complement). This allow mixing energy from the supply and the return pipe to feed the HEx. By doing so, a part of the energy will come from the return pipe and the temperature at the inlet of the HEx will drop. However, this temperature drop must be compatible with the buildings connected to the substation and must not cause a drop in the supply temperature at the secondary side of the HEx under the set point (usually a function of the outdoor temperature and fixed by a specific control curve, as it will be seen later). Therefore, the lower the set point temperature, the greater the acceptable temperature drop and the bigger the fraction of water coming from the return pipe. For this reason, using this configuration of the substation could be a good solution to connect low-temperature buildings to actual high-temperature networks.

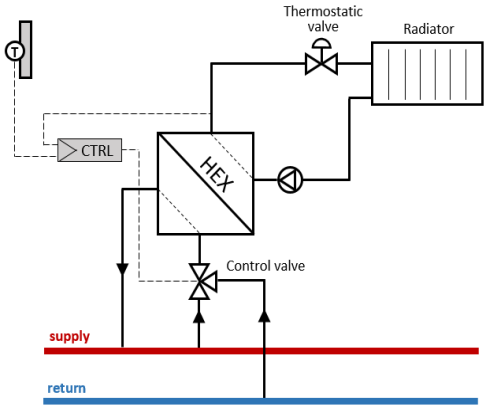

Figure 29 : Scheme of a substation connected to the supply and the return pipe

This project has received funding from the European Union's Horizon 2020 research and innovation programme under grant agreement No 731297.

Another potential solution consists in integrating HP in some substations which allows reducing the temperature level required in the secondary side of the substation without any actions at the building level. This type of modification will reduce also the heat consumption in the substation because part of the heat production will come from electricity grid.

6.2.3 Solutions at the production units' level

At the production level, optimal control of the supply temperature could help reducing energy losses in the pipes. Reducing the supply temperature reduces the temperature difference between the water in the pipes and the outdoor temperature and heat losses from the pipes. Besides, for the same power delivered, the mass flow rate increases when the supply temperature decreases which implies a reduction of the residence time of the water in the pipes and, hence, the distribution energy losses. However, some constraints need to be respected when reducing the supply temperature. Firstly, temperature needs to be high enough for reaching set point temperatures at the secondary sides of all the substations, otherwise the quality of the heating service will be altered. Secondly, mass flow rates must not become too high to avoid pumping energy or even exceeding the capacity of the pumps.

6.3 Overall methodology

Changes in DH systems must be implemented in accordance with multiple Decision Makers (DMs): the DH operator, the clients and the local authority owner of the DH infrastructure. A methodology is then necessary to provide these DMs with the relevant information for selecting alternatives among the various scenarios to improve the system.

The methodology has to be closed to the operational reality, by using real data extracted from different sources such as the Urban data platform (D2.7), 3D models (D1.12) or others. In that view, it needs to be robust as the datasets can be quite partial or unequally complete. Then, the impacts of the improvements have to be assessed by a DH model which will forecast the DH behaviour in the proposed new configurations. Finally, the relevance of different scenarios has to be evaluated, considering technical and non-technical criteria and taking into account the priorities of DMs, using MultiCriteria Decision Aiding (MCDA) tools developed in the framework of mySMARTLife (D2.8).

This project has received funding from the European Union's Horizon 2020 research and innovation programme under grant agreement No 731297.

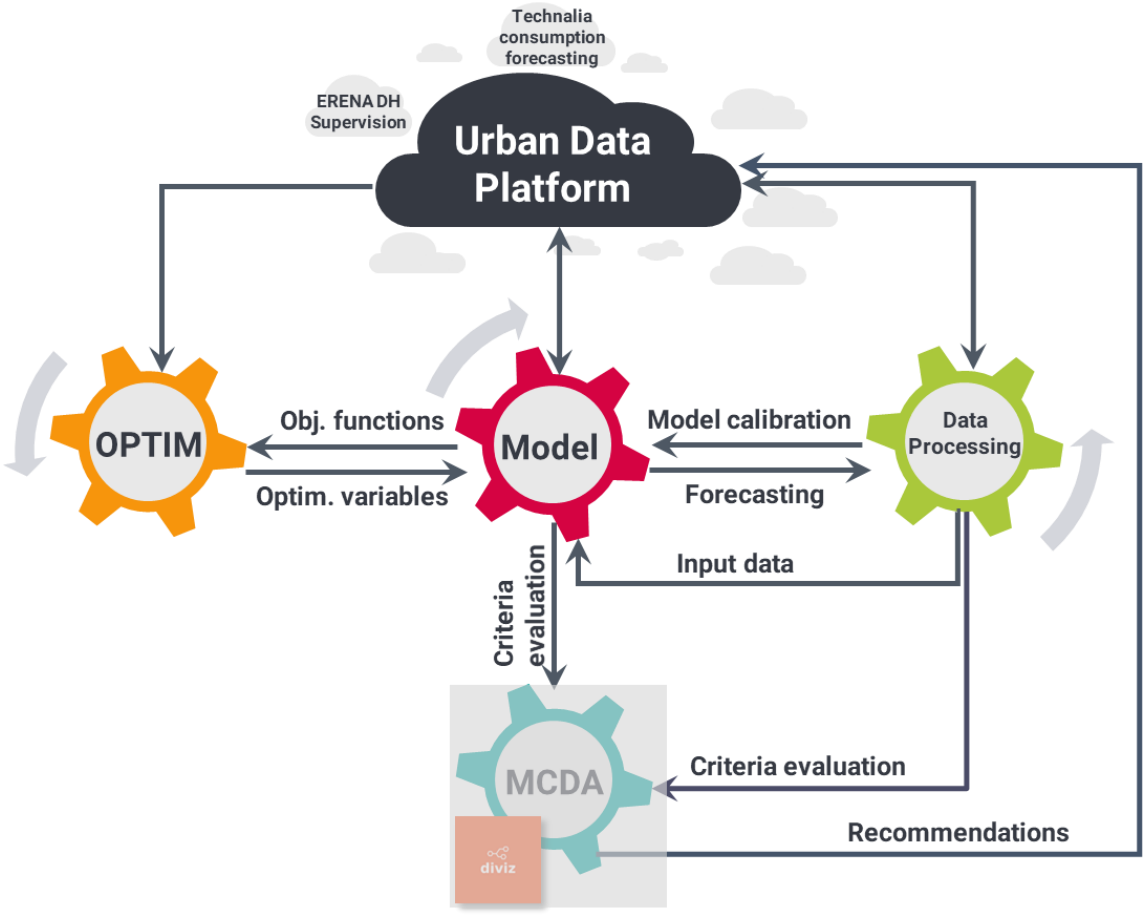

Figure 30: Overall methodology

The Figure 30 shows the systemic methodology which has been developed considering the conditions previously enumerated. The toothed disks illustrate the different processes of the methodology, whereas the arrows show the interaction between the processes.

The idea is the following: relevant data are extracted from the DH supervision tool and collected in the urban data platform[8]. They are processed and used in models as input and for their calibration. Results of simulations obtained from the model provide forecasting which integrates the set of data and can be centralized in the Urban data platform.

Besides, the model can be plugged to an optimization process when the studied scenario requires an optimization step. The optimization variables are defined according to the scenario studied. The model simulates the DH behaviour and evaluate the objective function of the optimization from the set of optimization variables. At the end, the model/optimization coupling provide solutions for an optimized behaviour of the DH.

[8] See footnote 5 of the section 5

This project has received funding from the European Union's Horizon 2020 research and innovation programme under grant agreement No 731297.

Finally, data from the urban platform as well as outputs from models/optimization can be used as indexes for the evaluation of technical criteria of a MCDA algorithm. MCDA gives tools and methods for assisting DMs in reaching a decision when faced with a set of scenario, described via multiple, often conflicting criteria (technical and non-technical). This last layer, highlight in grey in the schema of Figure 30, has been treated as an application case of action 2.5.3 (see D2.8)

In a first step, the overall methodology has been built, implemented and tested on a case study focused on a specific part of the DH named *Millerand*. This branch, located at the east of the Ile de Nantes, is connected to the rest of the DH by a single substation making this branch similar to a DH with a production on the top. This stand-alone part of the DH covers 35 substations for which a continuous and overlapped dataset is available.

6.3.1 Data processing[9]

As seen in the section 0, the use of data from the DH supervision can necessitate some specific processing depending on their use, their availability and quality.

Moreover, the optimization of DH is computationally cost intensive as it requires an important number of simulations, at each time steps, over long periods of time. This issue is a bottleneck clearly identified in the literature. A solution consists in simulating the system with several short time series, representative/typical of the whole period analysed. The challenge is then to define the typology of data supposed to be representative. In that view, a clustering methodology based on k-means algorithm is implemented. Figure 31 shows a diagram of the methodology: daily heat loads energy and variability are characterized from substation heat consumption time series. Then k-means algorithm is implemented, k, the number of clusters, been determined by MCDA. The typical days (TD) are then deduced from the clusters. The impacts of representing the time series with TD on the simulations are finally assessed.

[9] Results presented in *Haurant, P., Mabrouk, M., Lacarrière, B.,2019. Generation of daily load typology for district heating simulation and optimisation.5th International conference on Smart Energy Systems, 9-10 September, Copenhagen, Denmark.*

This project has received funding from the European Union's Horizon 2020 research and innovation programme under grant agreement No 731297.

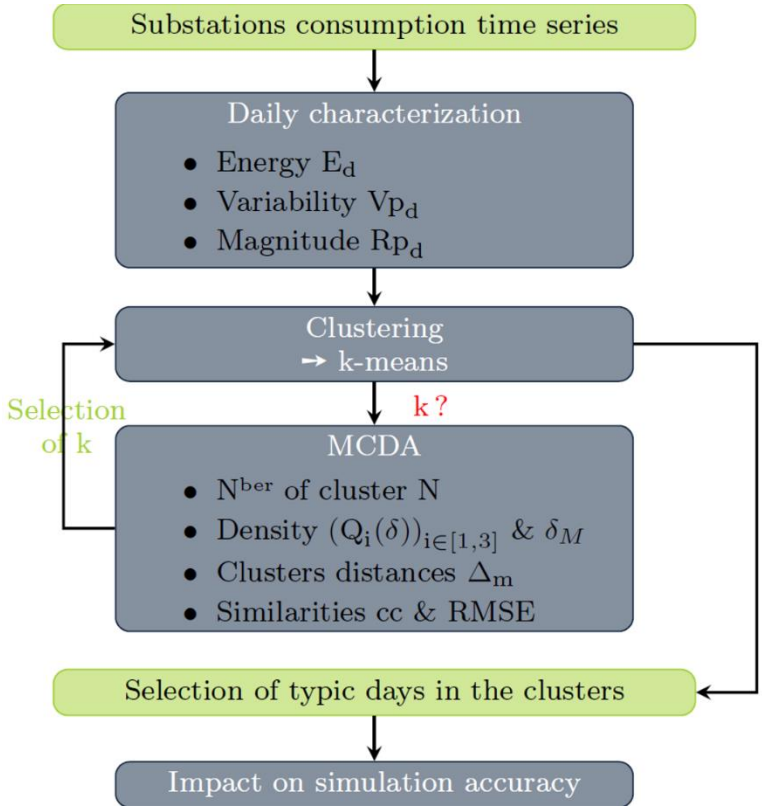

Figure 31: Diagram of clustering methodology for selecting TD

The clustering is realised from aggregated key parameters which characterized the daily behaviour of the loads of the set of substations:

- the daily total energies E_d is the integration of heat power demands $P_d(subs, h)$ in a day:

$$E_d = \sum_{subs} \sum_{h=1}^{24} P_d(subs, h) \,.\, dt \qquad (3)$$

  As we consider hourly heat demands, the integration is equivalent to a sum of $P_d(subs, h)$, with $dt = 1$

- the daily variations is the absolute difference between the heat power at times $h + 1$ and h;

$$V_{Pd} = \sum_{subs} \sum_{h=1}^{23} |P_d(subs, h+1) - P_d(subs, h)| \qquad (4)$$

- the daily maximum range of the variations:

$$R_{Pd} = \max(P_d) - \min(P_d) \qquad (5)$$

The three key parameters are normalized by their respective maximal value over the sample. Graphically, the load days can be represented in a three dimension scatter plot (Figure 32). Daily heat loads draw a cloud of point. The clustering consists in grouping closed point in subsets.

This project has received funding from the European Union's Horizon 2020 research and innovation programme under grant agreement No 731297.

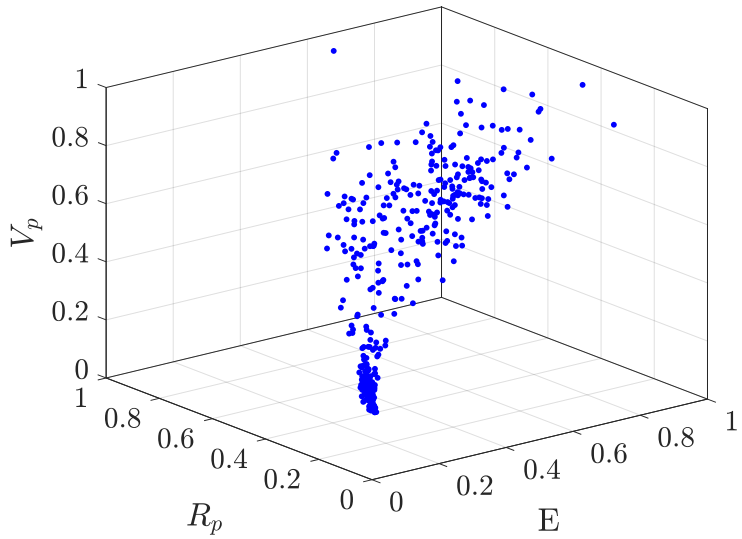

Figure 32: Load days behaviour characteristics (*Millerand*)

The clustering method used here is k-means (Forgy, 1965; MacQueen, 1967). It is the most popular clustering algorithm since it is robust, fast and easy to implement. It determines iteratively k-centroids that minimize a distance function between the centroid and the point of the associated clusters.

The main obstacle for implementing the algorithm is the choice of k, the number of clusters. Numerous methods have been explored for solving this issue (Pelleg and Moore, 2000; Pham et al., 2005). A good clustering allows maximizing the density of the clusters and maximizing the distance from each other at the same time. These two criteria are conflicting since the higher the value of k, the more clusters are drawn, and the more the number of clusters, the denser but the closest from each other they will be. Then a compromise between density and inter-clusters distances must be find. MCDA tools allow solving this kind of decision issues.

Thus, intra-cluster distances which characterise the density of cluster and inter-cluster distances are quantified through 5 indexes:

- $Q_1(\delta)$, $Q_2(\delta)$ and $Q_3(\delta)$ are respectively the first, second and third quartiles of distances between the points of the clusters and the centroids. These indexes characterise respectively the density of the core and the peripherals of the clusters. They have to be minimized.
- $\delta_M = \max(\delta)$ the distance between the farthest point of the cluster and the centroid, ot be minimized
- $\Delta_m = \min(\Delta)$ the minimum distance between centroids of clusters, to be maximized.

On another hand, two other indexes allow evaluating the similarity between daily loads of a same cluster:

- cc the correlation coefficient between days of a cluster to be maximized
- $RMSE$ the difference between days of a cluster to be minimized

This project has received funding from the European Union's Horizon 2020 research and innovation programme under grant agreement No 731297.

Figure 33 shows the trends of these indexes for $k \in [2,10]$. As the k-means method is iterative from a random initialisation, the clusters contents can vary for a same value of k, from a run to another. So, a few runs of the algorithm, with the same value of k have been proceed, leading to differences in the value of the metrics previously defined. We can observe that:

- Error bars are extended for δ_M : the differences between runs for a same value of k are link to the integration or not of farthest points to the clusters.
- $Q_1(\delta)$, $Q_2(\delta)$ and $Q_3(\delta)$ present same trends, with drops for $k \in [2,4]$. and then a step for $k \in [5,10]$.
- Δ_m drops for $k \in [2,4]$ and evolve for $k \in [5,10]$

These trends confirm the conflicts between the criteria. Besides, they are not discriminant since they do not allow selecting the clustering easily. This two reasons justify the need of MCDA.

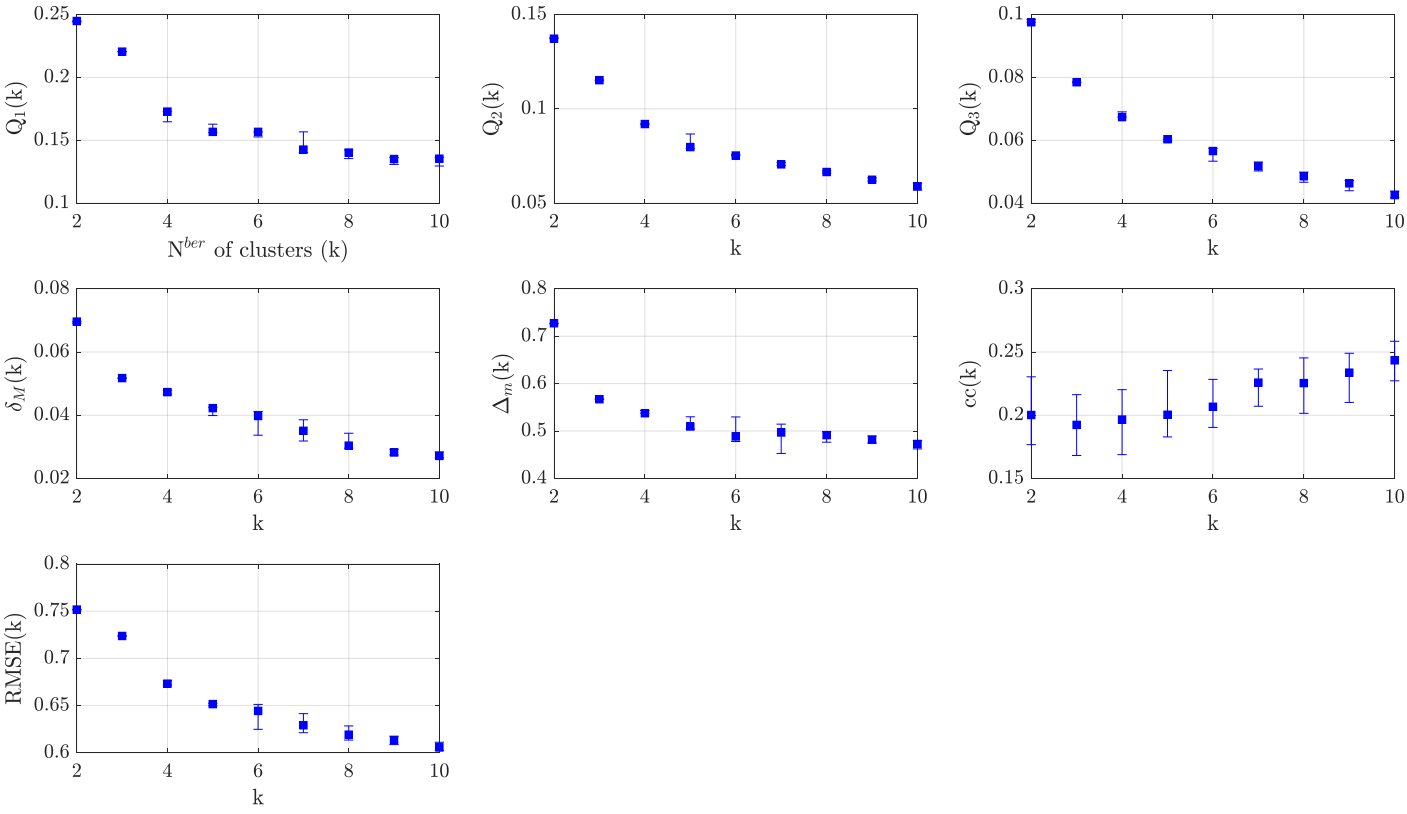

Figure 33: Indexes value for k ∈ [2,10]

The previous indexes define the set of criteria, completed by the number of clusters since it is necessary to reduce the computational time. A so-called performance table sums up the evaluation of each alternative (the clustering). Then, an outranking based MCDA algorithm compiles this table by comparing alternatives by pair. This method relies on a majority principle: an alternative is considered at least not less good than another if a majority of the criteria verifies it.

This project has received funding from the European Union's Horizon 2020 research and innovation programme under grant agreement No 731297.

The preference situation between alternatives, from insignificance to strict preference are determined by considering indifference and preference thresholds. These last allows discriminating the alternatives.

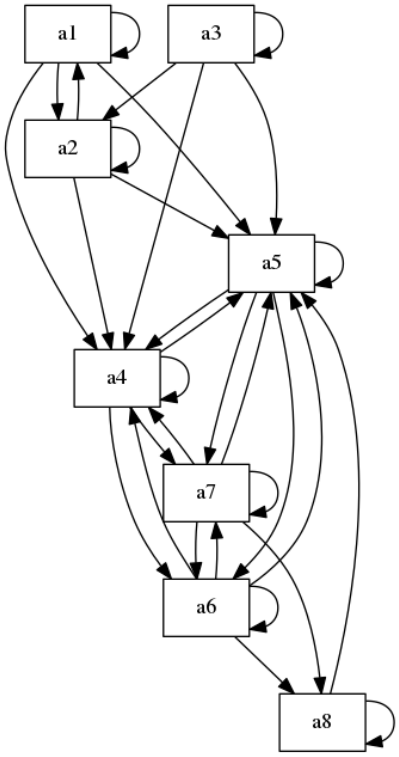

Figure 34: Outranking oriented graph

The MCDA algorithm leads to an outranking oriented graph (Figure 34) where nodes are the alternatives and arrows show the outranking relationships. The kernel groups the set of alternatives that cannot be exclude from the selection. In our case, it is composed with a_3 and a_7 but we can see in the oriented graph that a_3 for $k = 5$ only outranks the alternatives without being outranked, justifying the selection of $k = 5$.

Yet, the obtained clustering from data from *Millerand*'s DH subpart are presented in Figure 35:

This project has received funding from the European Union's Horizon 2020 research and innovation programme under grant agreement No 731297.

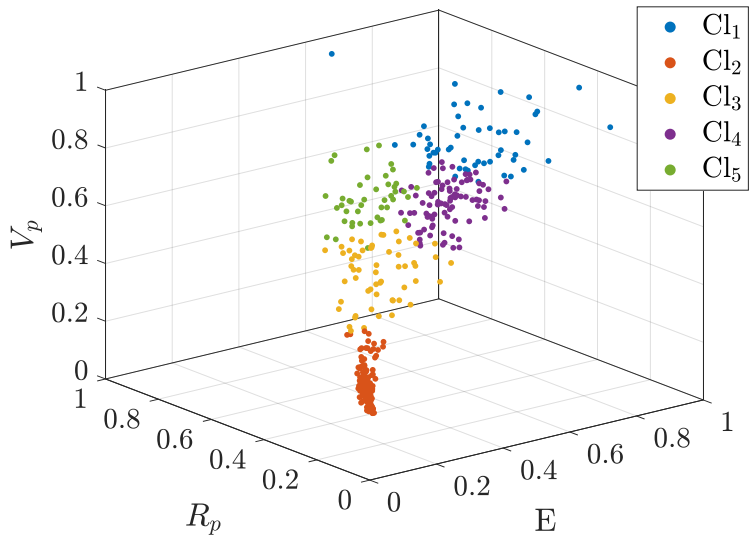

Figure 35: Clusters (*Millerand*)

We can see that the cluster Cl_2 groups summer days with low energy consumption, variability and range. Cl_5 and Cl_3 show medium energy and respectively more or less variation, and finally, Cl_1 and Cl_4 groups days with the higher energy consumption and more or less variations.

The TD are then extracted from the clusters. The idea is to select the real days which are the nearest from the centroids of the clusters instead of using the centroids themselves. Thus, the TD are made of real powers, with a real date so that it is possible to get data of other variables such as outdoor temperature, secondary temperatures etc., for the date of the TD.

Figure 36 shows all the days' loads times series of each cluster, with all the substations in a row and the associated TD. We can confirm the characteristics of each cluster, in terms of energy consumed and variability: Cl_2 groups days of low energy consumption, Cl_3 and Cl_5 group days with medium and respectively low and high variability, and Cl_1 and Cl_4 group high energy consumption days, Cl_1 been less variable than Cl_4.

We can also observe that the days grouped in each cluster present similar patterns and are different to days of other clusters. Finally, we can check that the extracted TD are representative of the days within the associated cluster.

This project has received funding from the European Union's Horizon 2020 research and innovation programme under grant agreement No 731297.

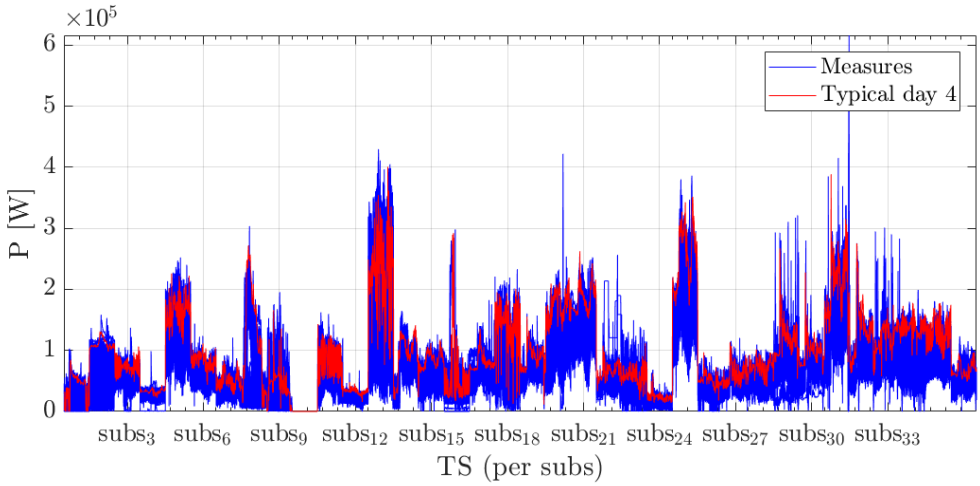

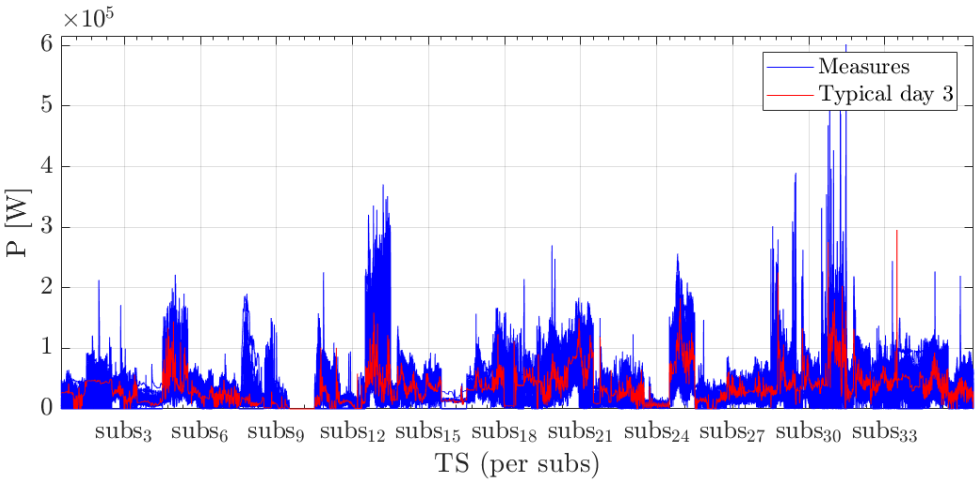

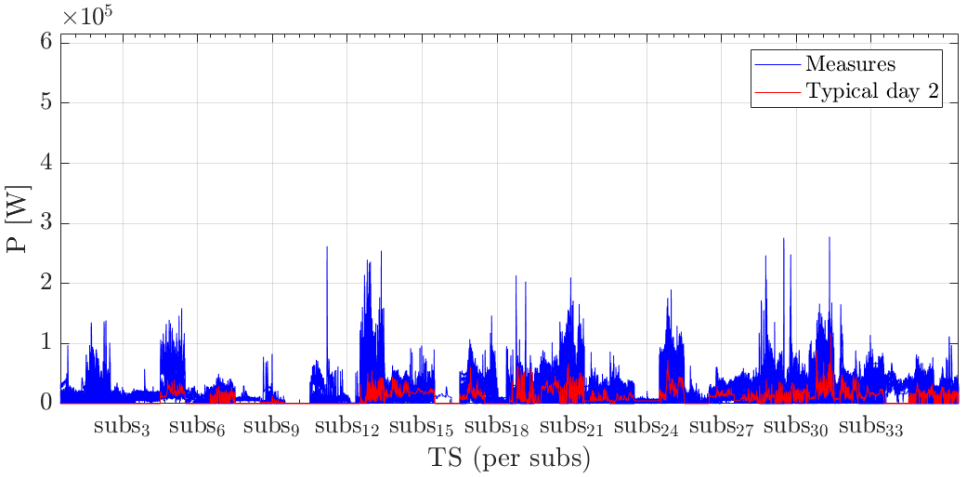

This project has received funding from the European Union's Horizon 2020 research and innovation programme under grant agreement No 731297.

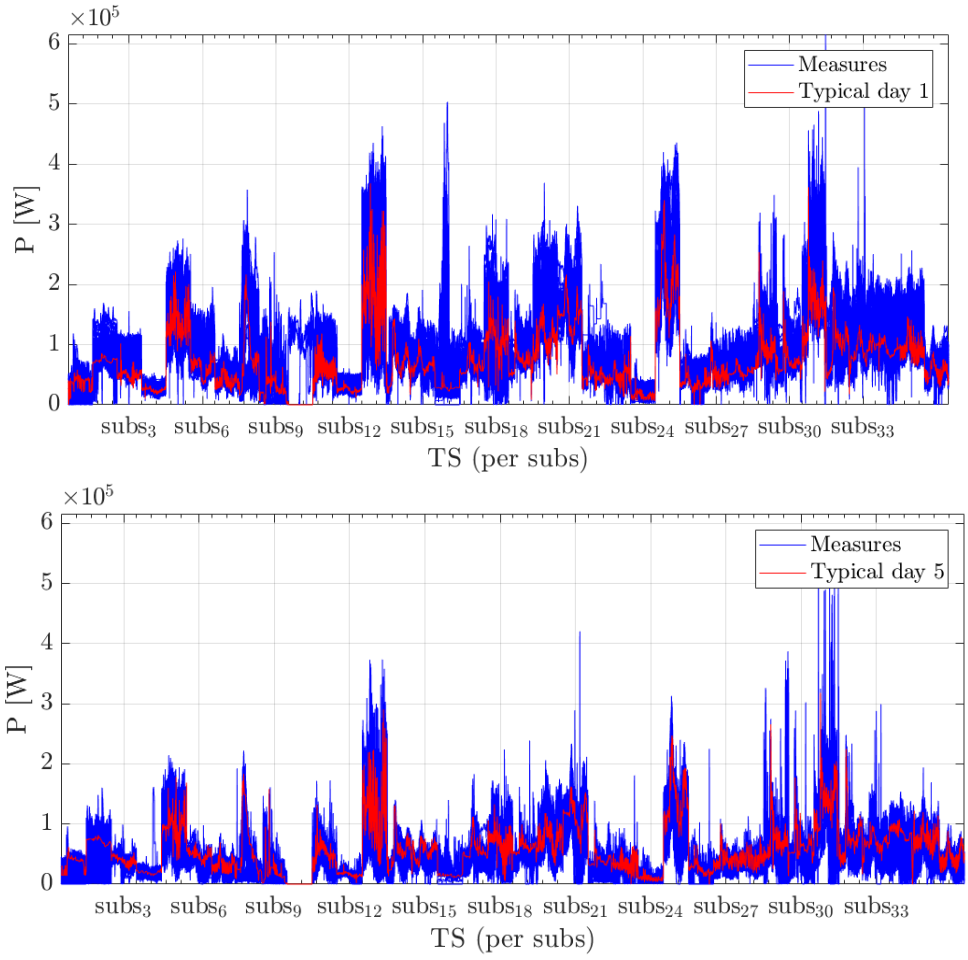

Figure 36: Days' loads times series of the clusters, with all the substations in a row and the associated TD.

A post-selection validation has been proceeded by comparing the measured time series of some variables to a generated time series from TD of the same variable, with different number of TD N_{TD}.

This project has received funding from the European Union's Horizon 2020 research and innovation programme under grant agreement No 731297.

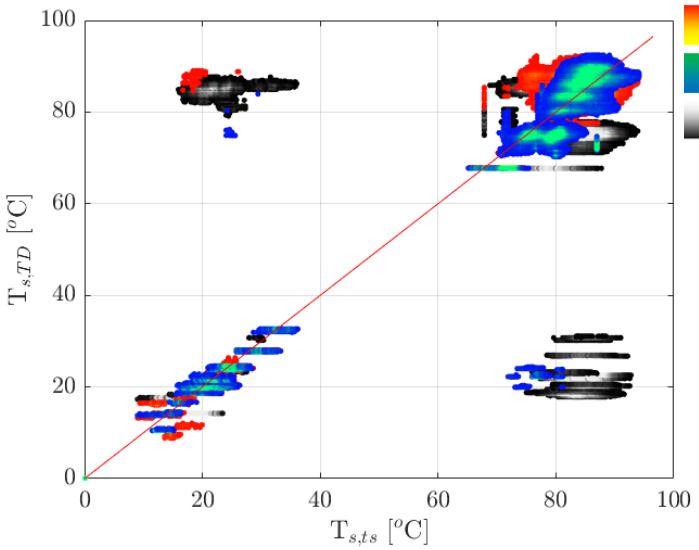

Figure 37: Supply temperatures time series generated from TD against supply temperatures time series from measurements in x-y scatter plots. The gradients of colours show the density of points.

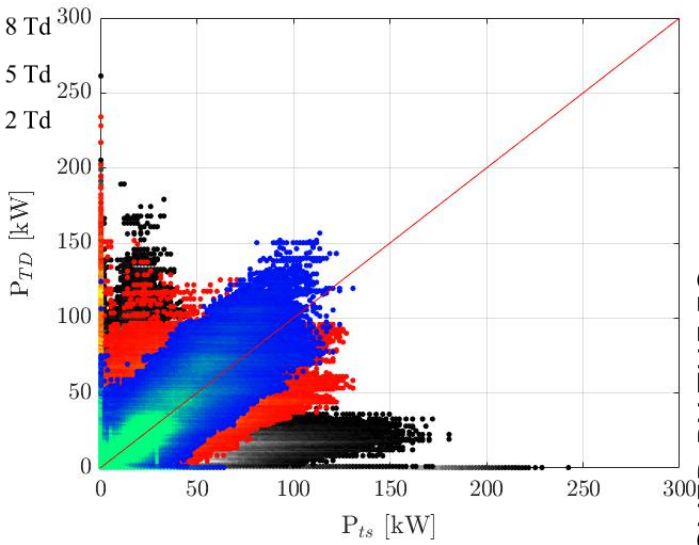

Figure 38: Heat power time series generated from TD against heat power time series from measurements in x-y scatter plots. The gradients of colours show the density of points.

Figure 37 and Figure 38 show x-y scatter plots of respectively supply temperature and power. We can observe that:

- Four clouds of points are visible on supply temperature x-y plot for 2 TD and 8 TD (Figure 37). Two of them follow the bisector showing a good concordance between the measures and the time series generated from TD. On the other hand, the two other clouds are far from the bisector: they illustrate periods when the supply temperatures generated from TD are at 20°C while the measured one are at 80°C and vice versa. For this clustering, at these periods there are confusion between heating and non-heating season. These confusions are more marginal with 5 TD.
- For powers times series, the clouds of points are more tightened on the bisector for 5 TD than for 2 TD and 8 TD (Figure 38)

From these observations we can deduce that the generated time series from 5 TD fits better the measured time series than 2 TD and 8 TD. These conclusions are not obvious *a priori* since it would be reasonable to think that the more there are TD, the better the time series would be fitted.

Now these first results can be generalized for all $N_{TD} \in [2,10]$. Figure 39 and Figure 40 show the boxplots of differences between measured and generated time series, respectively for power and supply temperatures. They show the dispersion of the differences

This project has received funding from the European Union's Horizon 2020 research and innovation programme under grant agreement No 731297.

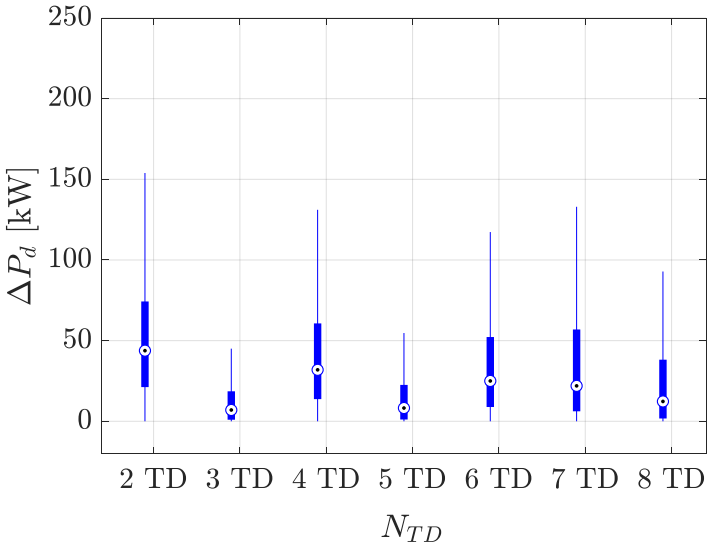

Figure 39: Boxplots of differences between load times series generated from TD and measured loads, as a function of the number of TD N_{TD}

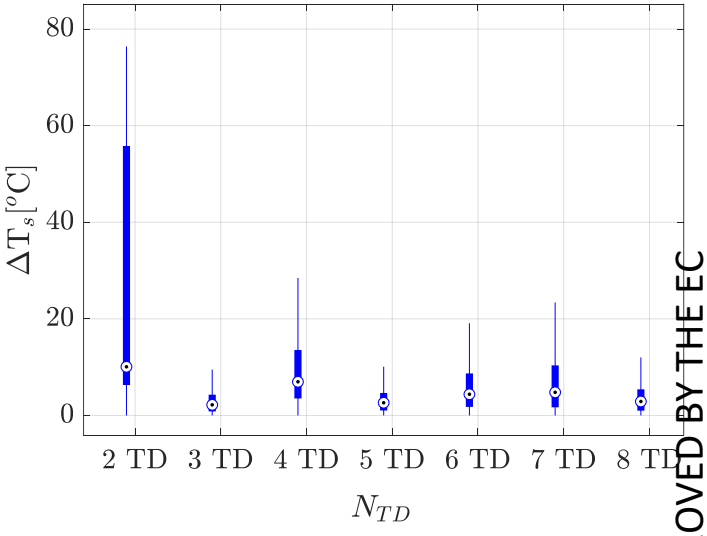

Figure 40: Boxplots of differences between supply temperatures times series generated from TD and measured supply temperatures, as a function of the number of TD N_{TD}

We can see that the differences are less dispersed for 3 TD and 5 TD than for the other value of N_{TD}. For example, for these two cases, the maximum difference achieves 15°C and half of the errors are below 8°C while the maximum difference is over 75°C and half of the differences are over 15°C for 2 TD. These figures confirm our choice. Using 5 TD has a smaller impact on the data of the studied variable.

In a next step (section 6.3.3), the impact the clustering can have on the output of simulations needs to be analysed.

6.3.2 District heating modelling

Modelling is an important step for understanding the behaviour of DH and for predicting the effect of the actions for enhancing the performance of the system. The main idea is to set up models able to reproduce as precisely as possible the behaviour of the real systems which constitute the DH. Models must also calculate different types of indicators to measure the expected impacts of each action. Testing the actions in the modelling environment is a cheap and fast solution to decide if the action is worth to be implemented in the real world.

For large systems like DH, having models that produce results with an acceptable accuracy and reasonable computing times is an absolute prerequisite to realize this decision process.

This section is dedicated to the modelling of the systems constituting DH including heat sources, substations, consumers and distribution networks. The first subsection draws an overview of existing tools and software for DH's simulation and planning. The second subsection focuses more on theoretical aspects and deals with the different mathematical approaches used to model DH systems. The next two subsections are dedicated to the Nantes' DH case and show how the models are calibrated to reproduce the behaviour of a real installation and what type of simulation results we can produce using the calibrated models.

This project has received funding from the European Union's Horizon 2020 research and innovation programme under grant agreement No 731297.

Modelling all the components of the DH is an important step to develop simulation tools which can reproduce accurately the real behaviour of such systems. These components are Heat production plants, distribution network and the consumers. Different modelling approaches are used to model these components:

6.3.2.1 Substation's HEx modelling

When the mass flow rates and inlet temperatures are known in both primary and secondary side in the HEx, outlet temperature can be calculated using the NTU method.

The HEx is defined by its dimensionless effectiveness which is a dimensionless and defined as:

$$\epsilon = \frac{\dot{Q}_{actual}}{\dot{Q}_{max}} \quad (6)$$

Where $\dot{Q}_{actual}$ is the heat transferred in the HEx. Under adiabatic conditions, this transferred heat is the same in both sides of the HEx:

$$\dot{Q}_{actual} = \dot{m}_p c_{p_p}(T_{ps} - T_{pr}) = \dot{m}_s c_{p_s}(T_{ss} - T_{sr}) \quad (7)$$

Where $\dot{m}_p$ and $\dot{m}_s$ are the mass flow rates in the primary and secondary sides of the HEx, T_{ps} and T_{pr} are supply and return temperatures in the primary side, T_{ss} and T_{sr} are supply and return temperatures in the secondary side and c_{p_p} and c_{p_s} are heat capacities of the primary and secondary exchange fluids.

The maximum heat that can be transferred in the HEx is actually the amount of heat needed to realize a temperature change equal to the maximum temperature difference in the HEx. The fluid that can realize this temperature change is the fluid that has the minimum $\dot{m}c_p$ value:

$$\dot{Q}_{max} = (\dot{m}c_p)_{min}(T_{ps} - T_{pr}) \quad (8)$$

The actual heat transfer is then equal to:

$$\dot{Q}_{actual} = \epsilon(\dot{m}c_p)_{min}(T_{ps} - T_{pr}) \quad (9)$$

The number of transfer units is defined as:

$$NTU = \frac{U_{global}A}{\dot{m}c_p} \quad (10)$$

Where U_{global} the global heat is transfer coefficient and A the heat exchange area of the HEx. We define also the ratio R as:

$$R = \frac{(\dot{m}c_p)_{min}}{(\dot{m}c_p)_{max}} \quad (11)$$

The effectiveness of the HEx is given by:

This project has received funding from the European Union's Horizon 2020 research and innovation programme under grant agreement No 731297.

$$\epsilon = \frac{1 - e^{-NTU(1+R)}}{1+R} \quad (12)$$

For a plate geometry, the global heat transfer coefficient can be obtained by:

$$U_{global} = \left[\frac{1}{\alpha_p} + \frac{1}{\alpha_s} + \frac{e}{\lambda} + R_{fp} + R_{fs}\right]^{-1} \quad (13)$$

Where α_p and α_s the convection heat transfer coefficients at the primary and secondary sides, e the thickness of the wall between the two streams, λ the conductivity of the wall's material and R_{fp} and R_{fs} are fouling thermal resistances for the primary side and the secondary side. Fouling is caused by the impurities carried by the fluid that are deposited on the surface and form an additional layer between the fluid and the heat exchange surface.

The heat exchange coefficient in both sides of the vary as a function of the mass flow rate of the fluid and this variation can be expressed as:

$$\frac{\alpha_k}{\alpha_{k0}} = \left(\frac{\dot{m}_k}{\dot{m}_{k0}}\right)^{c_1} \quad (14)$$

Where $k = p$ for the primary side $k = s$ for the secondary side, α_0 and $\dot{m}_0$ are the heat exchange coefficient and the mass flow rate at nominal conditions and c_1 is a constant.

At nominal operation the nominal power can be expressed as:

$$P_0 = \dot{m}_{p0}(T_{ps0} - T_{pr0}) = \dot{m}_{s0}(T_{ss0} - T_{sr0}) = U_{global}.A.\Delta T_{lm} \quad (15)$$

The model needs to be calibrated using actual data to reproduce the behaviour of the real system. This calibration consists of tuning some of the model's parameters to minimize the deviation between the model outputs and real data. Two cases arise, then, depending on data availability from the supervision:

- **When all temperature measurements are available**

In this case, the deviation between the actual and modelled values of the secondary side supply temperature is minimized. Input data of the model are the supply and return temperatures, the mass flow rate in the primary side and the return temperature in the secondary side. Data used to calibrate the model need to be physically feasible. For this reason, it is filtered by deleting the time steps where the return temperature at the secondary side is lower than the return temperature in the primary side and the time steps where measured heat rate in the HEx is greater than the maximum possible heat rate. Figure 41 shows the amount of raw and filtered data for each substation. In total there are 103 substations in *Beaulieu* DH for which all the temperatures are available.

The effect of the thermal conductivity of the wall and fouling resistances are automatically integrated to the heat exchange coefficient thanks to the calibration process which uses real data. Hence, tuned parameters for this case are: $P_0, \Delta T_{p0}, \Delta T_{s0}, \Delta T_{lm}$, and α_0 and c_1 for both sides (primary and secondary) . The number can reduce by setting typical values for α_0 (which gives good results) and by fixing some parameters of the HEx when available.

This project has received funding from the European Union's Horizon 2020 research and innovation programme under grant agreement No 731297.

Figure 42 to Figure 45 illustrates the results of this calibration with the example of four substations. It shows the good agreement between simulated and measured data.

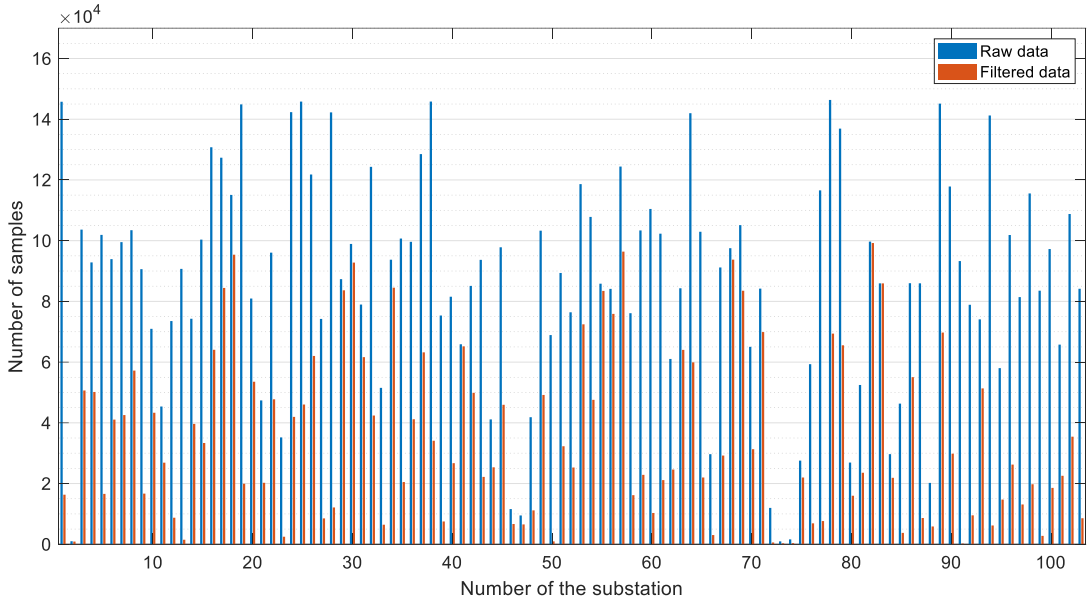

Figure 41: Number of samples in the raw data and the filtered data after eliminating negative power and physically infeasible points (data outliers)

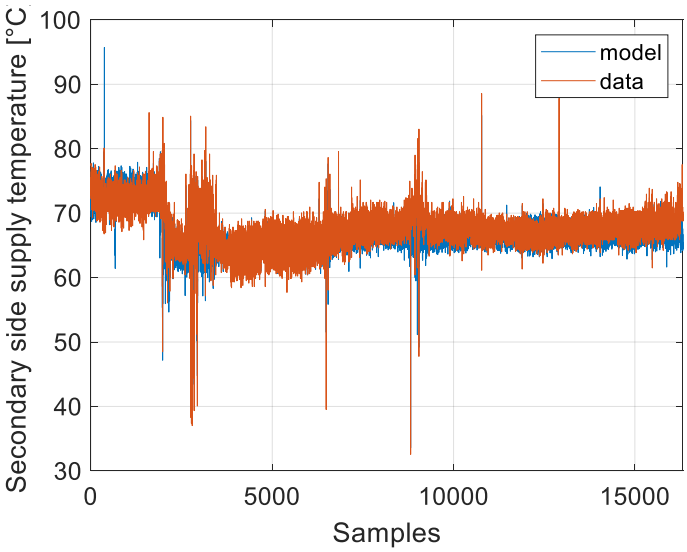

Figure 42: Secondary side supply temp. predicted by the calibrated model vs actual data (substation : *AC1*)

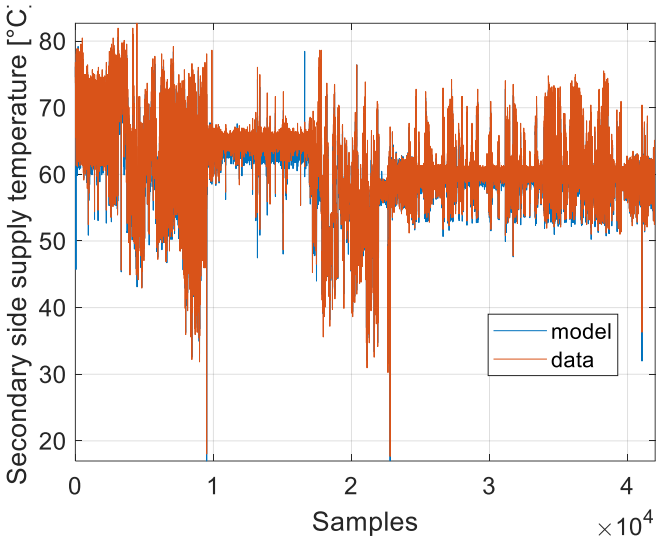

Figure 43: Secondary side supply temperature predicted by the calibrated model vs actual data (substation : *CPAM*)

This project has received funding from the European Union's Horizon 2020 research and innovation programme under grant agreement No 731297.

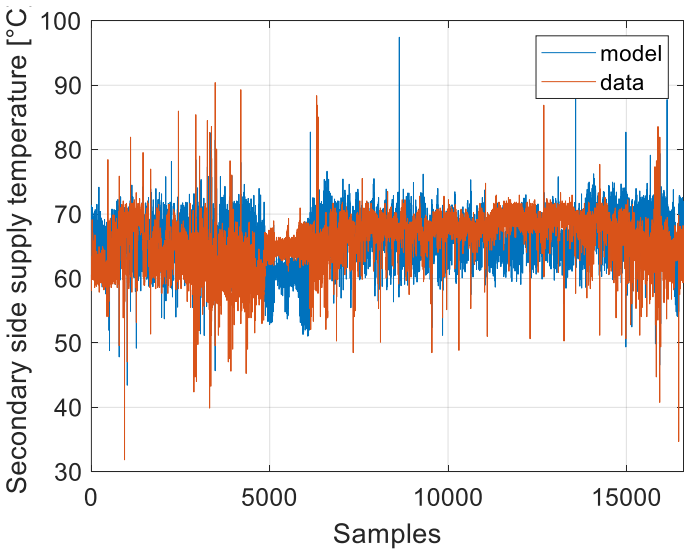

Figure 44: Secondary side supply temperature predicted by the calibrated model vs actual data (substation : *Aimé Césaire*)

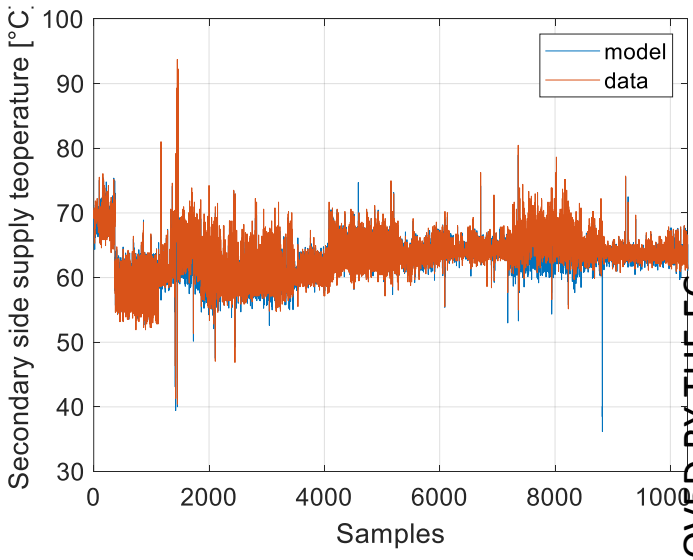

Figure 45: Secondary side supply temperature predicted by the calibrated model vs actual data (substation *MAN*)

- **When temperature measurements are available only for the primary side**

In this particular case, the deviation between the simulated and measured primary side return temperature is minimized to calibrate the model. The secondary side return temperature becomes then an additional parameter to be tuned instead of being an input variable. Figure 46 and Figure 47 show the output of the calibrated models against measured data. The figures show acceptable agreement for a certain range of return temperature. However, the model is unable to reproduce correctly the behaviour of the substations when the primary side return temperature drops under the value of the secondary side return temperature resulting from the calibration process. This shows clearly the importance of data availability in the calibration process and its impact on the accuracy of the prediction.

This project has received funding from the European Union's Horizon 2020 research and innovation programme under grant agreement No 731297.

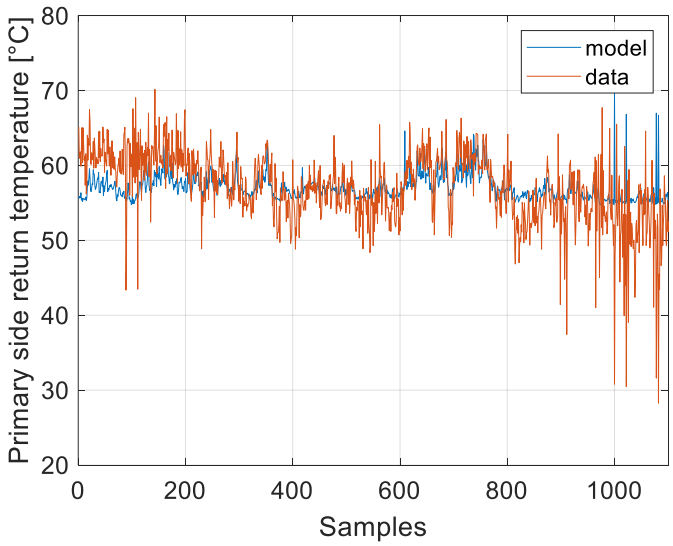

Figure 46: Primary side return temperature predicted by the calibrated model vs actual data (substation : *Fongecif*)

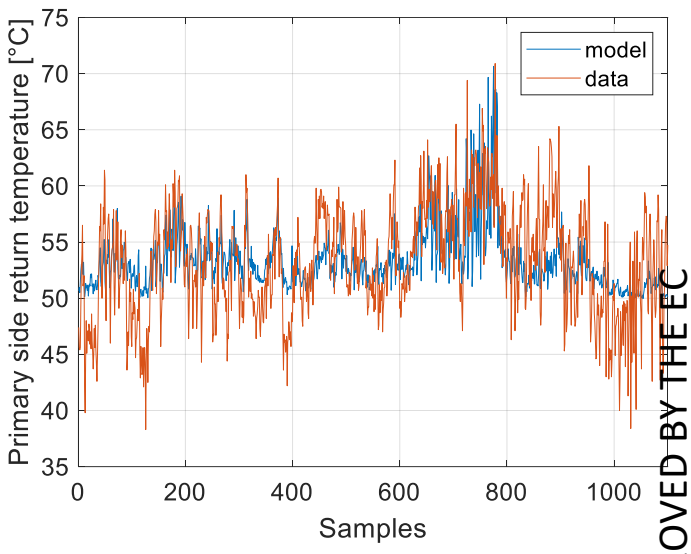

Figure 47: Primary side return temperature predicted by the calibrated model vs actual data (substation : *Clos Pergeline*)

6.3.2.2 Distribution model

As mentioned before, the DH is modelled by an oriented graph where each edge represents two pipes (supply and return) and nodes represents either production units or consumer substations. The model used in this paper is based on a thermal and hydraulic modelling of pipes, nodes and HEx at each node.

- Hydraulic model

Assuming the water flow throughout the pipes to be incompressible with constant properties, the head drop through a pipe connecting a node i to a node j can be expressed by:

$$H_j - H_i = k_{ij}\dot{m}_{ij}|\dot{m}_{ij}| \quad (16)$$

Where H_i and H_j are hydraulic heads at nodes j and j, $\dot{m}_{ij}$ is the water mass flow rate in the pipe and k_{ij} is a coefficient given by the Darcy-Weisbach equation:

$$k_{ij} = \frac{8L_p f}{gD_p^5 \rho_w^2 \pi^2} \quad (17)$$

where L_p, D_p, ρ_w and f are respectively the length and the diameter of the pipe, water density and the Darcy friction factor which is calculated using the usual correlations for laminar and turbulent flow regimes.

The mass flow balance in each node is given by the equation:

$$\sum_{j\in\{\mathrm{Pr}(i)\}} \dot{m}_{ji} = \sum_{k\in\{\mathrm{Su}(i)\}} \dot{m}_{ik} + \dot{m}_i \quad (18)$$

This project has received funding from the European Union's Horizon 2020 research and innovation programme under grant agreement No 731297.

where $\{\mathrm{Pr}(i)\}$, $\{\mathrm{Su}(i)\}$ are respectively the predecessors and the successors of the node and $\dot{m}_i$ is the mass flow rate going to the consumer or to the production unit depending on the node's type.

- Thermal model

The energy balance applied on the water in the pipes gives the general form of the thermal model that can be used to calculate the temperature profile along the pipe ($T_w(x)$) and, hence, the temperature drop between its inlet and outlet:

$$\rho_w \, c_{p_w} \frac{\partial T_w}{\partial t} + \frac{\dot{m}_w c_{p_w}}{A_c} \frac{\partial T_w}{\partial x} = \frac{P}{A_c} \, U_l (T_w - T_s) \tag{19}$$

Where T_s, $\dot{m}_w$, c_{p_w}, A_c and P are respectively the surrounding temperature, the mass flow rate of water, its heat capacity, the cross sectional area of the pipe and its perimeter. U is the heat transfer coefficient expressed with:

$$U = \left[\frac{d}{R_1 h_w} + \frac{d}{k_p} \ln\left(\frac{R_2}{R_1}\right) + \frac{d}{k_{ins}} \ln\left(\frac{R_3}{R_2}\right) + \frac{d}{k_g} \ln\left(\frac{d_g}{R_3}\right) \right]^{-1} \tag{20}$$

where h_w, k_p, k_{ins}, k_g are convective coefficient between the water and the pipe, and thermal conductivities of the pipe, the insulation and the ground and R_1, R_2, R_3 are respectively the inner and the outer radii of the pipe and the outer radius of the insulation layer.

The thermal model used here is a steady state model which takes into account the heat losses to the ground in the pipes. Applied to time series, this so called pseudo-dynamic model is preferable when the time step is long enough to reach the steady state. The temperature drops in the pipes due to the heat loss is given by:

$$T_{w,out} = T_s + (T_{w,in} - T_s) e^{-\left(\frac{2\pi d_g L_p U}{c_p \dot{m}}\right)} \tag{21}$$

where $T_{w,in}$, $T_{w,out}$ and T_s are temperatures at the inlet and the outlet of the pipe and the temperature of the surrounding atmosphere. d_g is the depth of the pipe in the ground.

For both supply and return networks, an energy balance is applied in each node relating outgoing and incoming mass flow rates $\dot{m}_{j,in}$ *and* $\dot{m}_{j,out}$:

$$\sum \dot{m}_{j,in} T_{j,in} = T_{out} \sum \dot{m}_{j,out} \tag{22}$$

The heat power consumed or produced by each node is expressed by:

$$\dot{Q}_i = \dot{m}_{p,i} c_p \left(T_{ps,i} - T_{pr,i}\right) \tag{23}$$

where $\dot{m}_{p,i}$, $T_{ps,i}$ and $T_{pr,i}$ are the primary side mass flow rate the node's HEx and the primary side supply and return temperatures.

The hydraulic and the thermal models need to be solved simultaneously knowing the energy consumption of all the consumers and the production of all the nodes except one of them which is used as a slack node to balance the

This project has received funding from the European Union's Horizon 2020 research and innovation programme under grant agreement No 731297.

system. This gives the mass flow rates in all the pipes and the supply and return temperature in all the nodes of the network and for each time step.

This model need also to be calibrated to reproduce the behaviour of the real system. The calibration consists of minimizing the deviation between simulated and measured values of the supply temperatures in the substations by tuning the values of the heat transfer coefficients in the pipes. Different calibration cases are defined:

- **Cal1:** 0.2 % of available data is considered for the calibration and heat transfer coefficients are constant and comprised between 0.1 and 2 W/m².K.
- **Cal2:** 0.2 % of available data is considered for the calibration and heat transfer coefficients are constant and comprised between 0.1 and 6 W/m².K.
- **Cal3:** 1 % of available data is considered for the calibration and heat transfer coefficients are constant and comprised between 0.1 and 6 W/m².K.
- **Cal4:** 1 % of available data is considered for the calibration and heat transfer coefficients are a linear function of the water velocity in the pipes.

The indicator used for the calibration process to measure the deviation between simulated and measured values of the supply temperatures in the substations is the mean value of all the Root Mean Square Errors in the substations.

Figure 48 shows these indicators for all the calibration cases and Figure 49 to Figure 52 present simulated data against measurements for the substation *Salicornes*. Cal4 is the best case and seems to be more suitable to reproduce the real behaviour of the system. At a first sight, the deviation indicator seems to be high. However, Figure 52 shows that the agreement between the model and real data is very good for the heating season (samples between 4000 and 8000) and less good for summer season which alters the deviation indicator without a great impact on total energy losses prediction because this period represent a low fraction of heat production.

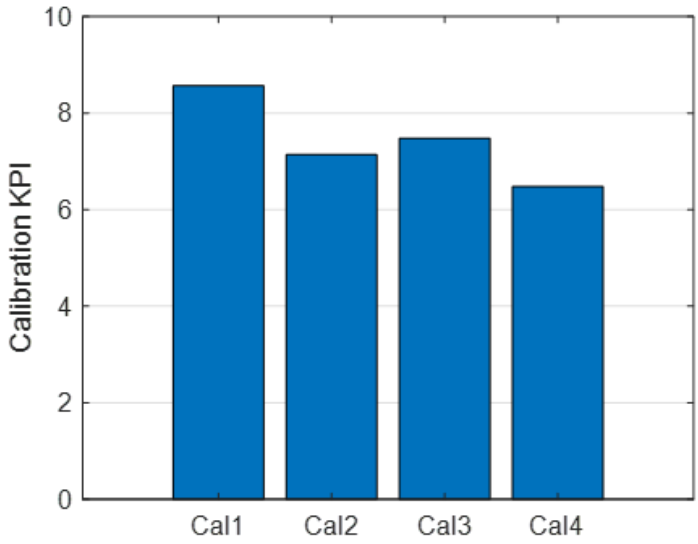

Figure 48: Deviation indicator for each calibration case

This project has received funding from the European Union's Horizon 2020 research and innovation programme under grant agreement No 731297.

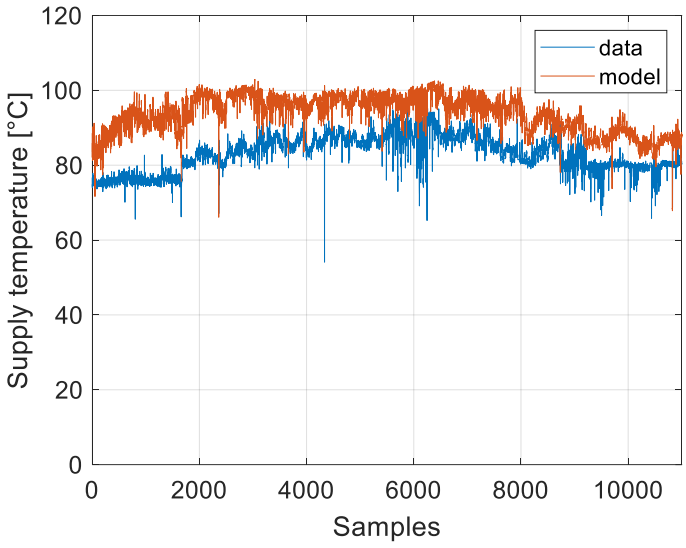

Figure 49: Supply temperature predicted by the calibrated model vs actual data (*Salicornes*, Cal1)

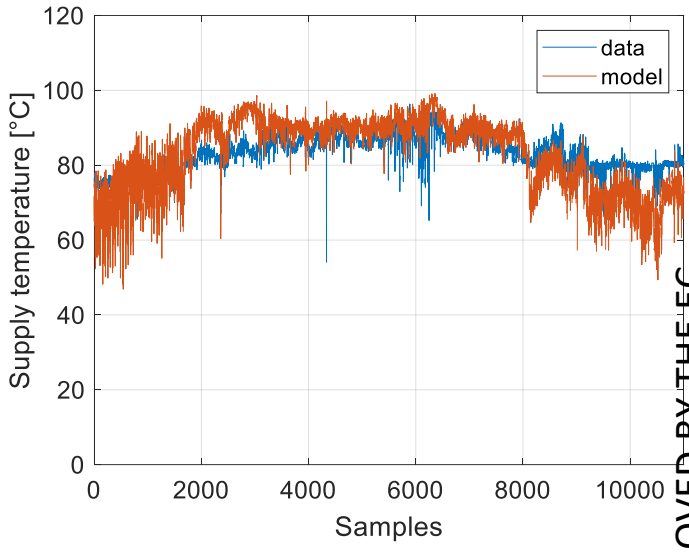

Figure 50: Supply temperature predicted by the calibrated model vs actual data (*Salicornes*, Cal2)

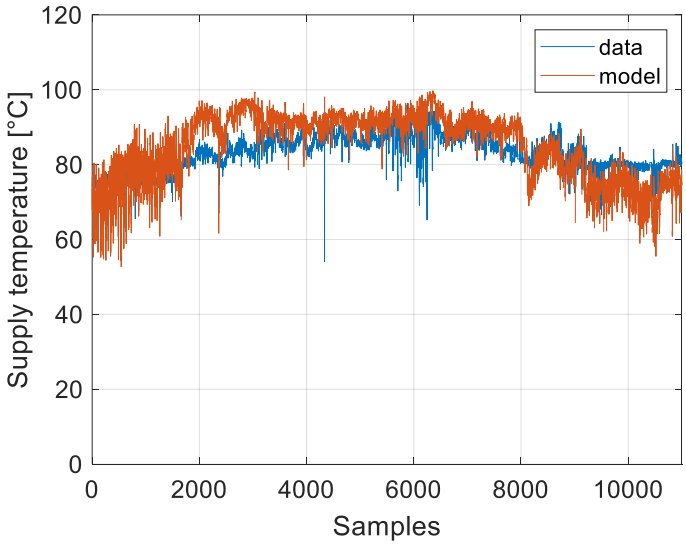

Figure 51: Supply temperature predicted by the calibrated model vs actual data (*Salicornes*, Cal3)

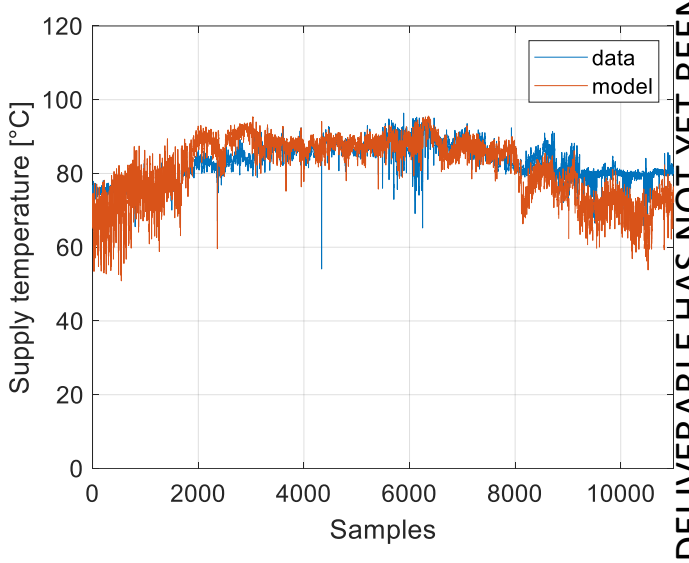

Figure 52: supply temperature predicted by the calibrated model vs actual data (*Salicornes*, Cal4)

6.3.3 Impact of typical day on simulations accuracy

Replacing real time series by representative TD (see section 6.3.1) induces some information losses and imprecisions. As a consequence, we can anticipate the use of TD instead of real times series as inputs of a DH model will have an impact on the results of simulations. To quantify this impact, outputs of simulations using TD as input where compared to those using real measurement times series as input. The boxplots on Figure 53 show the dispersion of differences between these outputs.

This project has received funding from the European Union's Horizon 2020 research and innovation programme under grant agreement No 731297.

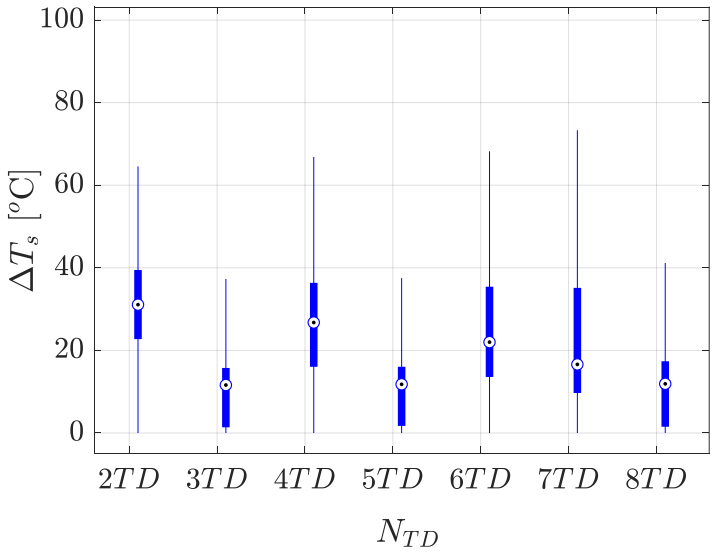

Figure 53: Boxplots of differences between supply temperatures simulated with TD and measured supply temperatures as input, as a function of the number of TD N_{TD}

We can observe that whatever the number of TD used for the simulations, the differences are quite high, the median being always over 15°C. Yet, we can see that the differences are more limited using 3 TD, 5 TD or 8 TD, confirming our choice of using 5 TD.

As said before, the use of TD is necessary for reducing drastically the computational costs of simulations and optimization, but as a drawback, it induces a loss of information so that the simulations integrate inaccuracies that cannot be reduced. For this reason, the results on fast dynamic phenomena must be carefully considered. However, for the purpose of assessing scenarios of DH improvement, the evaluation is based on the comparison between scenarios. As the data processing is the same for each scenario, the difference of performance is not affected.

Moreover, the results on aggregated variables such as global losses or total energy consumption suffer less of this issue. Indeed, Figure 54 shows the total energy consumption depending on the number of TD chosen. The black dashed line shows the measured value as reference. We can clearly observe that whatever the number of TD, the total modelled energy consumption remains quite closed from the real one: in the worst case (3 TD) it is underestimated by less than 5 %. Besides, the results confirm our choice of 5 TD since it gives the lowest difference between modelling and measurement.

This project has received funding from the European Union's Horizon 2020 research and innovation programme under grant agreement No 731297.

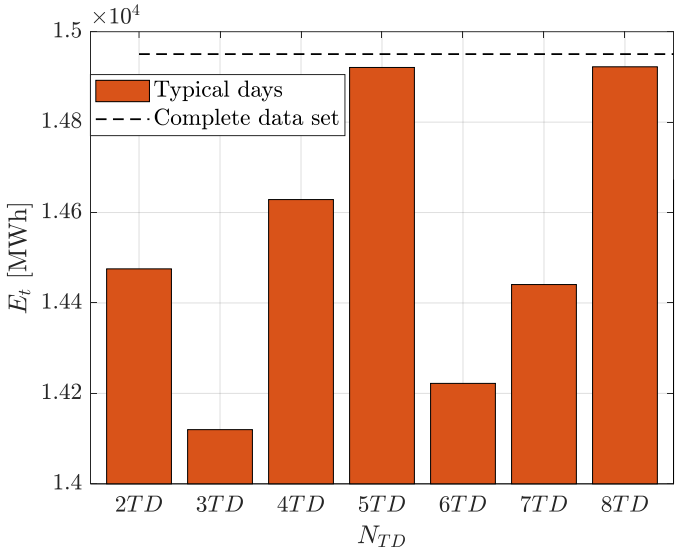

Figure 54: Total consumed energy E_t as function of the number of TD N_{TD}

In conclusion of this sub-section about DH simulation, the proposed methodology can be implemented with any simulation tools able to represent with a good level of confidence the physics described by the above models. In the frame of the mySMARTLife project the implementation has been done with models developed by ARMINES. However, for the purpose of flexibility and replicability, the section 9.1 lists a non-exhaustive list of tools compatible with the methodology.

6.3.4 Optimization algorithms

In general, models of DH can be used to optimize some criteria such as distribution losses, energy production costs or investment costs and operational costs of the distribution network or the energy production systems. Mathematically, an optimization problem is defined by:

$$\begin{gathered} Minimize: f(x) \\ subject\ to: g_i(x) \leq 0\ i = 1 \dots m \\ h_j(x) = 0\ j = 1 \dots p \\ x_{k,L} \leq x_k \leq x_{k,U}\ k = 1 \dots n \end{gathered} \quad (24)$$

$f(x)$ is called the objective function and represents a cost to be minimized. $g_i(x)$ and $h_j(x)$ are inequality and equality constraints that need to be satisfied by the solution x_{opt}. Every potential solution x compatible with these constraints is called feasible solution. $x_{k,L}$ and $x_{k,U}$ are the upper and lower bounds of the search space. Equality and inequality constraints are divided to two groups: linear and non-linear and can be evaluated using explicit functions or using implicit methods (e.g. numerical simulation). Optimization variables can be continuous or discrete and different techniques are used to solve these problems. Figure 55 shows the classification of these different methods depending on variables types.

This project has received funding from the European Union's Horizon 2020 research and innovation programme under grant agreement No 731297.

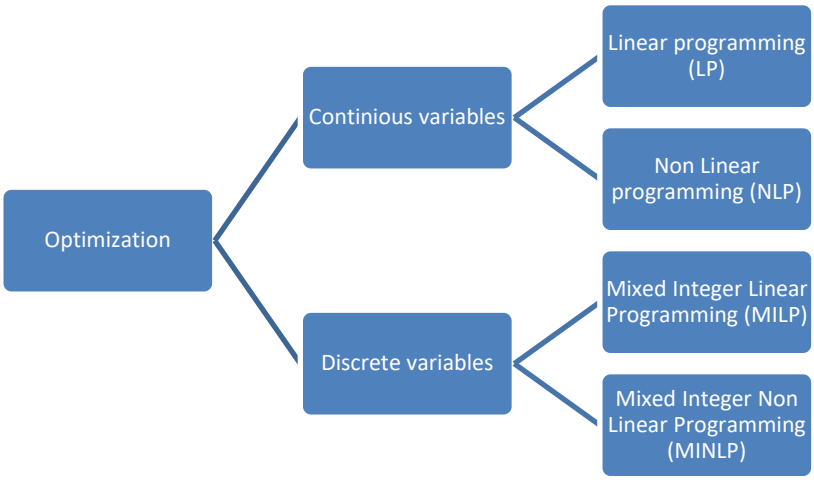

Figure 55: Classification of optimization methods based on variables' type

Optimization algorithms can be also classified depending on whether the algorithm allows global or local optimum search. Local optimization algorithms converge to the closest optimum to the initial point and global optimization algorithms explore the search space with the objective of finding the solution that optimizes better the objective function among all local optimums.

6.3.4.1 Local optimization methods

- **Direct search methods**

Direct search is defined as a sequential examination of potential solutions chosen using a certain strategy. These methods rely on comparison of objective function values without evaluating derivatives and can be used for both continuous and discrete variables' optimization problems. These methods remain popular as they are relatively easy to implement. They have also a high degree of flexibility and reliability. The most popular direct search methods are Generalized Pattern Search (GPS) and Nedler-Mead simplex procedures:

Nedler-Mead simplex algorithm was introduced by Nelder and Mead (1965), this algorithm requires a set of points that form an initial simplex. In each iteration, the objective function is evaluated at the corner points of the simplex which permits to determine the worst corner. The worst vertex is replaced by a new candidate. This new candidate is obtained by applying a number of operations about the centroid of the current simplex: reflection, contractions or other means.

Generalized Pattern Search was introduced by Torczon (1997), generalized pattern search methods generalize direct search methods by introducing an additional search step at the beginning of each iteration which consists in choosing the new solution by sampling the objective function at a finite number of points along a suitable set of search directions generated by some strategy aiming to improve the current solution. Another additional step called Poll step is executed in case of failure of the search step to find a better direction. This step evaluates the objective function on a function on a poll set which contains necessarily at least one feasible descent direction unless the current solution is a stationary point.

This project has received funding from the European Union's Horizon 2020 research and innovation programme under grant agreement No 731297.

- **Model based search methods**

These methods use surrogate model to guide the search algorithm. The idea is to create a posteriori database of cost function values and to generate a surrogate model using this database (linear or polynomial interpolation, artificial neural networks, support vector machine etc…). The surrogate model is then used instead of the real model to evaluate the function and its gradient during the optimization process. Among these model based methods one can find Trust region method and Implicit filtering:

Trust region method (Conn et al., 2000) uses smooth surrogate model that can be considered accurate locally within a trust region about the current solution. Some authors used linear interpolation and some others proposed quadratic models. For example, if a quadratic model is used to approximate the objective function, about a solution x_k the optimization problem is reduced to solving a trust-region sub problem :

$$\text{Minimize: } \mathrm{m_k(p)} = \mathrm{f(x_k)} + g_k^T p + \frac{1}{2} p^T B_k p \qquad (25)$$

$$s.t. \|p\| \leq \Delta_k$$

Where Δ_k is the trust-region radius and g_k and B_k are the gradient and the hessian at current point.

Instead of calculate them, g_k and B_k can be estimated in order to interpolate a set of sample points evaluated using the original model. The trust region radius is reduced or increased depending on whether we achieved a satisfactory reduction of the objective function in the current step and the quality of the approximation given by the surrogate function measured by the ratio between the actual and the predicted reductions.

In the same way as descent techniques when the gradient of the objective function, implicit filtering methods evaluate the gradient of the function to facilitate the search process. However, these methods use an approximation of the gradient obtained by forward or centred finite differences. Centred differences require twice function evaluations than forward differences but it is, in return more robust and less sensitive to noise.

6.3.4.2 Global search algorithms

Global optimization algorithms try to search for an optimum in the whole search space. Algorithms proposed in the literature cover different techniques to explore the space in a clever way to avoid premature convergence to local minimums. These models could be classified into three categories: Deterministic, model-based and stochastic search algorithms.

- **Deterministic global search algorithms**

This class encloses search techniques which do not use random processes when searching for the global algorithm.

The DIRECT algorithm is a good example of this category of methods (Jones et al., 1993). DIRECT (stands for DIviding RECTangles) is a black-box optimization algorithm which means that it needs only function evaluation to work and does not use derivative evaluations in the search process. The algorithm proceeds by normalizing the search space to transform it to an n-dimensional hypercube. It identifies a set of potentially optimal boxes. Each box is then

This project has received funding from the European Union's Horizon 2020 research and innovation programme under grant agreement No 731297.

partitioned to smaller rectangles with a sampled point at the center of each one. An efficient methodology for selecting potential optimal boxes is the key to a successful DIRECT method. The methodology needs to ensure a good balance between local search which accelerates the convergence and global search which enables the convergence to a global optimum.

- **Global model-based search algorithms**

As it is the case for local model-based optimization, the key idea here is to replace computational expensive objective function with a surrogate model or a distribution with lower fidelity and less computational cost. The local model used to approximate the objective function is usually called metamodel. Many types of models can be used such as distributions, classical or polynomial regressions, Support Vector Machines (SVM), Artificial Neural Networks (ANN), response surface methodology, etc…

- **Stochastic global search algorithms**

This category of algorithms is widely used in global optimization problems because it regroups many algorithms such as Genertic Algorithms, Particles Swarm Optimization, Simulated Annealing, Tabu Search, Scatter Search, etc… These algorithms are simple to implement and to adapt to different problems. As examples, the Genetic Algorithm and Particles Swarm Optimization are presented briefly hereafter:

Genetic algorithms were first proposed by Holland in 1975 (Holland, 1992) and take advantage of concepts inspired from biology such as mutation and selection. A genetic algorithm starts by creating a population of individuals usually called chromosomes. Each of these chromosomes is basically a vector representing a point in the search space. In each iteration, a new generation of chromosomes are created by applying selection, mutation and crossover process on the current generation. The selection process is guided by evaluating the objective function of each chromosome (also called fitness). Selecting the chromosomes is done according to their fitness. Additional chromosomes are also generated using crossover and mutation process to ensure a diversity of solutions in each generation.

Particles Swarm Optimization (PSO) proposed by Kennedy (1995) tries to find the global best value using a methodology inspired from the way a swarm of birds scatter and regroup. Like Genetic Algorithms, this algorithm is a population based algorithm although the population in this case is usually called swarm and its members are called particles. The position of each particle is a vector representing a point in the search space and it moves in the space with a velocity updated in each iteration using a self-accelerating factor and a global accelerating factor to ensure efficient global optimum search and the convergence of algorithm.

In conclusion of this sub-section about optimization, the proposed methodology can be implemented with any tools proposing the above methods. In the frame of the mySMARTLife project the optimization phases (calibration and optimization) have been done with tools developed by ARMINES based on Particle Swarm Optimization (Stochastic global search algorithm) and Generating Set Search method (global direct search method). However, for the purpose of flexibility and replicability, the section 9.21 lists a non-exhaustive list of tools with optimization functions.

This project has received funding from the European Union's Horizon 2020 research and innovation programme under grant agreement No 731297.

6.3.5 Multicriteria decision aiding layer

In the Figure 30, the last part of the methodology deals with the decision aiding step which is the purpose of the action 2.5.3 of the project. As mentioned before the action on DH optimization and monitoring and the action on Decision Aiding have been built in a strong collaboration making the coupling effective. The implementation of the decision aiding layer for DH optimization is presented and explained in the deliverable D2.8.

This project has received funding from the European Union's Horizon 2020 research and innovation programme under grant agreement No 731297.

7. Implementation

The implementation is done in two steps. In a first part the potential of improvement scenarios is evaluated on a part of the *Beaulieu* DH located in the area of *Millerand*. The selection of the Millerand area is justified as it is representative of the configuration of the whole DH. The topology, the consumption, the heterogeneity of the data available… makes this part a test bench of the methodology. More than this, working on a part of the DH, which does not necessary include systems and which is connected to an upper-scale DH, demonstrates the capacity of the methodology to assess scenarios in the realistic context of urban planning actions, usually located on a part of the urban area. As said before, the methodology can assess scenarios on the distribution, the sub-stations, the buildings, in complement of energy systems optimization (usually at the whole scale of the DH).

The second part of this section gives the methodology for generalizing the data processing phase of the methodology. A strategy made of adapted solutions is proposed in order to make the methodology of the action possible whatever the reality of the data available. It is indeed necessary as the situation and the level of knowledge of the DH can vary from location to location in a given DH, from a DH to another one.

Then an illustration of the methodology combined with the generalized data processing solutions is presented in the case of the whole Beaulieu DH branch.

7.1 Implementation to *Millerand* area

Millerand is a part of the DH composed of 33 substations which corresponds to 20 % of the total number of substations of *Beaulieu* DH (Figure 23). The secondary side of this Hex corresponds to the general supply of the area of *Millerand*. The 3D map and oriented graph representing this portion of the network are given in Figure 56 and Figure 57

7.1.1 Global actions on the distribution systems

All the scenarios will be assessed compared to a reference case which is simulated first. In the reference case, the supply temperature is constant and equal to 95°C and return temperature at the secondary side are taken from measurements when available. If data is not available for the secondary side, return temperature is constant and equal to the value resulting from the calibration process detailed in section 6.3.2.1. The supply temperature is fixed using a typical control law for standard heating systems. An illustration of control curves for standard systems, low temperature systems and sanitary hot water is given in Figure 58.

Five scenarios are considered and compared to the reference case:

- **Scenario 1:** return temperatures at the secondary side of all the substations are decreased and fixed to 40°C. This scenario can be the result of the implementation of an effective control strategy of the secondary side is implemented

This project has received funding from the European Union's Horizon 2020 research and innovation programme under grant agreement No 731297.

- **Scenario 2:** return temperatures at the secondary side of all the substations are decreased and fixed to 30°C. This scenario reflects the implementation of the same action as the scenario one coupled to the use of larger heat emitters allowing lower return temperature without reducing the comfort level in the building.
- **Scenario 3:** some emitters technologies such as underfloor heating or radiant emitter allow to reduce more the temperature levels of water in the heating system. In this scenario low supply and return temperatures in the secondary side are used. Indeed, in all the substations of the network, the secondary side supply temperature is controlled using a control law which is typical for low-temperature systems (cf. Figure 58). The secondary side return temperature is kept constant (30°C) thanks to an effective control system.
- **Scenario 4:** an optimization of the supply temperature of the heat source (being on top of the studied subnet the substation *Millerand* can considered as a source) is performed in each time step to reduce the operation temperature without altering the quality of service. This scenario aims to reflect an optimization of the production regarding the temperature control It could be realized by implementing a model-based temperature controller in the heat production sites.
- **Scenario 5:** this scenario is a combination of scenario 3 and scenario 4 meaning that all the substations require low temperature levels at the secondary side and an optimization of the supply temperature of the heat source is realized in each time step.

Figure 56: 3D Map of *Millerand* section

This project has received funding from the European Union's Horizon 2020 research and innovation programme under grant agreement No 731297.

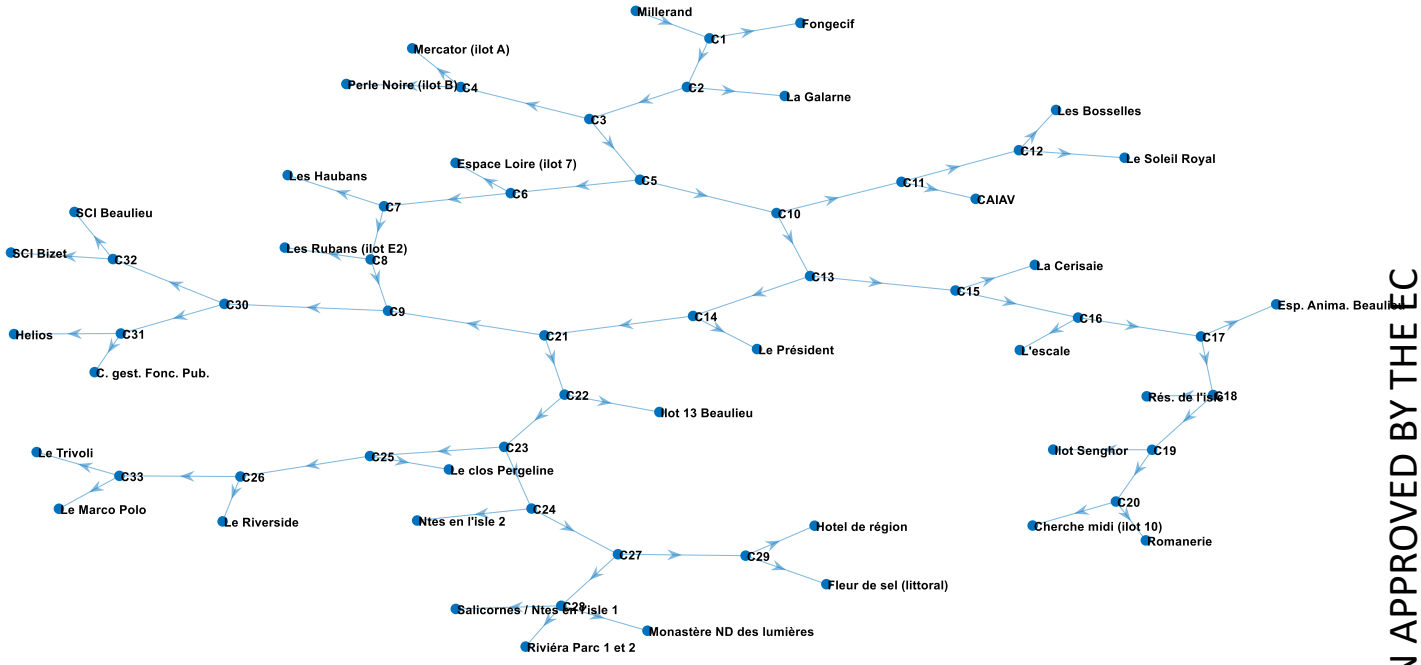

Figure 57: Topology of the network's digital twin (*Millerand*)

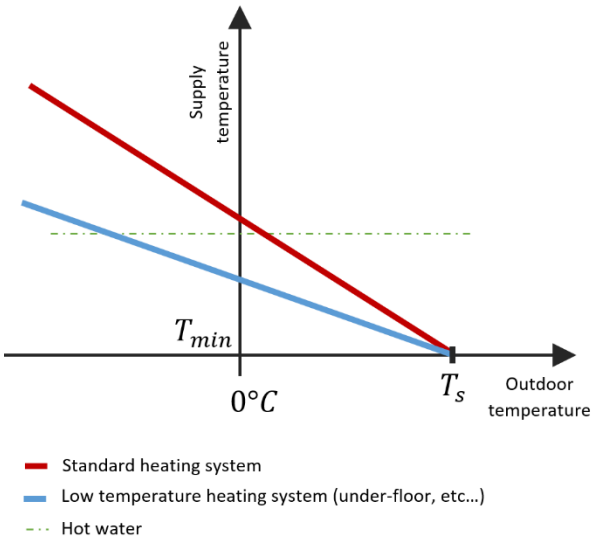

Figure 58: Control laws of the supply temperature for standard heating systems, low-temperature heating systems and hot water (case of two separate HEx for SH and DHW)

Figure 59 shows the total energy consumption in *Millerand* for 120 hours which corresponds to the 5 TD used for the simulation. Energy consumptions in the substations are the measured inputs for the simulation model which, for recall, calculates the mass flow rates in the pipes and the temperatures in all the nodes and the substations as well as the total energy produced by the heat source. The energy production for *Millerand* is given also in Figure 59 for the reference case and the 5 scenarios detailed previously. It demonstrates that the scenario 5 allows lower energy production in most of the time steps compared to the reference and all the other scenarios.

This project has received funding from the European Union's Horizon 2020 research and innovation programme under grant agreement No 731297.

Figure 60 shows the return temperature at the heat source (Top of the *Millerand* network) for the reference case and all the scenarios. Return temperature is higher than the reference in scenario 4 where the supply temperature is optimized without any other action. For the other scenarios, the return temperature is lower than the reference which can lead to additional energy savings in the production systems (not considered in this study). However, return temperatures are an indicator of the improvement of the performance of the DH.

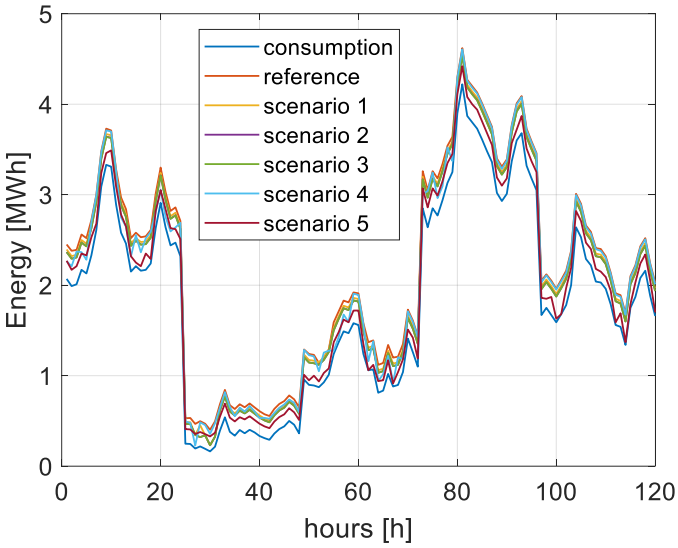

Figure 59: Energy consumption[10] in *Millerand* sector and total energy prod.[11] for the different scenarios (for the 5 TD)

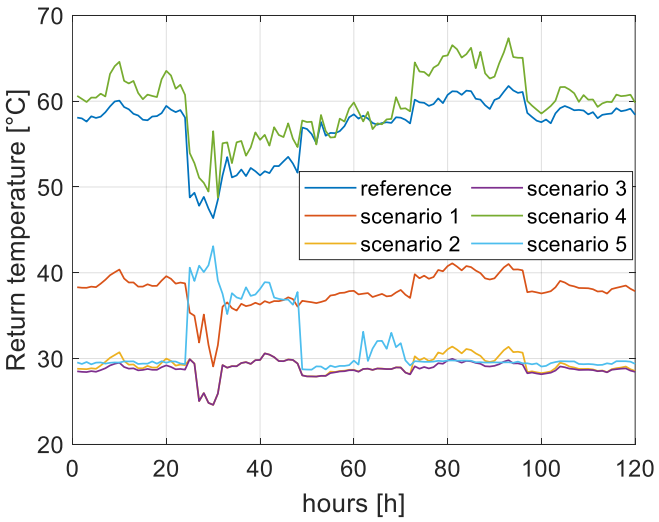

Figure 60: Return temperature at the source of *Millerand* sector for the different scenarios (for the 5 TD)

Total Energy consumption[8] and production[9] for the whole period are given in Figure 61 and energy savings are given in Figure 62 with the corresponding CO_2 emissions. The latter shows clearly the importance of source temperature control which leads to almost 5 percent without any other action. Reducing return temperature at the secondary side of the substations leads also to substantial energy savings and the lower these temperatures the more energy savings. Another interesting remark is that scenario 2 and scenario 3 give the same energy savings. Reducing the supply temperatures at the secondary side of the substation by retrofitting buildings' heating systems does not lead to any additional energy savings. This type of action is beneficial only when coupled with the optimization of the source temperature. This is the case of scenario 5 which gives the best impact among all the scenarios with energy savings higher than 9 % of the total consumption of the substations. These energy savings can be explained by the fact that the supply temperature of the source, in this case, is globally lower than the reference case and then scenario 4 which

[10] *Consumption* is defined as the energy consumed at the substation coming from the variables monitored by the supervision tool of the DH operator

[11] As the present study does not consider the production systems, in this work *Production* corresponds to the energy necessary for fulfilling the *consumption* plus the energy necessary for the distribution (losses).

This project has received funding from the European Union's Horizon 2020 research and innovation programme under grant agreement No 731297.

is allowed by lower supply temperatures at the secondary side. The drawback of scenario 5 is that it can be realized only if all the substations buildings are modified for low-temperature heating. If any buildings are still using high temperatures, scenario 5 will not guaranty the quality of service for those buildings.

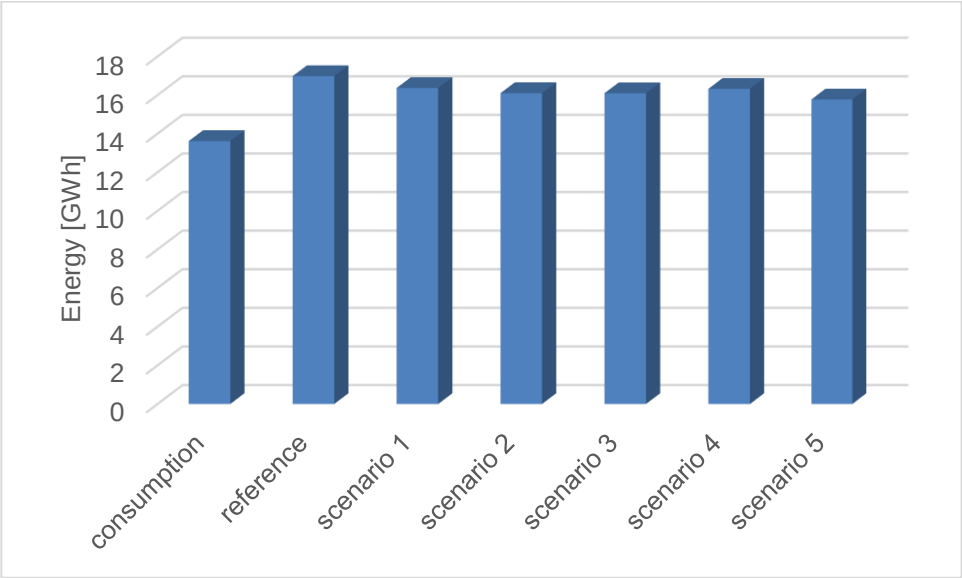

Figure 61: Energy consumption and energy production in the considered period for the reference case and five scenarios

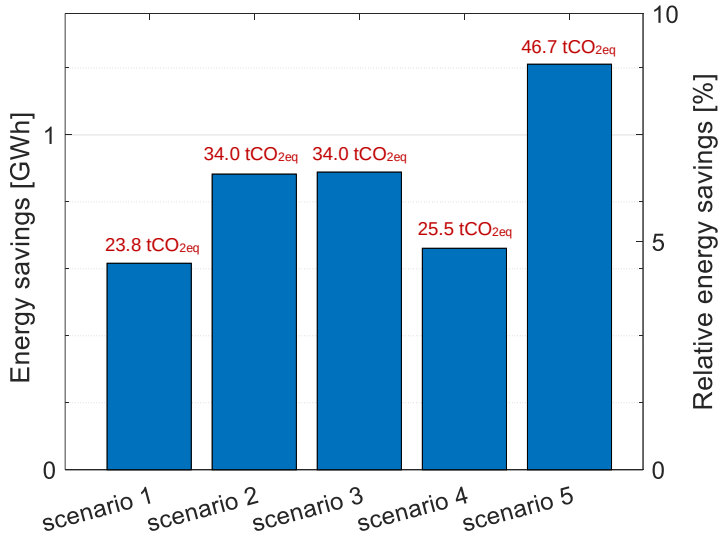

Figure 62: Energy savings and CO2 emissions for the 5 scenarios (absolute and percentage of total consumption).

7.1.2 Energy recovery from return pipes

Scenarios studied in the section 7.1.1 are global and require an implementation on a big number of substations. In this section, the actions investigated aim to recover heat from the return pipe as explained in section 6.2.2. For this, 2 scenarios are studied with only one substation modified each time to support energy recovery from the return pipe.

This project has received funding from the European Union's Horizon 2020 research and innovation programme under grant agreement No 731297.

The fraction of the mass flow rate coming from the return pipe is optimized for each time step using an optimization algorithm (Generating Set Search method).

As an illustration, results are given hereafter for two substations sst1 and sst5. The hourly consumption of these substations is given in Figure 63 and Figure 64 gives the ratio of energy savings of the modified substations. The absolute energy savings are given in Figure 65. These figures show globally small energy savings. For example, in the scenario where sst1 is modified, energy savings are most of the time under 1 % of the consumption of the substation. For sst5, relative and absolute energy savings are globally higher. However, for both cases, energy savings are constantly below 1 kWh for the period. These results show that connecting substations to the return must be coupled to another action. Moreover, buildings which require high supply temperature are not suitable for this type of modification.

Connecting substations to the return pipe could be more interesting for buildings equipped with low temperature heating systems. In order to verify this statement, 33 additional scenarios where investigated. In each of them, only one substation is modified by decreasing temperature levels at the secondary side and by connecting it to the return pipe. Relative and absolute energy savings are given in Figure 66 and Figure 67 and show a higher benefit than the connexion to the return pipe alone. Indeed, hourly absolute energy savings are sometime 50 times higher than previous cases. Total energy savings for the whole studied period (Figure 68) vary considerably from a substation to another. It depends on the heat consumption of the substation and the level of the return temperature. Both of them need to be high to observe high energy savings after the modification. Another important criterion which affects the potential of a substation is the mass flow rate of water in the return pipe. Typically, a substation located at the end of a branch does not have any potential to recover energy from the return pipe. Similarly, a substation with a high heat demand which is placed near to the end of a branch followed by substations which consume a low quantity of heat does not have an interesting potential either.

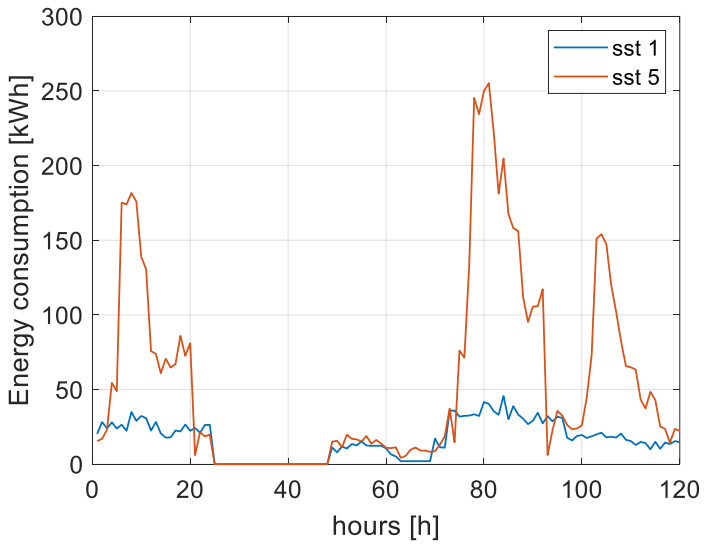

Figure 63: Energy consumption of substations 1 and 5 during the 5 TD

This project has received funding from the European Union's Horizon 2020 research and innovation programme under grant agreement No 731297.

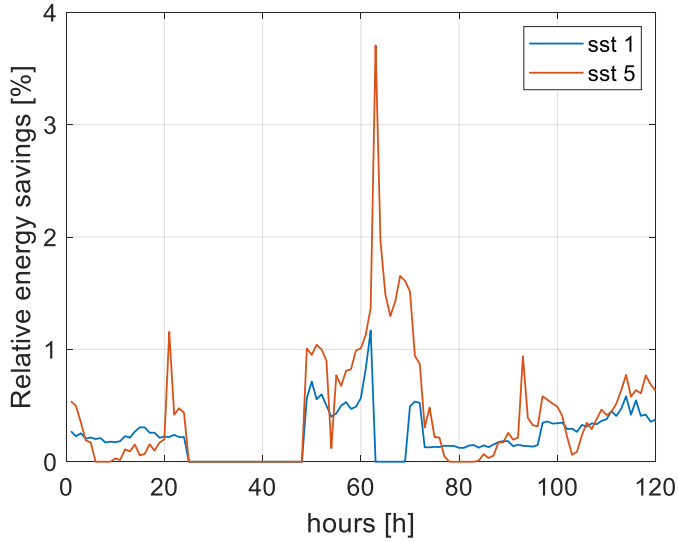

Figure 64: Relative energy savings for the scenario “recovering energy savings from return pipe”

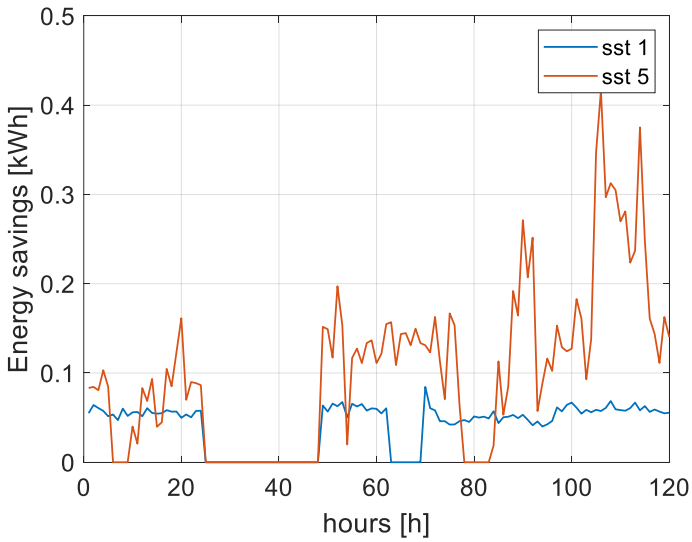

Figure 65: Energy savings for the scenario “recovering energy savings from return pipe”

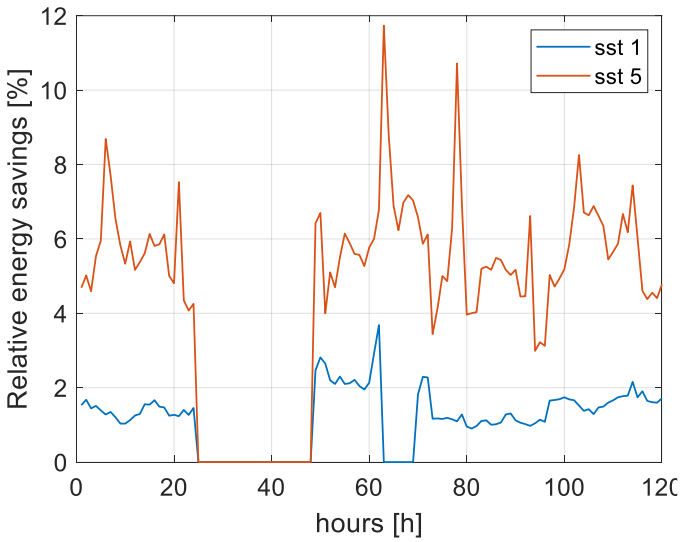

Figure 66: Relative energy savings for the scenario “recovering energy savings from return pipe coupled to a temperature reduction in the secondary side network”

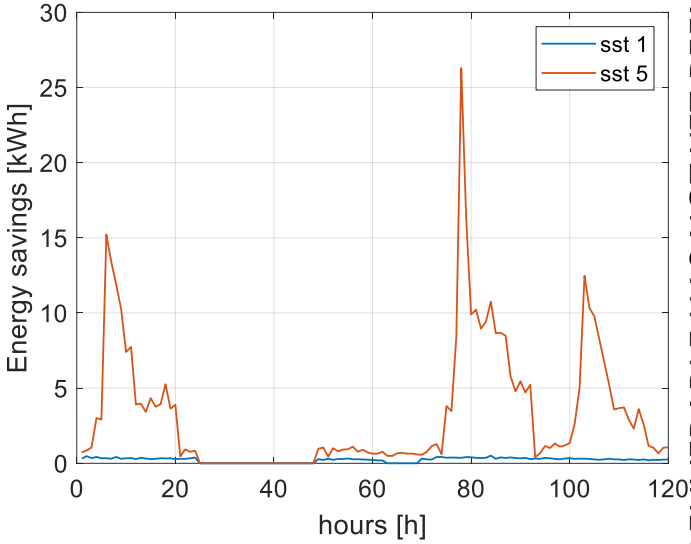

Figure 67: Energy savings for the scenario “recovering energy savings from return pipe coupled to a temperature reduction in the secondary side network”

This project has received funding from the European Union's Horizon 2020 research and innovation programme under grant agreement No 731297.

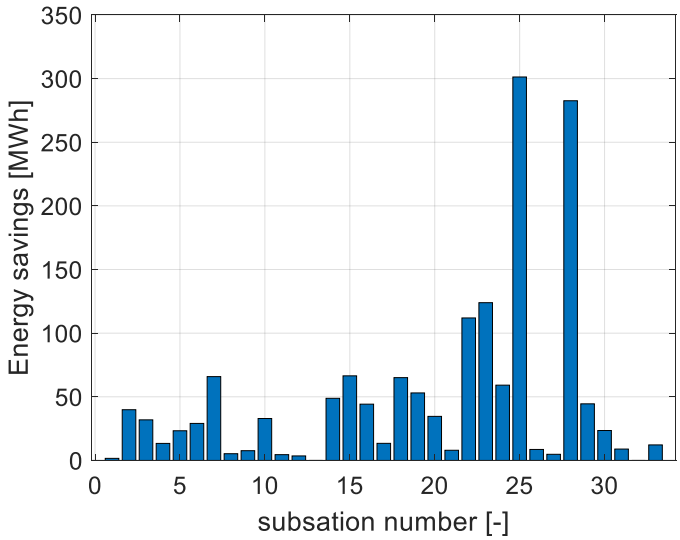

Figure 68: Total energy savings during the studied period for the 33 scenarios corresponding to connecting one substation to the return pipe coupled to a reduction of temp. levels at the secondary side of the modified substation.

Decreasing the return temperature at the heat source is another positive impact of modifying low temperature substations by connecting them to the return pipe. This effect is shown in Figure 69 for sst1 and sst5 where it can be seen that modifying sst5 allows to reduce the return temperature more than sst1. This is due to the fact that sst5 is able to recover more energy from the return pipe than sst1.

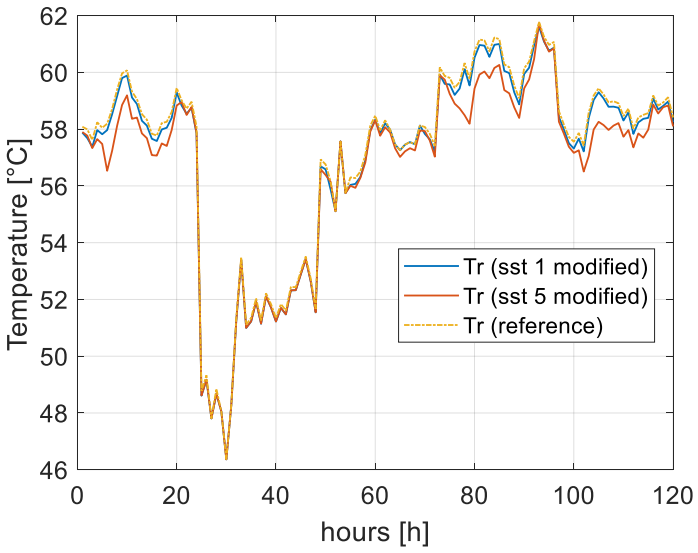

Figure 69: Return temperature of *Millerand* section for the reference as defined in 7.1.1 case and for two cases where only substation n°1 and or substation n°5 is modified

This project has received funding from the European Union's Horizon 2020 research and innovation programme under grant agreement No 731297.

7.1.3 Relevance of combined actions on limited and well selected substations

The potential to recover heat from the return pipe (Figure 68) is not homogeneous from substation to substation. This means that a reduced number of substations can be selected for making the modification efficient. The selection process needs to respect two important criteria: the substations with an interesting potential of heat recovery are privileged; the selected substations need to be far from each other (the modification of a substation reduces the return temperature nearby). To assess the effectiveness of such an approach, additional scenarios were studied in this section:

- Scenario 6: four substations (sst2, sst7, sst15, sst25) are modified by connecting them to the return pipe and by reducing temperature levels at the secondary side of the HEx.
- Scenario 7: four substations (sst2, sst7, sst15, sst25) are modified by connecting them to the return pipe and reducing temperature levels at the secondary side of the HEx. Besides, the supply temperature of the heat source is optimized in the same way as scenarios 4 and 5. Another constraint is taken into account in this scenario to avoid unfeasible cases. Indeed, maximum flow velocity[12] in the pipes of the network is limited to $10\ m/s$.
- Scenario 8: same as scenario 7 but the maximum flow velocity[12] in the pipes of the network is limited to $15\ m/s$.

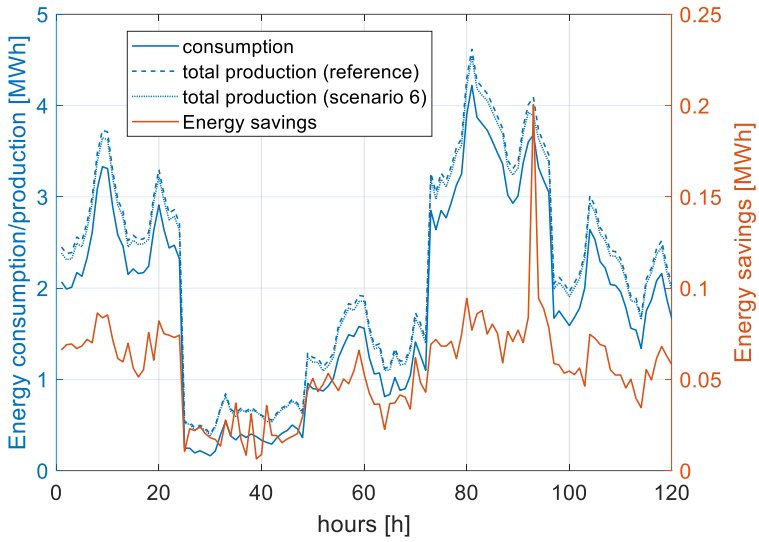

Figure 70: Hourly energy production and energy savings of scenario 6 compared to the reference

[12] A high velocity benefits the energy savings regarding the limitation of heat losses but implies a higher pumping cost

This project has received funding from the European Union's Horizon 2020 research and innovation programme under grant agreement No 731297.

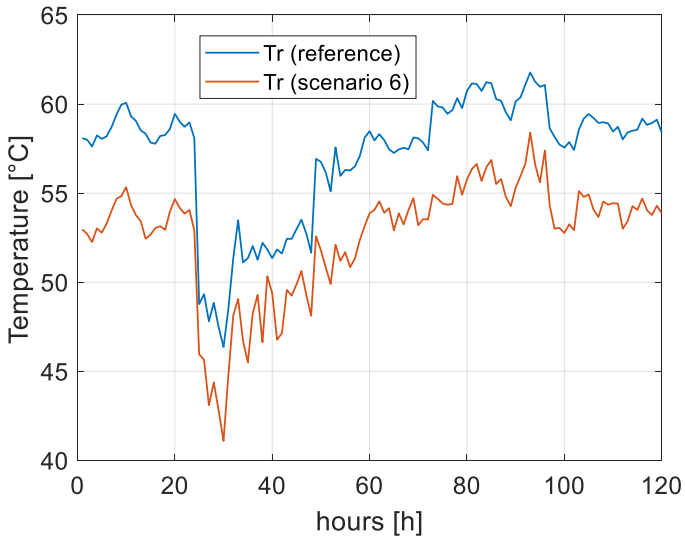

Figure 71: Hourly return temperature of scenario 6 compared to the reference

Figure 70 shows the total energy consumption of *Millerand* DH which is the same as previous scenarios, it shows also the total production of the reference case and scenario 6. Energy savings which are given in the same figure are globally lower for TD2 than the other typical days. However, they have the same order of magnitude in the TD1, TD3, TD4 and TD5. Figure 71, presents the return temperature at the source for scenario 6 compared to the reference. This figure reveals that return temperature are always lower than the reference case which represents an additional potential of energy savings at the production system level.

Optimizing the supply temperature of the heat source in addition to the modification of the four substations, leads to more energy savings almost in every time step as demonstrated by Figure 72. This is also confirmed by total energy savings presented in Figure 73 for scenarios 6, 7 and 8, where it can be seen that the modification of the four substations combined with the optimization of the heat source temperature is 5,9 % more efficient than the reference scenario when the water velocity in the pipes is limited to $10\ m/s$ and 8 % when this velocity is limited to $15\ m/s$. In fact, reducing the supply temperature in some substations leads to high mass flow rates which increases also pumping costs[10]. Pumping costs optimization is not in the scope of this work. However, the simulation solution proposed for modelling the DH can be used to assess the effect of the water velocity in each pipe and to identify possible bottlenecks. Associated solutions (e.g. to replace those pipes by larger ones) could be then coupled with solutions on energy issue and broaden the analysis by considering a multi-objective optimization.

Regarding return temperatures, scenario 6 have globally lower temperature levels than the reference case and scenarios 7 and 8 (Figure 74). Indeed, optimizing the supply temperature of the heat source can lead in some time steps to higher return temperatures than scenario 6 but rarely higher than the reference case.

This project has received funding from the European Union's Horizon 2020 research and innovation programme under grant agreement No 731297.

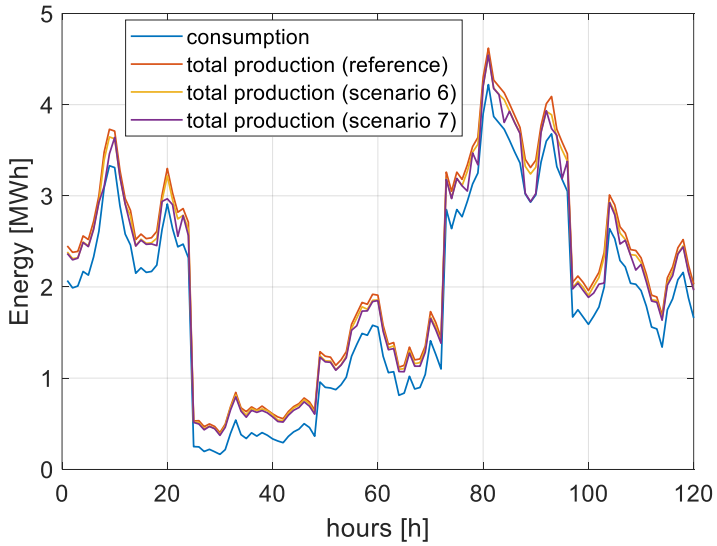

Figure 72: Hourly energy production of scenarios 6 and 7 compared to the reference

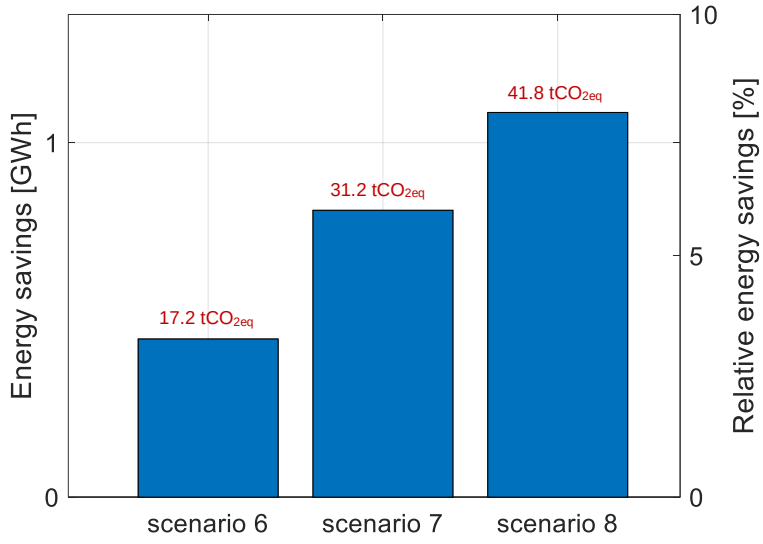

Figure 73: Total energy savings and CO2 emissions during the studied period for scenarios 6, 7 and 8

This project has received funding from the European Union's Horizon 2020 research and innovation programme under grant agreement No 731297.

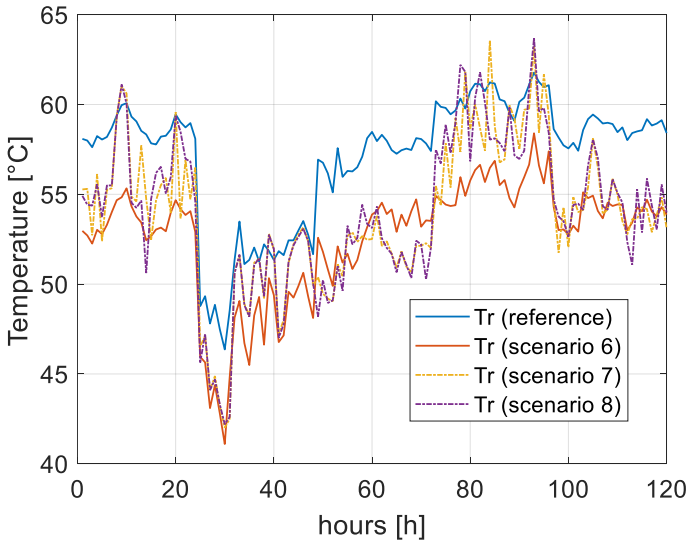

Figure 74: Return temperatures for scenarios 6, 7 and 8

7.1.4 Impact of actions on the buildings envelope (retrofitting)

In addition to actions on the distribution part of the DH, it is important for the DH operator to anticipate the effects of action done on the buildings. For instance, at a first glance it can be imagined actions aiming to lower the energy consumptions of the buildings connected to the DH should improve its efficiency (based on the a priori argument of less energy to be supplied). To study this assumption, the proposed methodology is implemented for different of energy performances of the *Millerand* buildings, using the present state as the reference. These rates cover the range from 0% of reduction up-to 80 % of energy savings. This latter value is not really realistic but allows the test of the methodology for such scenarios to be done.

In the Figure 75, the consumption and production time series are presented for the reference case (current state of the DH and the connected buildings) and when the buildings connected to the DH are 50 % more efficient than the reference. We can see the difference between the consumption and the production tends to be lower for the 50 % cut-off scenario compared to the reference one. This is clearly demonstrated with the Figure 76, where the network efficiency is plot as a function of the building efficiency rate. It can be seen the efficiency is not a growing function of the building performances. This counter-intuitive result is explained by an increase of relative energy losses in the pipes when the consumption decreases. This result does not mean the conventional DH are not compatible with energy retrofitting policy of the connected buildings. It underlines the necessity to couple different actions together (e.g. combination with an optimization of the production temperature, combination with appropriate control of the supply temperature of the secondary networks in the buildings…) and the needs to think actions on the buildings coupled with actions on the associated branch of the DH.

This project has received funding from the European Union's Horizon 2020 research and innovation programme under grant agreement No 731297.

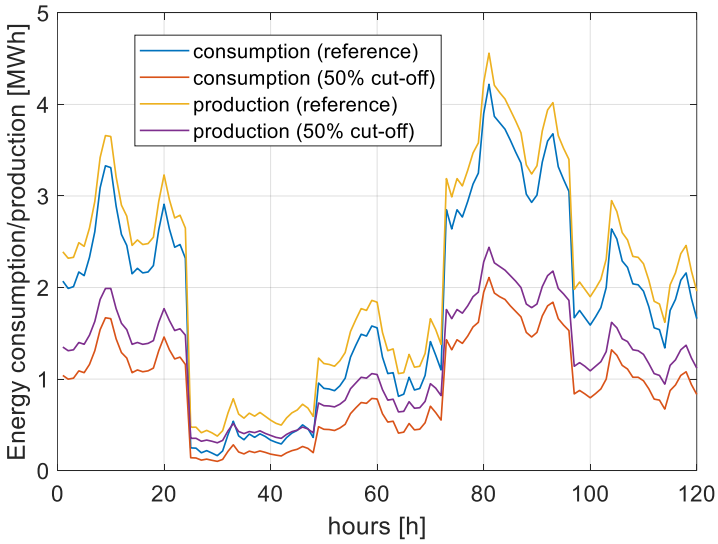

Figure 75: Consumption and production profiles for the TD (reference case and 50 % of energy savings applied to the connected buildings).

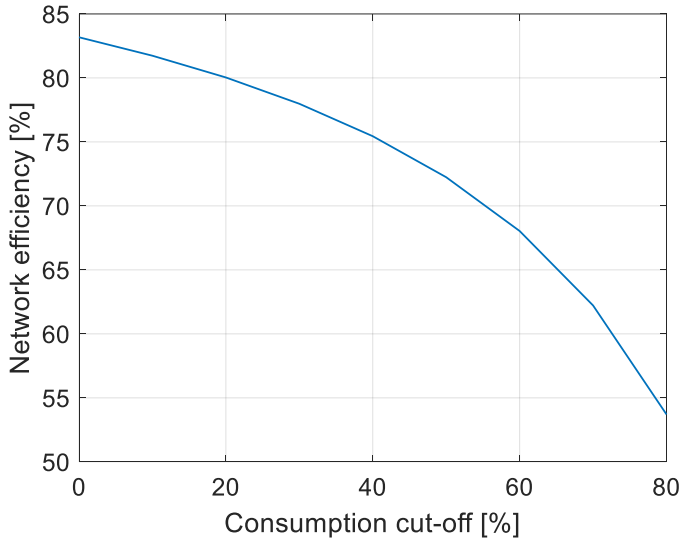

Figure 76: Influence of the level of the buildings retrofitting on the network efficiency.

In conclusion, with the case of *Millerand* part of the DH, the usefulness and the potential of the proposed methodology has been illustrated with a diversity of scenarios which cover different type of actions. The combination of simulation and optimization is revealed as a good support for assessing potential improvements of DH systems. In addition, this section shows the relevance of the data processing described in the previous section and particularly the capacity to base the simulation/optimization on real data, making the whole methodology strongly connected to the operational objective.

The implementation on a fragment of the DH demonstrates the methodology can be applied to any parts of the network, without the need to model all the DH. This capacity is, as already said, more compatible with real urban planning

This project has received funding from the European Union's Horizon 2020 research and innovation programme under grant agreement No 731297.

procedures. It is however necessary to be able to scale up the methodology from a part of the DH to bigger scale (either a bigger part of the DH or the whole system).

7.2 Data processing generalization

The aim of this section is to make the implementation of the methodology possible whatever the part of the DH studied and the size of this part (from a branch to the whole DH). We have seen the heterogeneity from substation to substation regarding the availability of the data is an important challenge for the purpose of a flexible methodology (see section 4.1).

Indeed, the reality of monitoring does not make the energy consumption of all the substations available at the same time. Figure 19 shows there is no overlapping dates for calculating heat loads on all the substations at the same time.

As a consequence, the construction of TD (see section 6.3.1) must be implemented to a selected subset of substations, with a representative amount of overlapping dates (like it has been done in the case of *Millerand* DH part).

In case of not enough overlapping dates when considering all the substations, a minimum number of daily consumption time series, statistically representative of the whole available data, must be determined thanks to a Kolmogorov-Smirnov (*KS test*) test (Figure 77). This defines the reference substations subset on which will be applied the clustering procedure (section 6.3.1).

Alternative processes must be implemented for determining the TD of the substations excluded of the reference subset (Figure 77) :

1. For substations for which they exist, the daily consumption time series associated to the dates of the selected TD must be extracted
2. Otherwise, the clusters must be refined from common dates between these substations and the reference ones. These existing dates are associated with the cluster indexes (defined in section 6.3.1.) The days the nearest from the centroid of the re-built clusters was designed as TD for the given substations.
3. Finally, for substations without enough data for generating TD, the energy difference between energy production and consumptions is spread over these substations. In complement, this needs an iterative calibration process done with the modeling module to account for the energy losses. This process is defined by the following steps:
    a. The model is calibrated as described in the section 6.3.2.2. Heat transfer coefficients in the pipes which cannot be calibrated are fixed to typical values.
    b. Total energy losses in the network are assumed using an initial guess
    c. The difference between energy production and consumptions added to energy losses is distributed on concerned substations, with respect to their heated surfaces.
    d. The energy losses are updated using the calibrated model
    e. Steps c. and d. are repeated to minimize the deviation between assumed and calculated energy losses.

This project has received funding from the European Union's Horizon 2020 research and innovation programme under grant agreement No 731297.

An alternative to the step 3 can be to use Energy & Buildings modelling tools to determine the consumption of the remaining substations. A list of possible tools is presented in the section 9.2).

Figure 77: TD generation for high heterogeneity data availability

This project has received funding from the European Union's Horizon 2020 research and innovation programme under grant agreement No 731297.

7.3 Implementation to *Beaulieu* DH

The methodology developed in this work is applied to the whole *Beaulieu* branch of the network. The oriented graph of the network is given in Figure 78. Three scenarios are selected based on previous results to illustrate the capacity of the network analysis performed on *Millerand* network to be implemented at a bigger scale. All the other scenarios presented for Millerand could be applied to *Beaulieu* branch or even the whole DH. The three scenarios are:

- **Scenario 9:** return temperatures at the secondary side of all the substations are decreased and fixed to 30°C.
- **Scenario 10:** in addition to scenario 9, a control law of typical for low temperature systems is used for all the substations and the supply temperatures at the production units are optimized.
- **Scenario 11:** 10 substations are selected and modified by reducing temperature levels at the secondary side and by connecting them to the return pipe. Supply temperatures at the production units are also optimized in this scenario.

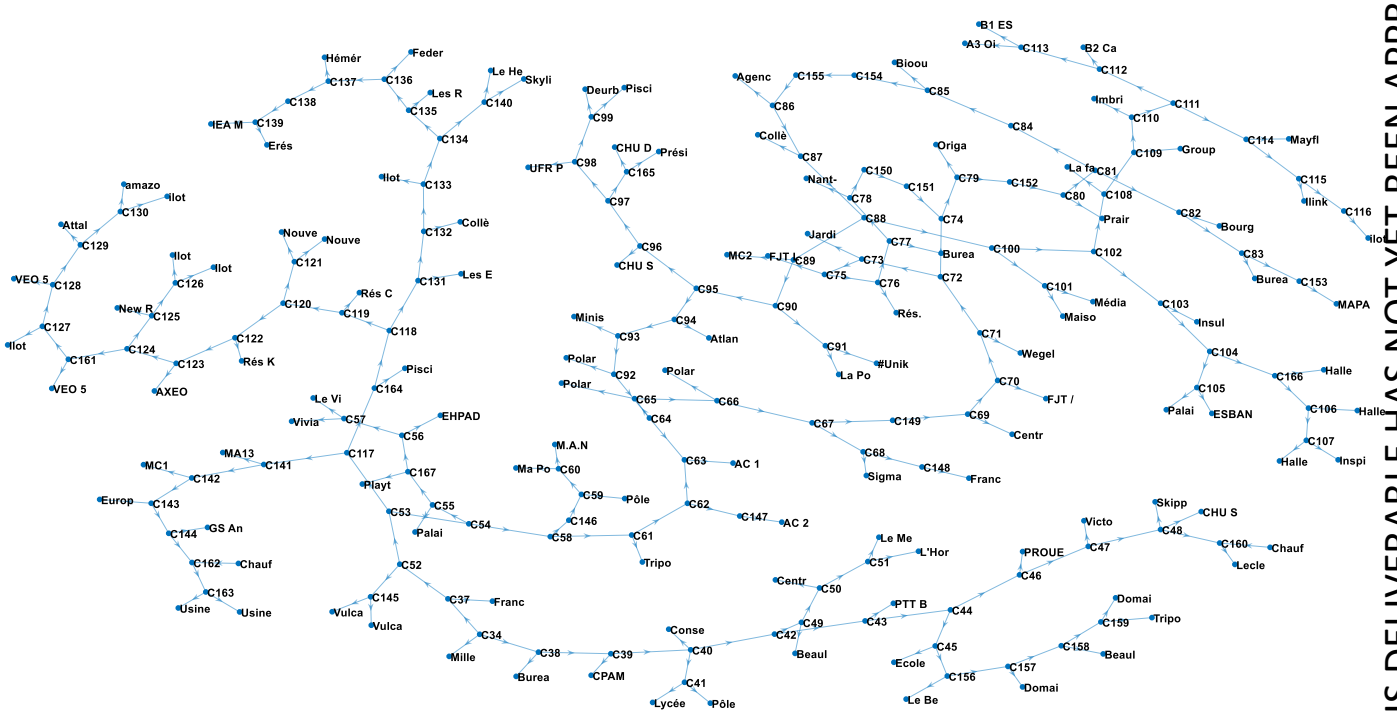

Figure 78: Topology of network's digital twin (*Beaulieu*)

The total energy consumption of *Beaulieu* network for the whole period is given in Figure 79 for the reference scenario and the three scenarios studied. The reference scenario corresponds to the return temperatures in the secondary side fixed to the measured values and the supply temperatures in the two production units (Malakoff and Californie) constant and equal to 95°C. Energy savings realized in scenarios 9, 10 and 11 are given in Figure 80. This figure shows that relative energy savings have the same trend as found in the case of *Millerand* area. Indeed, the best results are obtained when all the substations are modified to support low temperature heating and in the same time, the supply temperatures in the production units are optimized to follow outdoor weather conditions. In this case, 10.2 % of the

This project has received funding from the European Union's Horizon 2020 research and innovation programme under grant agreement No 731297.

total energy consumption can be saved. It appears also that modifying only 10 substations properly selected allows to realize substantial energy savings of about 7.4 % of the total consumption of the network. Scenario 9, gives the smallest amount of energy savings (4.3 %). CO_2 emissions savings are also given in Figure 80.

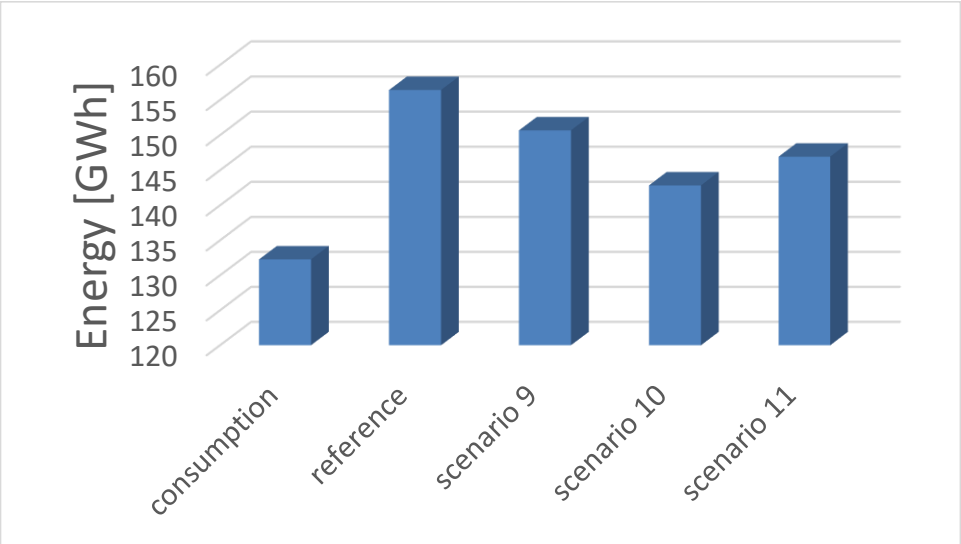

Figure 79: Energy consumption and energy production of *Beaulieu* network in the considered period for the reference case and three scenarios

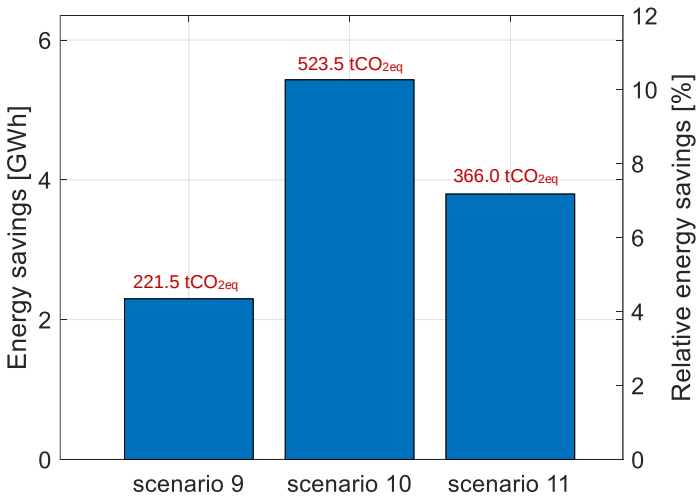

Figure 80: Energy savings realised in scenarios 9, 10 and 11 (absolute and percentage of total consumption)

The detailed time series are not presented here as they have been analysed in the case of Millerand. Similar analysis could be done at any scale of the DH as well as the assessment of any additional scenarios.

This project has received funding from the European Union's Horizon 2020 research and innovation programme under grant agreement No 731297.

7.4 Operationality of the methodology

As explained in the section 4 and illustrated in sections 7.1 and 7.3, to consider the physical variables at the distribution level and/or the substations level makes the methodology able to reflect various practical actions for improving the energy performance of the DH system. In addition, the methodology can also be used to assess more global actions for a better management of the DH.

7.4.1 Extension of the distribution network

The perimeter of the mySMARTLife project being the Ile de Nantes, regarding the DH the question of extending the network is not relevant as almost all the buildings of the island are already connected. However, in a perspective of extending another DH or another part of Nantes DH, a difference must be made between creating a new branch or connecting two existing branches or interconnecting two existing DHs.

In the first, case the proposed methodology is not appropriate as the DH has to be design in totality (topology, piping, HEx, energy systems…) what is well done by usual engineering technics.

In the two other cases, the methodology is fully relevant to assess the impacts the action will have. Indeed, we saw its implementation is appropriate to any scales of the DH including or not the systems. Thus, the DH to be connected or the branch to be interconnected just have to be considered as a part of a DH.

7.4.2 Sub-net connexion

In the concept of 4th generation DH we saw that having low temperatures is one of the main objective (see section 3). Here also, if the project of such DH is totally a new project for a low consumption district, it is then a pure engineering design issue. The proposed methodology reaches its full potential of interest when a low temperature branch is imagined to be connected to a conventional DH (temperature cascade). In this case, as it has been showed by Castro et al. (2016; 2018) who studied the impact of these configuration can have on the systems, the impact on the distribution cannot be neglected. In this sense, the methodology makes possible the assessment of these impacts and the feasibility of hybrid 3rd and 4th generation of DH. More precisely a use of the methodology in this regards corresponds to a combination of scenarios presented in the sections 7.1.1 to 7.1.4. This combination can also be used to determined where on the DH the connexion makes most of sense.

In addition, the action on the energy recovery from the return pipes evaluates this strategy as a function of the useful fraction of the mass flow rate from the return pipe (we saw the potential of recovery is different from substation to substation and directly represented by this fraction). In Figure 81 and Figure 82, we can see that for some substations the fraction can reach values close to 100 % making them low temperature subnets (connected to low energy consumption buildings for example). In the example of these substations, the figures show that sst2 is the less dependent to the energy from the supply pipe. The substations sst7, sst15 and sst25 are more dependant to the supply pipe but the mean value of mass fraction of water coming from the return pipe is relatively high (around 60 %). For all these substations, supply temperatures at the primary side are substantially lower than supply temperature in the other

This project has received funding from the European Union's Horizon 2020 research and innovation programme under grant agreement No 731297.

substations. Connecting some substations to the return pipe is a practical way to feed some substations at lower temperatures without using different circulation pipes for the different temperature levels of water.

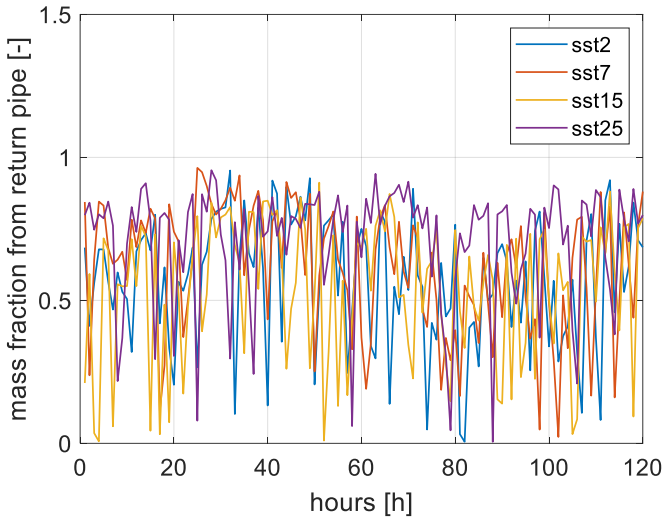

Figure 81: mass fractions of water coming from the return pipe for substations sst2, sst7, sst15 and sst25 in scenario 8 detailed in section 7.1.2

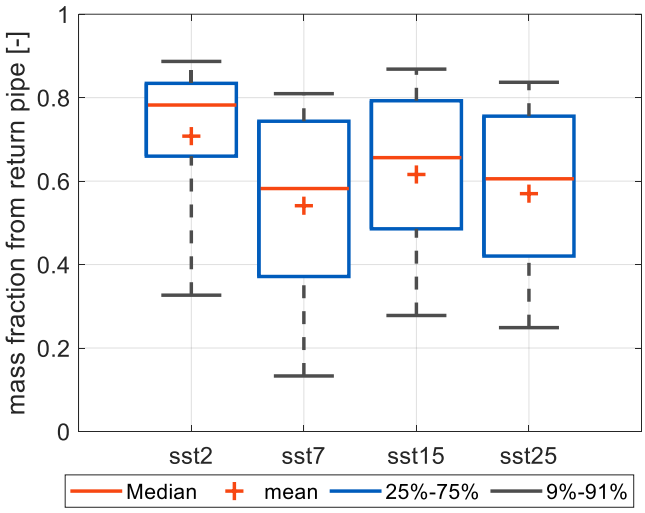

Figure 82: box plot of mass fractions of water coming from the return pipe for substations sst2, sst7, sst15 and sst25 in scenario 8 detailed in section 7.1.2

7.4.3 Energy carriers coupling

In the section 7.1.2, the solution of using the surplus of heat from the return pipe has been evaluated thanks to the proposed methodology. An alternative to this solution can be to use this energy locally by upgrading the return temperature with local Heat Pumps instead of using the supply flow as a complement. This has two positive consequences. The first one is a reduction of the energy consumption as part of it comes from electricity with a

This project has received funding from the European Union's Horizon 2020 research and innovation programme under grant agreement No 731297.

Coefficient of Performance (generally between 2 and 4). The other advantage is the local coupling between energy networks of different energy carriers what is seen as an important potential of flexibility for integrating intermittent renewable energy sources and then energy savings. The Figure 83, illustrates this coupling with a representation coming from a research work (Ayele et al., 2019) done by the ARMINES LTP (IMT Atlantique). The impact on the DH can be assessed like the action of the section 7.1.2 has been evaluated with the present methodology, illustrating again its usefulness for various possible actions.

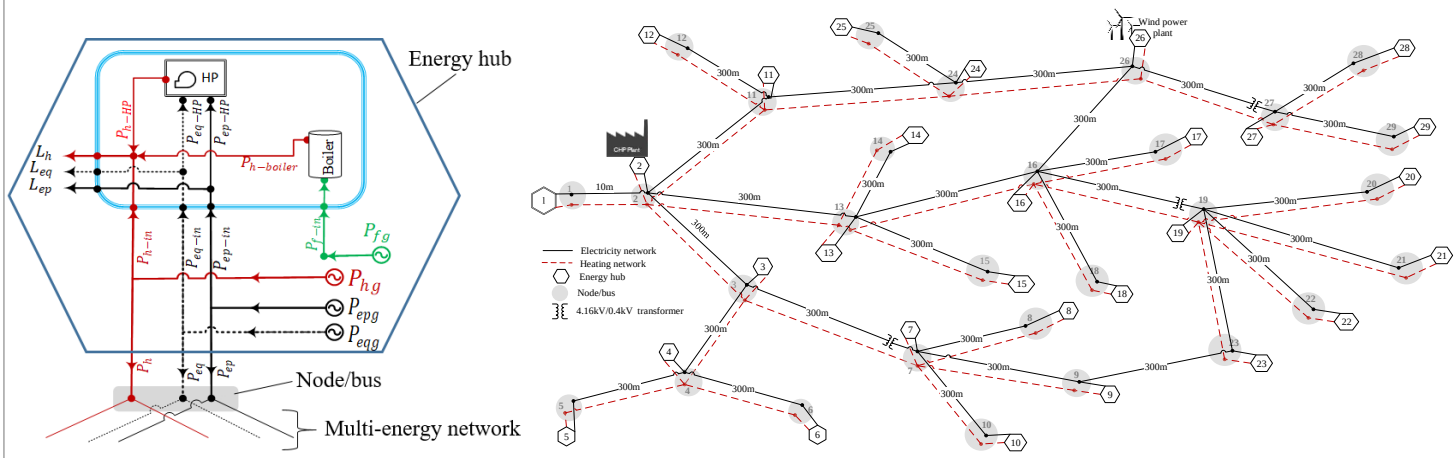

Figure 83: Interaction of DH and electricity grid using Heat Pumps. A connexion between the networks is done in an energy hub (Fig. left) and the connexion can be multiple (Fig. right)

7.4.4 Management of the energy systems

In the different scenarios studied, the impact of the actions has been illustrated with time series where the potential of the action to shave the production curves can be evaluated. This is of importance as it directly implies energy savings (like seen in the corresponding section) for the peak demand, reducing then the use of non-renewable energy systems (generally used for the peak loads because of their high flexibility). The methodology is then a good complementary tool of energy systems management, in combination with usual tools aiming to assess the merit order between the systems based on the load curves.

7.4.5 Energy savings and CO_2 emissions

As seen in the different case studied, the impact of the actions is given in energy saved and CO_2 emissions avoided. The conversion ratio used is defined in the section 4.1.

7.4.6 Awareness of end users

End-users are defined here as the users of the proposed methodology. It can be directly the DH operators or the local authorities who delegate the public service of managing the DH. It can be also third parties proposing them services with regards to energy efficiency actions, in urban planning for example (we saw the interest of considering actions on the buildings in combination with actions on the DH).

This project has received funding from the European Union's Horizon 2020 research and innovation programme under grant agreement No 731297.

The awareness can be seen under two aspects. It can be an information provided on new solutions for more energy efficiency. In this case, it has been illustrated in this section with a diversity of scenarios which explored not conventional ideas for most of them (as regularly discussed with the DH operator during the project[13]). It can also relate on the data quality as seen in the section 4. This section defined some indicators which can be part of a dashboard used by the different parties to assess the quality of the monitoring and the actions to be taken to improve it when needed.

[13] A concrete example of the awareness potential of the methodology is the proposition the DH operator made to ARMINES LTP IMT-Atlantique to write a description of the impact the methodology coupled to an Urban Platform can have, in order to include it in a response to a call for tender.

This project has received funding from the European Union's Horizon 2020 research and innovation programme under grant agreement No 731297.

8. Monitoring of the action

As stated in its definition the action does not aim to implement physical actions on the DH in the frame of mySMARTLife project. The purpose is to offer the different stakeholders in charge of the DH the possibility to forecast actions based on a realistic definition of the network in its current state. In this regards, the data collection and the associated analysis are as important as the modelling/optimisation parts (Figure 84). The main outcomes are the data analysis regarding their quality combined with the strategy to complement the information, and the assessment of the scenarios with the proposed methodology. In consequence, due to the particularity if the action, the monitoring proposed for the two next years will address these two pillars, at the distribution level (the perimeter of the action).

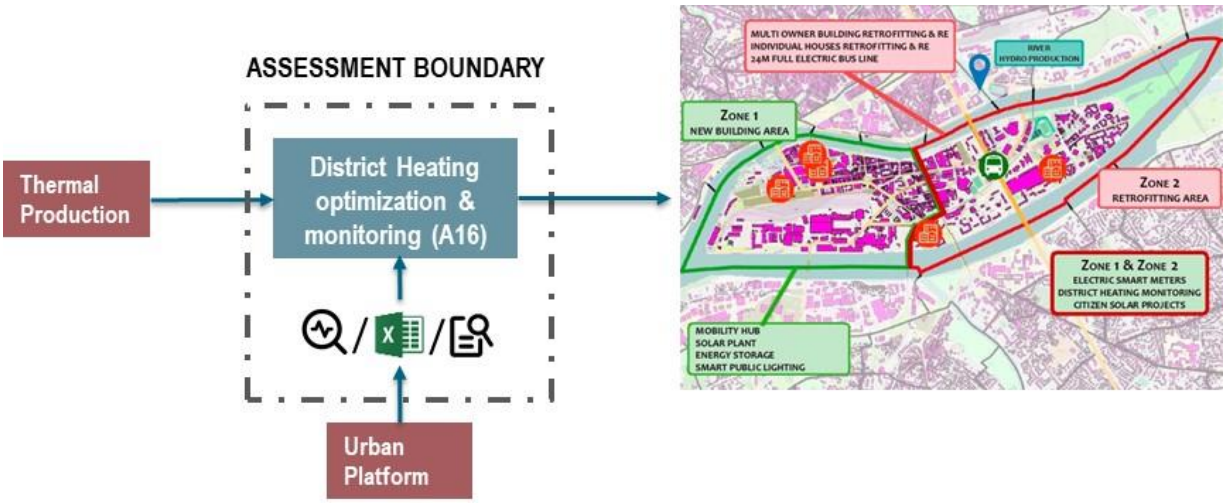

Figure 84: Boundary of monitoring the DH Action

- Regarding the Data, the DH supervision steps-up since its implementation in 2015. So a follow-up of the indicators defined in the section 0 will be done in order to assess the evolution of the data quality.
- In addition, the centralization of these data in the urban platform is in progress. The aim is to make the data available independently of the DH operator supervision tool constraints (limited access, manual extraction of the information…). An evaluation of this centralization will be done (amount of data and associated quality).
- An assessment of the ease of using the data from the urban platform instead of the data from the DH operator supervision will be done.
- The objective of the mySMARTLife program is to make the actions operational. With the different scenarios studied in this work, the methodology has already been proven *in operational environment* (TRL9). An evaluation of the usefulness of the present action for the stakeholders will demonstrate further its operational characteristic. This evaluation will cover both the use of the action on the DH system and its coupling with the action on the Decision Aiding.

This project has received funding from the European Union's Horizon 2020 research and innovation programme under grant agreement No 731297.

- A connection with real actions implementation on the DH will be done when it will be relevant. If such an opportunity occurs (independently of the present action), a posteriori comparison of the impacts of this action with the results given by the methodology will be done.
- Regarding the DH global performance studied in the section 4.1, a follow-up of the indicators defined in this section will be done and the indicators will be complemented with the additional information from the coming two years of monitoring.

In order to implement the monitoring, the main source of data will be the Urban Platform for which the centralization of data coming from the DH operator supervision tool is in progress. This information must be also complemented by the energy indicators of the energy systems (Energy production and the time series of the variables at each of the production sites). The proposed monitoring is then subject to having access to all this information that ARMINES do not own.

This project has received funding from the European Union's Horizon 2020 research and innovation programme under grant agreement No 731297.

9. Replicability of the methodology

As already mentioned, the methodology has been developed using modelling and optimization tools from ARMINES. The aim is to make the proposed work independent on them and compatible with other solutions (internal tools developed by the DH operator for example). This possibility also increases the flexibility of the solution as well as its replicability to other DH. This section lists some existing tools which can be used in the different parts of the methodology.

Depending on the tool alternative data sources are used reinforcing the flexibility and making them more appropriate depending on the operational objectives. Thus, the section also proposes a list of Energy & Buildings modelling tools which can be used in complement of the data processing generalization presented previously.

9.1 Existing Softwares and tools for DH modelling and optimisation

9.1.1 NetSim by Vitec

NetSim is a software developed by Vitec which is a Swedish software editor specialized developing software solutions for niche markets and offers products in various sectors such as associations, automotive industry, energy, education etc.

NetSim gives the possibility to run static and dynamic simulations of DH. The software has import tools from a number of network information systems on the market giving it the ability to creates a grid model from an existing Geographic information system (GIS) and to import consumption data from a billing system. Once the topology is created, NetSim calculates the mass flow rates and temperature over the network and can export the results in different formats including Excel, DXF/DWG of in the format of plots and animations. The graphical interface of the software gives the possibility to easily add or delete pumps, pipes, consumers or production units.

The software gives to the operator a greater knowledge level of the heating network and it can be used to size pipes and pumps, to enhance the temperature distribution and to lower the network's thermal inertia. These functionalities can be useful for engineers when realizing different tasks including: feasibility studies for connecting new costumers or new utilities, merging or sectioning networks and searching for "bottle neck pipes" or cold water stalls in summer time…

9.1.2 OpenUtilities by Bentley (formerly sysNet)

This software provided by Bentley is a GIS oriented management system rather than a physical modelling tool. This software is not specific for DH and can be used to manage electric, water, gas or district energy networks. It consists of three different and interconnected tools: OpenUtilities Designer, OpenUtilities Map and OpenUtility power view.

- **OpenUtilities Designer** is intended to speed up design workflow of utilities that are connected to a network by combining the MicroStation's functionalities and GIS systems. MicroStation is a CAD system developed by the same company and is used for design and drafting. Putting design in its geographical environment thanks

This project has received funding from the European Union's Horizon 2020 research and innovation programme under grant agreement No 731297.

to a GIS system allows project managers to review and approve projects and to keep track in the same time of costs and global progress at the network's level.

- **OpenUtilities Map** is the GIS system provided by Bentley that can be used along with OpenUtilities Designer and provides additional features such as network tracing, leak detection and outage planning.
- **OpenUtility power** view is intended to help managers to review workflows by providing reporting tools to track and approve changes and projects progress and to some analysis such as network tracing and leak detection. These tools are offered in a geolocalized fashion to help managers visualizing the whole system.

9.1.3 Apros

Initially developed for nuclear power plants modelling and simulation Apros can be used for DH modelling. Thanks to its component libraries, Apros is able to model the majority of the components that can be found in DH such as HEx, pipes, pumps, valves and heat storage systems. Control aspects can also be modelled using automation components (valve positions, pump power etc…). Apros provides also components to model services tunnels that are used in some DH especially those of first and second generations.

9.1.4 ForCity District heating and cooling

ForCity is a French startup working on urban modelling for decision making in different fields such as Energy, water, environment and buildings. Forcity relies on modelling systems in their geographical context and offers data visualization in 3D maps to facilitate the decision making process for decision makers. Forcity proposes to go further in data visualization by integrating the time factor and proposes predictive data visualization.

ForCity DH is one of the solutions proposed by ForCity and offers many functionalities such as demand side modelling, network's geometry optimization and decision making.

Demand side modelling allows to forecast energy demands across the city by integrating urban projects and buildings retrofitting impact based on different scenarios. Heat demand density tends usually to decrease in the cities because of new environmental transition requirements and network's must keep their growth to maintain their economic profitability. The tool offers also functionalities to assess network's densification scenarios by modelling substations which are candidates to be connected to the network and by evaluating the impact of annual expansion plans in terms of cost and environmental footprint reduction. It is possible also to take into account urban changes that will occur in the future (planned construction projects, new infrastructure etc…).

9.1.5 Hysopt

Hyspot was released recently in 2019 and has a friendly user interface that allows to draw quickly heat network plans over the top of maps. Different types of buildings can be created and connected to the network such as office buildings and apartment blocks. These buildings are represented with a limited number of parameters. The network is the ready for simulation considering the loads of the buildings. These loads are generated thanks to a load generator. Equivalent models are also used to calculate the pressure drop, mass flows and return temperatures of the buildings. These models can also be tuned using measured data from the buildings.

This project has received funding from the European Union's Horizon 2020 research and innovation programme under grant agreement No 731297.

Hysopt includes also a library containing a number of models for generation units (heating and cooling) with a certain level of details (distribution circuits, control, pumps, valves etc…) these models take into account the dynamic behavior of the system and allows to analyze various performance indicators such as efficiency, heat contribution etc.

The software uses also diversity factors for hot water and central heating in order to calculate heat demands for buildings of various sizes. Diversity is also used for aggregation to calculate mass flows and pipes diameters and to avoid oversizing them.

In Hysopt, different variants and scenarios can be assessed and compared based on different KPIs which give the user an idea about the economic, environmental and energetic performance of the installation for each scenario.

9.1.6 Termis

Initially developed by 7 technologies, Termis is now a Schneider Electric product. It allows to model DH in different modes: offline or real-time. The offline mode is used in planning and design phase and allows to perform different tasks such as pipes and pumps sizing, determine maximum capacity or to perform temperature optimization.

Same models can be used in real-time mode which permits to tune the model and adapt model's parameters to the real network. This is achieved by integrating the software to the SCADA system of the network. In this second mode, Termis will predict the behavior of the network and will optimize pumps' powers and energy production in a predictive manner.

9.1.7 MODEST

Modest is a part of Energy Plan which is a model for Energy Systems Analysis. It has been developed and expanded in Alborg University since 1999. The purpose of Energy plan is to design and analyse large energy systems in hourly steps for one years. It allows to perform technical studies by calculating energy balances, fuel consumption and CO_2 emissions of an energy system knowing energy demands and production capacities and efficiencies. The software allows also feasibility studies in terms of total annual costs by considering investment costs and fixed operational and maintenance costs over the lifetime periods of the systems. Energy plan has also the ability to perform market economic simulations and to optimize the supply side by minimizing both short-term electricity costs and short-term DH costs. MODEST can be used for studying any Energy system including DH. It allows studies at the design stage to decide what type of production units to connect to the system or at operation stage to decide which production units to use at each time step.

9.2 Demand modelling: models, existing (Commercial) software and tools

Heat demand (consumption) is an important parameter which needs to be modelled and predicted (when it cannot be monitored) with accuracy to enable a good understanding of DH systems. Some data are needed to obtain realistic prediction of heat demand. These data can be related to the building itself including its physical and geometric characteristics. They can also be related to the building environment such as outdoor temperature, humidity rate or the intensity of the solar radiation. Consumer's behaviour is also an important factor that needs to be modelled

This project has received funding from the European Union's Horizon 2020 research and innovation programme under grant agreement No 731297.

accurately and increases the randomness and uncertainties. Different methods have been proposed in the literature to model heat demand in DH systems. Existing techniques can be categorized into different categories: historical methods, simulation-based methods and time-series predictive models:

- **Historical methods**

These methods take advantage and combine different types of data (supply, demand, weather etc…).

1. **Heating degree day:** This method uses the assumption that heat losses in buildings is proportional to the difference between indoor and outdoor temperatures:

$$\dot{Q}_{loss} = U_{Overall} \times (T_{indoor} - T_{outdoor}) \quad (5)$$

The overall heat loss coefficient $U_{Overall}$ $[kW.K^{-1}]$ is a global coefficient which includes all sources of heat losses in the building (convection, radiation and air infiltration and renewal). This method does not give a good degree of accuracy and take into account only of thermal resistance of the envelope and not its thermal capacitance. It does not take into account neither the behaviour of the occupants nor eventual internal heat sources. For these reasons, this method is usually used for predesign purposes and essentially for small buildings.

2. **Measurements:** when measurements are available, they can be used as inputs to DH models. This method can be used only for existent buildings that has suitable equipment. Besides, a minimum history of one year is needed to capture the real consumption of the building and its variation over the seasons.
3. **Archetype buildings**: data can be used to categorize buildings in different classes representing different building's archetypes. Clustering techniques can be used to classify the buildings and reference buildings are defined for each class.

- **Simulation-based methods**

These deterministic methods use mathematical models for the components of the buildings (walls, roof, windows etc…), the heat balance between these components and the environment and between each other produce the heat demand profile of the building. These models can be complex or simplified:

1. **Complex models:** these models are widely used in buildings simulation software such as TRNSYS, Comfie and Energy plus and require detailed data about the geometry of the building, the materials used and weather conditions. It requires also extensive computational cost. For these reasons, complex models are used to model small-scale systems mainly at the design stage and are not suitable for modelling a large number of buildings connected to DH.
2. **Simplified models:** complex models can be simplified to minimize computation times and to model large scale systems. Models based on the analogy with electricity are often used for this. The details of the geometry and the materials characteristics are wrapped in global parameters. The components of the building (envelope, indoor air) are associated to capacities and resistances.

- **Predictive time series methods**

This project has received funding from the European Union's Horizon 2020 research and innovation programme under grant agreement No 731297.

These models are essentially data driven and rely on the curve fitting relations in order to predict the demand based on historical data. Different predictive models exist like for example: time-series ARMA models, Kalman filter, and artificial intelligence (AI) methods.

1. **ARMA time-series:** ARMA stands for Auto-Regressive Moving Average (also called Box-Jenkins). It predicts the demand using a linear model of several past observations and current perturbations:

$$z(t) = Y_p(t) + Y(t) \quad (26)$$

where $Y_p(t)$ depends essentially on the time of the day and usual weather patterns for the design day, and $Y(t)$ accounts for the effect of deviations from usual weather patterns due to random effects.

2. **Kalman Filter:** this model estimates the value of the variables for future time steps $(t + \Delta t)$ based on the values of the variables at its current time step (t) using a linear dynamic system written in state space format. The Kalman filter is a sequential estimation procedure. It tries to produce the best estimation of the set of variables by updating the estimate of state at each step using previous observations (Morrison and Pike, 1977).
3. **Artificial Intelligence:** many artificial intelligence methods exist and can be used for load prediction such as Artificial Neural Networks (ANN), Feed-forward Neural Network (FNN), and Support Vector Machine (SVM). The ANN is a general purpose model that has been used for predicting loads and particularly in forecasting electricity consumption of buildings (Zhang et al., 1998). The popularity of Artificial intelligence methods comes from the fact that it shows generally more accurate results compared with other simulation based methods. Besides, these methods are easily adaptable to different types of buildings without significant modifications in the mathematical model. In addition, inputs such as social parameters are included to the model as they are included in the training data sets. Despite these advantages, Artificial intelligence methods are not widely used yet because of some drawbacks like over-fitting problems and data requirements for the training process.

The list presented above is not exhaustive and focuses on methods and tools suitable for the action linked to the DH. Further tools exist and a benchmark is proposed in the deliverable D2.2

This project has received funding from the European Union's Horizon 2020 research and innovation programme under grant agreement No 731297.

10. Conclusion

District Heating is recognized as a key system for implementing the energy transition policies and for reaching the associated objectives. Like in the building sector the challenge is more the improvement of existing systems rather than developing new networks.

In this regards, the present work proposes a methodology able to guide the different stakeholders (DH operator, Local authority) for improving the DH or part of it. In particular, the combination of a good data processing with modelling and optimization make possible the assessment of a diversity of scenarios on the different main parts of DH (systems, distribution and substations).

This methodology has been built in order to be compatible with the reality of data and information owned by the stakeholders. Regarding this aspect, a data processing methodology is proposed to assess the performance of the system with appropriate indicators which are relevant for evaluating scenarios of improvement.

To fulfil with the objective of a flexible, scalable and replicable solution, the different bricks of the solution are totally modular and can be implemented by different tools (commercial, open source, developed internally by the different stakeholders).

To illustrate its potential, the methodology has been applied to different scenarios of actions which affects the different parts of the DH. The results show substential potential energy savings thanks to them.

The action has been developed in connexion with other actions in the mySMARTLife project like the action on Decision Aiding and the Urban Platform with real links between the respective outcomes of these actions.

This project has received funding from the European Union's Horizon 2020 research and innovation programme under grant agreement No 731297.

11. References

Castro Flores, J., 2018. Low-temperature based thermal micro-grids: Operating strategies and techno-economic assessment. IMT Atlantique et KTH, Stockholm, Sweden.

Conn, A.R., Gould, N.I.M., Toint, P.L., 2000. Trust Region Methods. Society for Industrial and Applied Mathematics. https://doi.org/10.1137/1.9780898719857

Forgy, E., 1965. Cluster analysis of multivariate data: efficiency versus interpretability of classifications. Biometrics 21, 768–780.

Frederiksen, S., Werner, S., 2013. District Heating and Cooling. Lund, Studentlitteratur.

Holland, J.H., 1992. Adaptation in Natural and Artificial Systems. MIT Press, Cambridge, MA, USA.

Jones, D.R., Perttunen, C.D., Stuckman, B.E., 1993. Lipschitzian optimization without the Lipschitz constant. J. Optim. Theory Appl. 79, 157–181. https://doi.org/10.1007/BF00941892

Kennedy, J., Eberhart, R., 1995. Particle swarm optimization. Proc. IEEE Int. Conf. Neural Netw. 4, 1942–1948. https://doi.org/10.1109/ICNN.1995.488968

Lund, H., Werner, S., Wiltshire, R., Svendsen, S., Thorsen, J.E., Hvelplund, F., Mathiesen, B.V., 2014. 4th Generation District Heating (4GDH). Energy 68, 1–11. https://doi.org/10.1016/j.energy.2014.02.089

MacQueen, J., 1967. Some Methods for Classification and Analysis of Multivariate Observations, in: Le Cam, L.M., Neyman, J. (Eds.), Proceedings of the 5th Berkeley Symposium on Mathematical Statistics and Probability - Vol. 1. University of California Press, Berkeley, CA, USA, pp. 281–297.

Morrison, G.W., Pike, D.H., 1977. Kalman Filtering Applied to Statistical Forecasting. Manag. Sci. 23, 768–774.

Nelder, J.A., Mead, R., 1965. A Simplex Method for Function Minimization. Comput. J. 7, 308–313. https://doi.org/10.1093/comjnl/7.4.308

Pelleg, D., Moore, A., 2000. X-means: Extending K-means with Efficient Estimation of the Number of Clusters, in: In Proceedings of the 17th International Conf. on Machine Learning. Morgan Kaufmann, pp. 727–734.

Pham, D.T., Dimov, S.S., Nguyen, C.D., 2005. Selection of “K” in ’K -means clustering. Proc. Inst. Mech. Eng. Part C J. Mech. Eng. Sci. 219, 103–119. https://doi.org/10.1243/095440605X8298

Torczon, Virginia., 1997. On the Convergence of Pattern Search Algorithms. SIAM J. Optim. 7, 1–25. https://doi.org/10.1137/S1052623493250780

Zhang, G., Eddy Patuwo, B., Y. Hu, M., 1998. Forecasting with artificial neural networks: Int. J. Forecast. 14, 35–62. https://doi.org/10.1016/S0169-2070(97)00044-7

This project has received funding from the European Union's Horizon 2020 research and innovation programme under grant agreement No 731297.